Ψ_k Newsletter

AB INITIO (FROM ELECTRONIC STRUCTURE) CALCULATION OF COMPLEX PROCESSES IN MATERIALS

Number 59   October 2003

Contents

1 Editorial

We start this newsletter with the **General News** section where we write about changes to downloading latex files of the current and future newsletters. There we also have a call for scientific highlights for the next year's newsletters and abstracts of newly submitted papers. Future workshops/meetings are announced in the **RTN2** section and in the **General Workshop/Conference Announcements** section. A number of reports are published in the **ESF** and **UK's CCP9** sections. They contain both programmes and abstracts, some rather extensive, of presented papers. More abstracts can be found in the usual **Abstracts** section. We have quite a few of available position announcements in the **General Job Announcements** section. The newsletter is finished with the scientific highlight on "**Exchange interactions, spin waves, and transition temperatures in itinerant magnets**" by Ilja Turek (Brno and Prague), Josef Kudrnovský (Prague), Vaclav Drchal (Prague), and Patrick Bruno (Halle). Please check table of contents for further details on this newsletter.

The *Networks* have a home page on World Wide Web (WWW). Its *Uniform Resource Locator* (URL) is:

http://psi-k.dl.ac.uk/

The above contains information on the Psi-k 2003 workshops and hands-on courses (subject to funding). In these pages you can also find information on how to apply for funding to make collaborative visits.

Please submit all material for the next newsletters to the email address below.

The following email addresses, which remain in operation, are repeated for your convenience, and are the easiest way to contact us.

	function
psik-coord@daresbury.ac.uk	**messages to the coordinators, editor & newsletter**
psik-management@daresbury.ac.uk	**messages to the NMB of all Networks**
psik-network@daresbury.ac.uk	**messages to the whole Ψ_k community**

Dzidka Szotek and Walter Temmerman
e-mail: psik-coord@dl.ac.uk

2 General News

-o-o-o-o-o-o-o-o-o-o-o-o-

2.1 Availability of the Psi-k Newsletters on the Web

-o-o-o-o-o-o-o-o-o-o-o-o-

This is just to inform you about changes regarding availability of the latex files of the present and future Psi-k newsletters on the Psi-k web-pages. Until now, Psi-k newsletters could be downloaded from the web either in the latex version, together with eps-files of all figures, as a postscript file or in the pdf-form. However, starting with this newsletter we have changed the previous practice and replaced the latex-file, with eps-files of the figures, by a gzipped file containing both the latex file of the newsletter and the eps-files of all the necessary figures. The current newsletter contains 37 figures, 15 belonging to the report on the Summer School on "New Magnetics", that took place in Poznan, Poland, on 15-19 September, and 22 figures associated with the scientific highlight of the month on "Exchange interactions, spin waves, and transition temperatures in itinerant magnets" by Ilja Turek (Brno and Prague), Josef Kudrnovský (Prague), Vaclav Drchal (Prague), and Patrick Bruno (Halle). Note that both the postscript- and pdf-files are available for downloading as usual. We hope that the gzipped file, with the latex file and figures, will be easier to deal with.

-o-o-o-o-o-o-o-o-o-o-o-o-

2.2 Call for Contributions to Psi-k Newsletters

-o-o-o-o-o-o-o-o-o-o-o-o-

Note that the next newsletter will be the 60th issue, and the last of this calendar year. As you all know, we publish six newsletters every year, every two months a new issue, always starting with the February- and finishing with the December issue. The newsletters have grown in size mostly because they cover activities of several networks or programmes, but also owing to our readers and their individual contributions. We do value these contributions very much, since they reflect living and active scientific community. In particular, abstracts of newly submitted papers are the most direct way of keeping the whole Psi-k community aware of our common interests and research efforts at any particular time, and hopefully can stimulate more collaborations between scientific institutions across Europe. So, we would like to encourage all of you to send us your abstracts. The abstract template is given below. Do not wait until your paper is accepted or

published, because it misses the point of the **Abstracts** section.

Other contributions we are greateful to our readers for are the scientific highlights. Recently, we have had a number of very elaborate highlights of both highly scientific and at the same time broadly educational value. We would like to encourage our readers to contribute highlights in the field of their expertise. We do realize the effort involved, but this is an effort spent for our community and the benefits are invaluable to all of us. If you want more people to be aware of your field and perhaps even start new collaborations this way then please do contribute a highlight. We need six highlights for the next year, but at the moment have only one offer. Note that we need to know at least two months ahead of time of any forthcoming highlights to plan accordingly. All other contributions to the subsequent newsletters need to reach us at least a few working days before the end of the months preceeding the publication months of the newsletters, i.e., a few days before the end of January for the February issue, a few days before the end of March for the April issue, a few days before the end of May for the June issue, a few days before the end of July for the August issue, a few days before the end of September for the October issue, and a few days before the end of November for the December issue.

Abstract template

```
%%%%%%%%%%%%%%%%%%%%%%%%%%%%%%%%%%%%%%%%%%%%%%%%%%%%%%%%%%%%%%%%%%%
%%%%%%%%%%%%%%%%%%%%%%  Abstract xx %%%%%%%%%%%%%%%%%%%%%%%%%%%%%%%
%%%%%%%%%%%%%%%%%%%%%%%%%%%%%%%%%%%%%%%%%%%%%%%%%%%%%%%%%%%%%%%%%%%
\newpage
\null
\vskip 2em
\begin{center}
\Large{\bf t i t l e  \par}
\vskip 1.5em
{\large \lineskip .5em \begin{tabular}[t]{c}
a u t h o r s \\
{\it  a f f i l i a t i o n s}\\
\end{tabular}\par}
\end{center}
\begin{abstract}
t e x t  of  a b s t r a c t
\end{abstract}

\noindent
(Submitted to  n a m e  of  j o u r n a l)\\
Contact person: N a m e  and  e m a i l \\
```

3   News from the RTN2 ("f-electrons")

"Ab initio computation of electronic properties of f-electron materials"

3.1   RTN2 Workshop Announcements

3.1.1   Workshop in Aarhus, Denmark

The Physics of f-electron Solids

November 6-7, 2003, Aarhus, Denmark

Sponsors: RTN2, ESF Psi-k, Danish Natural Science Foundation

The Workshop's web site:

http://www.phys.au.dk/∼svane/f-workshop.htm

The workshop will focus on new developments in experiments and theory of f-electron solids. The workshop is organized in the frame of the RTN2 network 'Psi-k: f-electrons' but will be open for anyone interested. Financial support is available for network participants. Registration: by email to A. Svane, see below.

Time and place: November 6-7, in Århus, Denmark

Tentative programme:

Thursday 6/11:

9:00-9:35   B. Johansson*, *on Theory*
9:35-10:10   F. Wastin, *on Experiments*
10:10-10:30   Coffee
10:30-11:05   J.-C. Griveau, *on Superconductivity*
11:05-11:40   R. Caciuffo, *on NpO_2 orbital ordering*
11:40-12:15   I. Opahle, *Electronic structure of $PuCoGa_5$ and related compounds*
12:30-13:30   Lunch
13:00-14:05   G. Kotliar, *on DMFT theory of Pu*
14:05-14:40   M. Brooks, *on Theory of Actinides*
14:40-15:15   O. Eriksson, *on Theory of$PuCoGa_5$*

15:15-15:45 Coffee

15:45-16:20 M. Richter, *Surface geometry and electronic structure of U/W(110)*

16:20-16:55 M. Lüders, *Local SIC implemented in the KKR method*

18:30-   Dinner

Friday 7/11

9:00-10:00   RTN Board meeting

10:00-10:30 E. Wimmer, *on Industrial f-electron systems*

10:35-10:50 Coffee

10:50-11:25 S. Biermann, *on DMFT*

11:25-12:00 K. Held, *The Cerium volume collapse: An LDA+DMFT study*

12:00-12:35 A. Lichtenstein*, *on DMFT*

12:35-13:30 Lunch

13:30-14:05 G. Zwicknagl, *on Uranium heavy fermion compounds*

14:05-14:40 L. Petit, *on SIC-LSD theory of Actinides*

14:40-15:15 L. Nordstrom, *on Theory of MAE of Gd*

15:15-15:45 Coffee

15:45-16:20 R. Laskowski, *Non-collinear magnetism in UO_2*

16:20-16:55 G. Santi, *Coexistence of ferromagnetism and superconductivity in $ZrZn_2$*
             * unconfirmed.

Organisers:

- Axel Svane
  Department of Physics and Astronomy, University of Århus, Denmark
  Phone: +45-8942-3678, Fax: +45-8612-0740,
  `svane@phys.au.dk`

- Walter Temmerman
  Daresbury Laboratory, UK
  Phone: +44-1925-603227, Fax: +44-1925-603634,
  `W.M.Temmerman@dl.ac.uk`

4 News from the ESF Programme

"Electronic Structure Calculations for Elucidating the Complex Atomistic Behaviour of Solids and Surfaces"

4.1 Reports on Collaborative Visits

Report on a collaborative visit of Julien GODET (Laboratoire de Métallurgie Physique, University of Poitiers, France) to Professor José SOLER's group (Dep. de Fisica de la Materia Condensada, Universidad Autónoma de Madrid)

June 1 - July 12, 2003

Within the STRUC-Ψ_k ESF Programme, I spent over six weeks (4.06.2003-12.07.2003) at the Dep. de Fisica de la Materia Condensada, Universidad Autónoma de Madrid, in the group of Professor José SOLER starting a collaboration on the problem of dislocation nucleation at surface steps in silicon using ab-initio techniques.

The formation of dislocation at surface defects is a process of particular importance in nanostructured materials submitted to large stresses, such as whiskers, nanograins or heteroepitaxial thin films (as those used for microelectronic devices). The very first stages of dislocation nucleation being still out of the scope of experimental investigations, the atomic scale simulations are expected to provide useful information.

The studied system is a slab of silicon with steps on the surface corresponding to the emergence of a perfect dislocation with a $1/2 < 110 >$ Burgers vector[1]. To apply a uniaxial stress, the system is deformed following the strain deduced from anisotropic linear elasticity. The problem requires minimizing the energy of an ensemble of at least several hundreds of atoms to avoid spurious interaction between steps and between surfaces. To realize an ab-initio calculation with a large number of atoms, we had to find the smallest basis set for silicon to reduce the calculation time. So we checked several atomic orbital basis sets with the code SIESTA and compared the results with previous ones obtained with a code of plane waves on the calculation of the homogeneous shear of the 111 planes along the $< 110 >$ direction of bulk silicon[2]. A minimal basis set (simple zeta) gives good results, but the system is limited to about 200 atoms to keep a reasonable calculation time. To model bigger systems we had to try the order-N method of the SIESTA code. The first tests have shown few problems of convergence. In fact, the use of the order-N method requires systems with a large band gap to have a good convergence

of the energy. In our systems, the band GAP is relatively small and the (100) surfaces rebuilt 2×1 are conductive. To solve this problem, we tried to saturate the dangling bond of silicon on the surface with hydrogen. We are looking forward for the results.

To summarise, during my stay at the Dep. de Fisica de la Materia Condensada we began a collaboration on the problem of dislocation nucleation at surface steps in silicon using the ab-initio code SIESTA. The goal being to validate the mechanism of dislocation nucleation at surface step obtained with empirical potentials in the scope of my Ph-D.

I am grateful to the Psi-k network for its support.

Julien Godet
Ph-D student
Laboratoire de Métallurgie Physique
CNRS - Université de Poitiers
UMR 6630, B.P. 30179
86962 Futuroscope Chasseneuil Cedex, France
julien.godet@etu.univ-poitiers.fr

Poitiers, August 30.

References

[1] Surface step effects on Si (100) under uniaxial tensile stress, by atomistic calculations. J. Godet, L. Pizzagalli, S. Brochard, P. Beauchamp, Scripta Materialia 47, 481, 2002

[2] Comparison between classical potentials and ab initio for silicon under large shear. J. Godet, L. Pizzagalli, S. Brochard, P. Beauchamp, submitted to Journal of Physic: Condensed Matter

4.2 Reports on ESF Workshops

4.2.1 Report on FHI-Berlin Workshop

Workshop on
Application of Density-Functional Theory
in Condensed Matter Physics, Surface Physics
Chemistry, Engineering, and Biology

21–30 July 2003

Fritz-Haber-Institut, D-15195 Berlin, Germany

This ten-day course was focused on the application of density-functional theory to electronic-structure calculations in different scientific fields and aimed at providing a practical introduction to the handling of pertinent software packages. The workshop programme combined morning lectures, which elucidate the theoretical concepts and numerical procedures, with hands-on sessions in the computer laboratory where realistic research problems were tackled. In addition to condensed matter physics, special emphasis was placed on fields like biology and surface chemistry.

The workshop was organized by a team of researchers at the Fritz-Haber-Institut der Max-Planck-Gesellschaft in Berlin (Peter Kratzer, Catherine Stampfl, Ricardo Gomez Abal, Arno Schindlmayr, Jörg Neugebauer and Matthias Scheffler). As conference venue, we had chosen Harnack-Haus, i.e., the Conference Center of the Max-Planck-Gesellschaft in Berlin, just across the street from the Theory Department of the Fritz-Haber-Institut. For the practical sessions, a computer lab with thirty LINUX PCs had been set up. During these afternoon sessions, post-docs and Ph.D. students from the Theory Department at the Fritz-Haber-Institute were available to answer questions from the participants and to assist them in tackling the practical exercises.

The workshop was attended by about sixty scientists from all over the world, in particular Ph.D. students and young researchers. Thanks to financial support by ESF, we could give out bursaries to some Ph.D. students from European labs, that covered part of their local costs. In order to guarantee computer access and individual attention during the tutorial sessions, the number of participants had to be limited to about sixty, although we had received more than eighty applications. We tried our best to ensure a fair selection but obviously could not do justice to all applicants. Thus here comes a big "SORRY" to those we had to reject.

Aimed especially at young researchers and Ph.D. students in the wider field of electronic-structure calculations, the workshop programme was concerned with a detailed discussion of

basic aspects of density-functional theory and its application in different contexts. In particular, it was interesting to hear about the various implementations of density functional theory directly from the experts: P. Blaha presented the linearized augmented-plane-wave method (LAPW) and the APW+lo approach for all-electron calculations, while P. Bloechl introduced the projector-augmented plane-wave method (PAW) to the audience. As an example of an all-electron method based on localized orbitals, the code Dmol^3 was discussed by J. Behler. The pseudopotential-plane-wave method was explained in detail in several lectures (J. Neugebauer, S. Boeck, E. Pehlke, M. Fuchs). Special attention was paid to an assessment of the reliability and computational performance of the various methods (M. Scheffler, P. Kratzer). *Ab initio* molecular dynamics (L. Ismer) and perturbative schemes for excited states, such as the *GW* approximation (A. Schindlmayr) and time-dependent density-functional theory (K. Tatarczyk), as well as the exact-exchange functional (A. Qteish), were also covered. Besides the lectures, there were six hands-on sessions in which the practical use of the SFHIngX computer code (a plane-wave pseudopotential implementation recently developed at the Fritz-Haber-Institut), the construction of pseudopotentials and the calculation of quasiparticle band structures in the *GW* approximation (code from the group of R. Godby, York) were taught.

More detailled information (the workshop programme, complete with abstracts and full lecture notes) is available at

<p style="text-align:center">http://www.fhi-berlin.mpg.de/th/Meetings/FHImd2003/</p>

From the response by the participants, we trust that the knowledge provided in the lectures, and in particular in the practical sessions, was most helpful in boosting their scientific projects. The workshop programme left ample time for individual study at the computer lab in the evenings or during the weekend, and many of the participants took this opportunity to improve their acquaintance with electronic-structure calculations. Summarizing our own experience with this workshop, the organizers judge that the selection of participants had resulted in a good mixture of novices and already somewhat experienced researchers in the field. Thus the participants could benefit not only from the lectures and practical sessions, but also from discussions with other participants. The lively discussions at the poster session (35 posters were presented) showed that many participants are already successfully pursuing their own research projects in the field.

4.2.2   Report on the Summer School on NEW MAGNETICS

15-19 September, 2003 Będlewo near Poznań, Poland

Sponsored by
EU RT-Network *Computational Magnetoelectronics*
ESF Working Group *Complex Magnetism and Nanostructures*
the Centre of Exellence *MMMFE*[(*)]
Institute of Molecular Physics of the Polish Academy of Sciences
Committee for Scientific Research

Organized by
Andrzej Jezierski, Andrzej Kowalczyk
Institute of Molecular Physics, Polish Academy of Sciences, Poznań, Poland
Stefan Blügel
Institut für Festkörperforschung, Forschungszentrum Jülich, Germany

The School on *New Magnetics* was organized at Będlewo near Poznań over the week of September 15-19, 2003. 61 participants from 8 countries took part in the Summer School. The nice atmosphere of the conference site stimulated cummunication and a lot of discussions till late in the evening.

The School provided an international forum for the presentation and discussion of state-of-the-art methods, novel ideas and experimental results of new magnetic materials, and to expose graduate students to the field on an educational level. Therefore, the invited lectures were given 90 min of lecturing time to provide detailed information on an level comprehendable for graduate students. The program of the school covered the following topics:
- first-principles investigations of the magnetic nanostructures (J. Hafner)
- nonequilibrium transport in Kondo quantum dots (H. Kroha)
- non-collinear magnetism of complex magnetic materials

(J. Hafner and L.Nordström)
- soft nanocrystalline alloys (J. M. Greneche)
- nanomagnetism investigated by spin polarised scanning tunneling spectroscopy

(R. Wiesendanger, J. Kirschner and S. Blügel)
- relativistic density functional theory (H. Eschrig)
- magnetism of ultrathin layers (K. Baberschke)
- application of SIC-LSD to half-metallic transition metal oxides and f-electron systems (Z. Szotek and W. Temmerman)
- heavy fermion systems (H von Löhneysen)
- magnetic and spectroscopy properties of metal cluster (H. Ebert)
- magnetism in low-dimensional systems (K-H. Mueller and V. Eyert)

- magnetic tunnel junction (F. Petroff)
- transport, magnetic properties and electronic structure of ferromagnetic semiconductors (O. Eriksson and T. Jungwirth)
- electronic structure and magnetic properties of d- and f- electron systems
(A. Ślebarski)

The main objective of the school was to bring together graduate studentes and scientists from the Western, Central and Easter European countries involved in research and application of novel magnetic materials. During the school 10 short (at least 20 min.) oral communications and 20 posters were presented. The Proceedings will be published as a regular issue of the *Molecular Physics Reports.*

Stefan Blügel and Andrzej Jezierski

————————————————————————————————————

SCHEDULE

Sunday, September 14

16.00-18.00 Transportation to Bedlewo and Registration

19.00 Reception and get-together

Monday, September 15

8.50- 9.00 OPENING

Chairman: **W. Temmerman**

9.00-10.30 **J. Hafner** *First-principles investigations of magnetic nanostructures*

10.30-11.00 Coffee

11.00-12.30 **H. Kroha** *Nonlinear transport of electrons and spins in correlated mesoscopic structures*

12.30-13.00 **M. Kosuth** *Electronic, magnetic and transport properties of ferromagnet-semiconductor heterostructure systems*

13.00-14.00 Lunch

Chairman: **J.A. Morkowski**

14.30-16.00 **L. Nordström** *Unconstrained non-collinear calculations of complex magnetic materials*

16.00-16.30 Coffee

16.30-18.00 **J.M. Greneche** *Magnetically soft nanocrystalline alloys*

18.00-18.30 **A. Postnikov** *Ab-initio simulations of molecular magnets*

19.00 Dinner

===

Tuesday, September 16

Chairman: **K.-H. Mueller**

9.00-10.30 **R. Wiesendanger** *Frontiers of nanomagnetism investigated by spin- polarized scanning tunneling spectroscopy*

10.30-11.00 Coffee

11.00-12.30 **H. Eschrig** *Relativistic density functional approach and magnetism*

12.30-13.00 **J. Hafner** *Non-collinear magnetism and phase-stability of Mn*

13.00-14.00 Lunch

Chairman: **R. Wiesendanger**

14.30-16.00 **K. Baberschke** *The magnetism of ultrathin trilayers: A playground to study fundamentals*

16.00-16.30 Coffee

16.30-18.00 **D. Szotek** *SIC-LSD description of half-metallic transition metal oxides*

18.00-18.30 **M. Richter** *Magnetocrystalline anisotropy of strained transition metals and rare-earth intermetallics: density functional calculations*

19.00 Dinner

20.00-22.00 Posters

===

Wednesday, September 17

Chairman: **J. Hafner**

9.00-10.30 **J. Kirschner** *Recent developments in nanoscale magnetism*

10.30-11.00 Coffee

11.00-12.30 **H. von Löhneysen** *Heavy fermion system near a magnetic instability*

12.30-13.00 **M. Przybylski** *Fe-based spin aligners grown on semiconducting substrates*

13.00-14.00 Lunch

Chairman: **H. von Löhneysen**

14.30-16.00 **H. Ebert** *Magnetic and spectroscopy properties of free and supported transition metal clusters*

16.00-16.30 Coffee

16.30-18.00 **K.-H. Mueller** *Magnetism in low-dimensional cuprates*

18.00-18.30 **F. Stobiecki** *Magnetoresistance of $Ni_{80}Fe_{20}/Au/Co/Au$ multilayers*

18.30-19.30 Oral Session (**M. Zwierzycki / J. Dubowik / B. Idzikowski**)

20.00 Banquet

==

Thursday, September 18

Chairman: **H. Eschrig**

9.00-10.30 **S. Blügel** *Magnetism under scanning tunneling microscope*

10.30-11.00 Coffee

11.00-12.30 **W. Temmerman** *Self interaction corrected electronic structure calculations for correlated systems*

12.30-14.00 **V. Eyert** *Ab-initio calculations for low-dimensional magnetic systems*

14.00-15.00 Lunch

Chairman: **K. Baberschke**

15.30-17.00 **F. Petroff** *Magnetic tunnel junctions: review of experimental results and perspective*

17.00-17.30 Coffee

17.30-19.00 **T. Jungwirth** *Transport and magnetic properties of ferromagnetic (III,Mn)V semi-conductors*

19.30 Bonfire

==

Friday, September 19

Chairman: **S. Blügel**

9.00-10.30 **O. Eriksson** *Electronic structure of dilute magnetic semiconductors*

10.30-11.00 Coffee

11.00-12.30 **A. Ślebarski** *Electronic structure and thermodynamical properties of some ternary d and f electron intermetallics*

12.30-13.15 **J.A. Morkowski** *Fast magnon relaxation*

13.15-13.45 **S. Krompiewski** *Ferromagnetically contacted metallic carbon nanotubes with spin-selective interfaces*

14.00-15.00 Lunch

15.00 Excursion

20.00 Dinner

==

NM'03 – INVITED LECTURES

THE MAGNETISM OF ULTRATHIN TRILAYERS: A PLAYGROUND TO STUDY FUNDAMENTALS

Klaus Baberschke

Institut für Experimentalphysik, Freie Universität Berlin, Berlin, Germany

Ferromagnets of few atomic layers only allow to manipulate magnetism as it is not accessible in 3D bulk. Special growth of ultrathin films produces artificial crystallographic structures like tetragonal Ni for which changes of $\approx 0.05 \mathring{A}$ in the geometry enlarge the magnetic anisotropy by $10^2 - 10^3$. For Fe, Co, Ni the Curie-temperatures can be adjusted by varying the number of layers to any value between zero and T_C^{bulk}. In particular we focus on experiments in coupled FM films like Co/Cu/Ni. X-ray magnetic circular dichroism (XMCD) enables us to measure separately T_C^{Ni} and T_C^{Co}. They influence each other dramatically due to enhanced spin fluctuations in 2D [1]. This is a case study which cannot be explained in a mean-field approach of $< S_z >$ but needs higher order contributions of spin dynamics by S^2. With ferromagnetic resonance (FMR) of coupled trilayers we monitor the optical and acoustical modes of the spin waves and determine the interlayer exchange coupling, its strength (eV/particle) and its temperature dependence [2]. From the linewidth we show conclusively that 'non Gilbert-like' damping at interfaces of nanostructures may be dominant. Finally, we discuss the alignment of orbital and spin moment at interfaces, i.e. the brakedown of the third Hund's rule [2].

[1] K. Baberschke and P. Poulopoulos in *Band-Ferromagnetism*, edited by K. Baberschke, M. Donath, W. Nolting (Springer, Berlin 2001), p. 27 and p. 283

[2] J. Lindner et al., Phys. Rev. Lett. **88**, 167206 (2002);

F. Wilhelm et al., Phys. Rev. Lett. **87**, 207202 (2001)

MAGNETISM UNDER THE SCANNING TUNNELING MICROSCOPE

S. Heinze[1], D. Wortmann[2], G. Bihlmayer[2], and S. Blügel[2]

[1] *Institute of Applied Physics, University of Hamburg*
D-20355 Hamburg, Germany
[2] *Institut für Festkörperforschung, Forschungszentrum Jülich*
D-52425 Jülich, Germany

At surfaces one experiences magnetic structures on a wide range of different length scales. These include the microscopic length scale at which magnetic domains form, or mesoscopic length scale determined by nano-patterning or the natural occurance of steps at surfaces and then the atomic length scale of clusters, wires and atomic scale magnetic structures such as for example the antiferromagnetic structure. In this frontier field of nano-magnetism observing and understanding complex magnetic structures is crucial. In the recent years the spin-polarized scanning tunneling microscope (SP-STM) developed to a tool to unravel complex magnetic superstructures on different length scales. For setting a frame of reference, in this lecture we will first present a list of results for atomic scale magnetic structures, give some explanation how to understand those and then we will move to the discussion of the spin-polarized scanning tunnelng microscope. We will extended the model of Tersoff and Hamann to the situation of an STM with a spin-polarized tip with an arbitrary magnetization direction and a sample with an arbritary magnetic structure and discuss the different operation modes of a SP-STM: We show that the spectroscopy mode (SP-STS) is ideal to analyse complex magnetic structures on a mesoscopic length scale created by atomic-scale ferromagnetism and we propose the application of the constant current mode of a SP-STM to the investigation of surfaces of complex atomic-scale magnetic structures of otherwise chemically equivalent atoms. We will discuss several examples. The results presented are obtained within the standard-model for describing magnetic transition metals, which is the density functional theory. The results are obtained with the full-potential linearized augmented plane wave method in the vector-spin density formulation to treat complex non-collinear magnetic structures in low-dimensional systems.

MAGNETIC AND SPECTROSCOPIC PROPERTIES OF FREE AND SUPPORTED TRANSITION METAL CLUSTERS

H. Ebert

Department Chemistry / Physical Chemistry, University of Munich, Germany

Magnetic clusters receive recently a lot of attention in academic but also in technological research. On the one hand side, the interest is caused by the fact that clusters provide a bridge between atoms and bulk material often showing quite peculiar properties. On the other hand, the ongoing need for miniaturizing, in particular in data storage technology, leads to smaller and smaller functional units leading finally to small clusters. The lecture will give an overview on the activities in this rapidly growing field, including free transition metal clusters, that can be seen as reference systems. While a number of experimental results will be presented and discussed in the first part of the lecture, emphasize will be put on concepts and results of theoretical investigations. In particular, it will be demonstrated that theory is able to provide very important and helpful information to understand the various properties of magnetic clusters that in general strongly depend on their composition, size and shape. This applies especially if one considers properties that are caused by spin-orbit coupling as the magnetic anisotropy. Another example is the linear and circular magnetic dichroism showing up in electron spectroscopies that are for that reason very powerful tools to investigate the properties of magnetic clusters.

ELECTRONIC STRUCTURE OF DILUTE MAGNETIC SEMICONDUCTORS

Olle Eriksson

Uppsala University

A brief background to the technological implications of dilute magnetic semiconductors is given after which several materials related issues are discussed for this class of compounds. The focus of the talk will be on electronic structure related phenomena, such as magnetic ordering, critical temperatures and defect formation energies. In addition to commonly discussed dilute magnetic semiconductors (e.g. Mn doped GaAs) several novel materials will be discussed, e.g. Co-oxides that recently have been predicted from first principles theory to be ferromagnetic semiconductors. The results of a newly developed theory for transport properties on magnetic nano-structures will be discussed with focus on spin-filtering applications.

RELATIVISTIC DENSITY FUNCTIONAL APPROACH AND MAGNETISM

H. Eschrig, M. Richter and I. Ophale

IFW Dresden, P.O.Box 27 01 16, D-01171 Dresden, Germany

The derivation of Kohn-Sham-Dirac types of equations is revisited and a number of subtleties is focussed on, including several accuracy issues. A survey over typical relativistic effects in the electronic structure of solids as on the symmetry of the states, effects on valence, binding and on optical properties is given. The interplay of spin-orbit coupling and correlation in the formation of the magnetic ground state of solids without and with an applied magnetic fields is considered in some more detail. An extended version of the presented material including computational details will appear in: H. Eschrig, M. Richter and I. Opahle, Relativistic Solid State Calculations, in: Relativistic Electronic Structure Theory-Part II: Applications, edited by P. Schwerdtfeger, Elsevier, Amsterdam, 2003, Chap. 12.

AB-INITIO CALCULATIONS FOR LOW-DIMENSIONAL MAGNETIC SYSTEMS

Volker Eyert

Institut für Physik, Universität Augsburg, Augsburg, Germany

Low-dimensional physical systems keep on receiving a lot of attention due to the occurrence of fascinating behaviour deviating distinctly from the notions connected with the three-dimensional world. In particular, materials with reduced dimensionality may exhibit new kinds of excitations such as spinons and holons as well as ordering phenomena as, e.g., Peierls transitions and charge density waves. Further interest grows out of the deviations from strict one- or two-dimensionality as arising from interactions between the low-dimensional units. They lead to a range of different coupling strengths and may increase the spectrum of low-temperature phases. Magnetic systems are no exception in this respect but bear the additional attraction of being subject to the Mermin-Wagner theorem, which prohibits long-range magnetic order at finite

temperatures for one- and two-dimensional arrangements of localized magnetic moments. On the experimental side this has motivated the preparation and characterization of magnetic layer materials, chain compounds or spin-ladder systems with localized moments arising from unfilled transition metal or f-electron atoms. Theoretically such compounds have been investigated using first principles methods, model approaches or combinations of boths aiming particularly at an understanding of the coupling mechanisms as well as the long-range ordering of the magnetic moments. In the talk I will illustrate the magnetic properties of low-dimensional systems by considering, in particular, magnetic chain compounds using first principles methods as based on density functional theory. After a short account of the capabilities offered by first principles methods I will discuss the electronic and magnetic properties of a rather new class of magnetic chain compounds, a prototype being the cobaltate $Ca_3Co_2O_6$. All members of this class are characterized by strong interactions between the magnetic ions of each chain across non-magnetic transition-metal atoms. In contrast, the magnetic coupling between different chains is very weak. Forming a triangular lattice, antiferromagnetic interchain coupling as displayed by some of these compounds may give rise to interesting frustration effects and a broad range of different magnetic structures.

NANOCRYSTALLINE ALLOYS: STRUCTURAL ASPECTS AND MAGNETIC PROPERTIES

J.-M. Greneche

Laboratoire de Physique de l'Etat Condens,
UMR CNRS 6087 Universitdu Maine, 72085 Le Mans Cedex 9, France
e-mail : greneche@univ-lemans.fr

Nanocrystalline alloys as Finemet, Nanoperm, and Hitperm, are fascinating systems because of their two phase behaviour. Their structural properties can be thus described by the emergence of crystalline grains in a residual amorphous matrix when a subsequent annealing treatment is applied to the as-quenched precursor alloy. The proportions of those two components are strongly dependent on the annealing temperature but less dependent on the annealing time. Both the structural and magnetic characterization of the nanocrystalline alloys requires the use of different techniques. A large debate occured during the last ten years. During the presentation, a few words will be first devoted to the preparation of those materials and the thermodynamical aspects. Then we concentrate on the structural characterization of both the crystalline grains and the amorphous residual phase, as well as the nature and the role of the interfacial zone which is located between these two components. Then, we discuss the magnetic properties from a macroscopic point of view and also from a local point of view, in order to clarify some concepts and to discuss the role of the amorphous remainder and the intergranular phase on the magnetic properties, as a function of the crystalline fraction. Finally, some perspectives of applications will be reported after reviewing the magnetic performances of the nanocrystalline alloys, in comparison with usual materials.

FIRST-PRINCIPLES INVESTIGATIONS OF MAGNETIC NANOSTRUCTURES

Jürgen Hafner and Daniel Spisak

Institut für Materialphysik and Center for Computational Materials Science
Universität Wien, A-1090 WIEN, Austria

The physics of magnetic nanostructures is of great scientific and technological interest: the magnetic properties of nanostructures are found to be very often drastically different from those of the bulk material, they vary with the dimensionality and the size of the nanostructures. The structural and magnetic characterization of nanostructures in the laboratory turns out to be difficult and almost necessarily in complete. E.g., the total magnetization of a thin films can be measured using magnetic X-ray circular dichroism (MXCD), but layer-resolved information on the magnetic structure of the film is not available. Under these circumstances, theoretical modelling with a predictive capacity is of particular importance.

Ab-initio local-spin-density theory has proved to be an immensly valuable tool for the investigation of the energetics and the geometric, electronic and magnetic properties of nanostructures. In my lecture I shall very briefly outline the foundations of the approach and the capacities and limitations of modern density-functional codes. Applications to nanostructures from 0 to 2 dimensions will be reviewed:

(i) Structural and magnetic properties of metallic clusters, including noncollinear structures.

(ii) Nanowires and nanostripes: Fe-nanowires on stepped Cu-templates, magnetism in nanowires formed by 4d- and 5d-transition metals, striped Fe-phases on reconstructured Ir-surfaces.

(iii) Ultrathin films. Particular attention will be devoted to the correlation between structure and magnetism of ultrathin Fe-films on Cu(100) and Cu(111) films and their correlation with the magnetic properties of alpha- and gamma-Fe.

NONCOLLINEAR MAGNETISM AND PHASE-STABILITY OF Mn

Jürgen Hafner and Daniel Spisak

Institut für Materialphysik and Center for Computational Materials Science
Universität Wien, A-1090 WIEN, Austria

Manganese is probably (except perhaps plutonium) the most complex of all metallic elements. At ambient pressure and low temperatures, the stable phase, alpha-Mn, has a complex body-centred cubic structure with 29 atomsd in the primitive cell. At higher temperatures, Mn undergoes successively structural transformations to a simple cubic (beta-Mn), a face-centred-cubic (gamma-Mn) and a body-centred-cubic (delta-Mn). Under pressure, Mn transforms to a fifth phase which has been tentively described as close-packed hexagonal (epsilon-Mn). Below a Neel temperature of $T_N = 95K$, alpha-Mn transforms to a complex noncollinear antiferro-magnetic structure. The magnetic transition is coupled to a tetragonal distortion of the crystal structure. Beta-Mn has been characterized as a spin-liquid, geometric frustration suppresses magntic ordering down to the lowest temperatures. The remaining three polymorphs also show complex low-spin/high-spin transitions. So far, the explanation of the complex structural and magnetic phase diagram of Mn remained a massive challenge to theory. In this lecture, a first-

principles local-spin-density investigation of noncollinear magnetism and phase stability in Mn will be presented.

TRANSPORT NAD MAGNETIC PROPERTIES OF FERROMAGNETIC (III, MN)V SEMICONDUCTORS

T. Jungwirth

Institute of Physics, Academy of Sciences of the Czech Republic, Prague, Czech Republic

The basic microscopic origins of ferromagnetism in the (III,Mn)As and (III,Mn)Sb compounds appear to be well understood within a model of carrier induced magnetic interactions between Mn local moments. Efficient computation methods have been developed, based on the effective Hamiltonian description of the system, which are able to model their magnetic, transport, and optical properties on a semi-quantitative level. In this presentation we focus on the ferromagnetic transition temperature and remanent magnetization, and discuss also the comparison between theory and experiment for the anisotropic magnetoresistance effects and the anomalous Hall effect. We also discuss a microscopic theory of the Gilbert damping of magnetization precession and the spin-transfer process in diluted magnetic semiconductor heterostructures.

RECENT DEVELOPMENTS IN NANOSCALE MAGNETISM

J. Kirschner [*]

Max-Planck-Institut für Mikrostrukturphysik, Weinberg 2, 06120 Halle, Germany

An actual field of research in magnetism is the analysis of nanostructures. I will report on two lines of development aiming at spatial analysis of nanostructures and at the dynamics of collective excitations at small wavelengths, down to the unit cell at surfaces. Spatial analysis may be obtained by spin-polarized tunneling spectroscopy, if a suitable electronic structure of tip or sample is available. We introduced a more general approach which probes the spin-dependent density of states in the sample, leading to a change in tunneling current upon reversing the tip magnetization. While our previous development was confined to perpendicularly magnetized structures in the sample, we are now able to probe in-plane magnetized domains. This is achieved by using a tip on a disk-shaped electrode which is magnetized along the sample surface. Examples for both approaches are given. The quest for the study of short-wavelength magnetic surface excitations has been long-standing. We report on the development of spin-polarized electron energy loss spectroscopy, by means of which the dispersion relation of surface magnons may be mapped up to the zone boundary. First examples for Co films on Cu(100) are given.

[*] **work done in collaboration with W. Wulfhekel, H. F. Ding, U. Schlickum, R. Vollmer, H. Ibach, A. Kumar, and M. Etzkorn**

NONLINEAR TRANSPORT OF ELECTRONS AND SPINS IN CORRELATED MESOSCOPIC STRUCTURES

H. Kroha

Physikalisches Institut der Universität Bonn, Bonn, Germany

In nanoscopic quantum dots the strong charging energy can induce a local magnetic moment on the dot, and due to the coupling to the leads can lead to dynamical electron and spin correlations, in particular the Kondo effect. Since spectroscopy as well as transport on such systems require in general a finite bias voltage, it is necessary to descibe such correlated systems in a nonequilibrium situation. We describe a newly developed poor mans scaling renormalization group method for Kondo systems at finite bias voltage. Several applications will then be discussed in detail, namely the nonequilibrium quasiparticle distribution in quantum wires with Kondo impurities, including its relevance for the low-temperature dephasing problem and the use of quatum dots in a local magnetic fields as spin filters.

HEAVY-FERMION SYSTEMS AT A MAGNETIC INSTABILITY

H. von Löhneysen

Physikalisches Institut, Universität Karlsruhe, D-76128 Karlsruhe, Germany
and Forschungszentrum Karlsruhe, Institut für Festkörperphysik, D-76021 Karlsruhe, Germany

The groundstate of a number of metals, notably those with strong electronic correlations such as heavy fermion systems or weak itinerant magnets, is in close proximity to a magnetic instability. The transition from a Pauli-paramagnetic to a magnetically ordered state can be tuned by chemical composition, pressure, or magnetic field. Often pronounced deviations from Fermi-liquid behavior are observed in the vicinity of the quantum critical point (QCP) where the magnetic ordering temperature vanishes, which are commonly referred to as non-Fermi-liquid (NFL) behavior.

The scenario of incipient magnetic order is exemplified by $CeCu_6$ with a nonmagnetic ground-state, and long-range incommensurate antiferromagnetism in $CeCu_{6-x}Au_x$ for $x > x_c = 0.1$. The magnetic instability can be tuned by alloying or applying external pressure p. At the QCP, the specific heat C varies as $C/T \sim a ln(T/T_0)$, independent of whether the Néel temperature T_N is tuned to zero by variation of x or p, and one observes a linear resistivity contribution $\Delta\rho \sim T$ [1]. These NFL features can be explained by quasi two-dimensional critical fluctuations, as observed for x = 0.1 with inelastic neutron scattering [2]. In addition, unusual dynamic scaling laws for the dynamical susceptibility are found in the vicinity of the QCP in $CeCu_{6-x}Au_x$ which are incompatible with simple spin-fluctuation scenarios [3].

A particularly clean system where the magnetic order - a long-wavelength incommensurate structure - can be tuned to $T = 0$ by hydrostatic pressure is MnSi. Here an unusual $T^{1.5}$ dependence of the electrical resistivity is observed far beyond the critical pressure [4]. Recent elastic neutron scattering indicate that near the QCP the system becomes orientationally disordered, with some resemblance of liquid crystals [5]. The archetypal weak ferromagnet $ZrZn_2$ has long been considered a candidate for p-wave superconductivity if samples can be made sufficiently pure. We recently found evidence for superconductivity in $ZrZn_2$ single crystals of unprecidented purity [6]. Surprisingly, super-conductivity (with $T_c \approx 0.3K$) exists over the entire pressure range where ferromagnetism exists, and vanishes when ferromagnetism is suppressed at sufficiently high pressure.

[1] H. v. Löhneysen, J. Phys.: Cond. Matt. **8** (1996) 9689-9706

[2] O. Stockert et al., Phys. Rev. Lett. **80** (1998) 5627-5630

[3] A. Schroeder et al., Nature **407** (2000) 351-355

[4] C. Pfleiderer et al., Nature **414** (2001) 427-431

[5] C. Pfleiderer et al., to be published

[6] C. Pfleiderer et al., Nature **412** (2001) 58-61

MAGNETISM IN LOW-DIMENSIONAL CUPRATES

K.-H. Mueller

IFW Dresden, POB 270116, D-01171 Dresden, Germany

The interest in quasi low-dimensional cuprates originated from the discovery of high-Tc superconductors typically consisting of intermediate valence ("doped") copper oxide planes with strongly correlated d-electrons. For understanding the mechanism of superconductivity in these materials their magnetic properties, even in the non-doped state, have to be considered. The magnetism of the cuprates mainly originates from the d-electrons of copper in the oxidation states $Cu^I, Cu^{II} or Cu^{III}$. In an ionic approximation the Cu species are described by charge states, e.g. Cu^{II} by Cu^{2+}. According to this approximation the ground state of Cu^I compounds has no magnetic moment and they exhibit diamagnetism or van Vleck paramagnetism. Cu^{2+} has an odd number of d-electrons resulting in so called Kramers degeneracy. Its paramagnetic moment is well approximated by the spin-only value of 1.73 Bohr magnetons. Depending on its anionic surrounding the paramagnetic moment of Cu^{3+} corresponds to the high-spin value of 2.83 Bohr magnetons (as in K_3CuF_6) or it may be zero (low spin) as usually in cuprates. In the ionic approximation a certain overlap of wave functions results in exchange interactions of the magnetic moments which may lead to antiferromagnetic or ferromagnetic long-range order. In the case of cuprates the dominating type of interaction is superexchange via oxygen anions. In a more realistic description covalence or, more generally, overlapping electron-wave functions combined with electron correlation have to be taken into account in order to explain effects as (i) the existence of well localized magnetic moments (in spite of delocalized wave functions), (ii) the real electric charge of the species usually being much smaller than following from the formal valency, (iii) the metallic or insulating behavior of particular compounds as e.g. $LaCuO_3$ or La_2CuO_4, respectively, and (iv) the special crystallographic structures which in the case of Cu^I compounds usually contain O-Cu-O dumbbells. In most cases the Cu^{II} cuprates contain quasi two-dimensional or quasi one-dimensional networks of CuO_4 plaquettes and they mostly behave like quantum spin-1/2 antiferromagnets of low dimensionality (d = 1 or d = 2). Usually a crossover to three-dimensional behavior occurs in these compounds at sufficiently low temperatures because, actually, they are three-dimensional solids. Ladder compounds are a special interesting group of cuprates. In the ideal case where non-interacting ladders have antiferromagnetic interactions between spin-1/2 sites, with the same strength of the interaction along the rungs and the legs, two types of behavior can be distinguished. Even-leg-ladder compounds reveal a spin gap, resulting in an exponentially vanishing magnetic susceptibility c whereas in the odd-leg-ladder compounds c remains finite for temperature $T \to 0$. This simple picture

becomes more complicated if there are deviations from the ideal cases. In particular phenomena have been observed which can be attributed to crossovers between effective dimensionalities of d = 0, 1, 2, and 3.

UNCONSTRAINED NON-COLLINEAR CALCULATIONS OF COMPLEX MAGNETIC MATERIALS

L. Nordström

Department of Physics, Uppsala University, Uppsala, Sweden

A short review of spin-dependent density functional theory will be given followed by a historic account of the development within applications: collinear, atomic moment based non-collinear, and fully unconstrained non-collinear. After a description of how this can be implemented in a full potential electronic structure method, some examples of applications will be given. These will touch upon e.g. relativistic effects, spin density waves, and spin waves.

MAGNETIC TUNNEL JUNCTIONS REVIEW OF EXPERIMENTAL RESULTS AND PERSPECTIVES

F. Petroff

Unité Mixte de Physique CNRS/Thales, Domaine de Corbeville, 91404 Orsay, France and Université Paris-Sud, 91405 Orsay, France

Stimulated by the discovery of the Giant Magnetoresistance effect [1] in 1988, spin electronics or spintronics has developed into one of the most vigorous field of research in condensed matter physics. One of the areas of considerable interest concerns the research on magnetic tunnel junctions and the associated Spin Dependent Tunneling (SDT) effect reported for the first time at room temperature in 1995 by Moodera et al. [2]. Within a few years, the understanding of the fundamental physics underlying SDT has considerably evolved while important advances towards applications such as magnetic random-access memories were made. After a general introduction on magnetic tunnel junctions, I will review some of the recent experiments performed to identify the relevant parameters driving the SDT effect and discuss its current understanding. Some perspectives and new directions for further research will be discussed at the end of the lecture.

[1] M.N. Baibich et al, Phys. Rev. Lett. **61**, 2472 (1988)

[2] J.S. Moodera et al, Phys. Rev. Lett. **74**, 3273 (1995)

ELECTRONIC STRUCTURE AND THERMODYNAMICAL PROPERTIES OF SOME TERNARY d AND f ELECTRON INTERMETALLICS

A. Ślebarski[a], A. Jezierski[b]

[a]*Institute of Physics, University of Silesia, 40-007 Katowice, Poland*
[b]*Inst. of Molecular Physics, Polish Acad. of Sciences, 60-179 Poznań, Poland*

CeNiSn and CeRhSb exhibit an puzzled ground state in the Kondo lattice. The class of these materials, e.g., "Kondo insulators", is characterized by their electronic properties, which at high temperatures is associated with a set of independent localized 4f moments interacting with the conduction electrons, while at low temperatures the electronic properties resemble those of narrow gap of the order $\approx 10K$. The energy gap is due to the hybridization between the strongly correlated 4f electrons and a conduction band, which is almost half filled. The compounds CeNiSn and CeRhSb are only two in the equiatomic ternary series which show a hybridization gap in the electronic density of states at low temperatures and a paramagnetic ground state. While the Ce-based ternary Sn-compounds are antiferromagnetically ordered (e.g., $CeCuSn, CeAgSn, CePdSn$) the equiatomic antimonides $CeMSb$ (M=Ni, Pd, Pt) are ferromagnets. Recently we have discovered, that the electrical resistivity, magnetic susceptibility and specific heat measurements of $CeRhSn$ have power law with low exponents, characteristic of a non-Fermi liquid ground state. The main goal of this presentation is to find the influence of transition metal M on the coherent gap formation at the Fermi level. We also discuss a similar semiconductor-like resistance anomaly of Fe_2TiSn. Fe_2TiSn reveal the occurence of weak ferromagnetism and heavy fermion-like behavior. A similar feature in the electronic structure and semiconductor-like resistance anomaly have been observed in FeSi and CeNiSn, which both are classified as Kondo insulators.

SIC-LSD DESCRIPTION OF HALF-METALLIC TRANSITION METAL OXIDES

Z. Szotek[1], W.M. Temmerman[1], D. Ködderitzsch[2], A. Svane[3], L. Petit[3], G.M. Stocks[4], W. Hergert[2], and H. Winter[5]

[1] *Daresbury Laboratory, Daresbury, Warrington WA4 4AD, UK*

[2] *Fachbereich Physik, Martin-Luther-Universität Halle-Wittenberg, Friedemann-Bach-Platz 6, D-06099 Halle, Germany*

[3] *Institute of Physsics and Astronomy, Univ. of Aarhus, DK-8000 Aarhus C, Denmark*

[4] *Metals and Ceramics Division, Oak Ridge National Laboratory, Oak Ridge, TN 37830, USA*

[5] *INFP, Forschungszentrum Karlsruhe GmbH, Postfach 3640, D-76021 Karlsruhe, Germany*

In this talk we discuss an application of the self-interaction corrected local spin density approximation (SIC-LSD) to half-metallic transition metal oxides, and among them double perovskites and magnetite (Fe_3O_4). We show that also such simple transition metal monoxides as NiO and MnO can acquire half-metallic characteristics when doped with vacancies. We concentrate on the electronic and magnetic properties of these compounds and in magnetite, in addition, issues of charge order are also thoroughly investigated.

SELF INTERACTION CORRECTED ELECTRONIC STRUCTURE CALCULATIONS FOR CORRELATED SYSTEMS

W. Temmerman, Z. Szotek and M. Lueders

Daresbury Laboratory

A. Svane

Institute of Physics and Astronomy, University of Aarhus

L. Petit

Center for Computational Sciences, Oak Ridge National Laboratory

P. Strange

Department of Physics, University of Keele

A. Ernst

MPI Halle

D. Ködderitzsch

University of Halle

H. Winter

INFP, Forschungszentrum Karlsruhe

An overview is given of applications of SIC-LSD calculations for correlated d and f electron systems. In particular it is shown that SIC-LSD splits d and f bands into a manifold of localized states, occuring well below the bottom of the valence band, and a band-like manifold represented essentially by the LSD potential. This split of the states allows for the introduction of the concept of nominal valence, which is the number of electrons left on the site to participate in band formation. Examples, such as the progression of trivalent to divalent to trivalent to divalent through the rare earth series will demonstrate these concepts. In another example, using Yb compounds, a comparison will be made with a semi-phenomelogical method of calculating valences. Applications to actinides and actinide compounds such as PuO_2 will be presented as well as some selected applications to d electron systems, namely $YBa_2Cu_3O_7$ and $La_{0.7}Sr_{0.3}MnO_3$. Finally we remark that SIC-LSD is a scheme well suited to describe static correlations when the electrons are well localized. A road map will be presented how to incorporate dynamic correlations.

FRONTIERS OF NANOMAGNETISM INVESTIGATED BY SPIN-POLARIZED SCANNING TUNNELING SPECTROSCOPY

Roland Wiesendanger

Institute of Applied Physics and Microstructure Adv. Research Center Hamburg (MARCH)
University of Hamburg, Jungiusstr. 11, D-20355 Hamburg, Germany
http://www.nanoscience.de, wiesendanger@physnet.uni-hamburg.de

In order to probe and tailor magnetic properties at the spatial limit we have combined the scanning tunneling microscope (STM) with spin-sensitivity [1-3]. This is achieved by the use of ferro- [4,5] and antiferromagnetically [6,7] coated probe tips offering a high degree of spin-polarization of the electronic states involved in the tunneling process. Magnetic domain imaging with sub-nanometer-scale spatial resolution has been demonstrated for magnetic transition metal [8,9] as well as rare earth metal films [10,11]. Ultra-sharp domain walls were discovered in ultra-thin iron films [12] while for ferromagnetic [13] and antiferromagnetic [14] samples, the different

magnitude or orientation of magnetic moments could directly be made visible at the atomic level.

The phenomenon of magnetic hysteresis was observed for the first time at the single- digit nanometer length scale and has directly been correlated with microscopic processes of domain nucleation and domain wall motion [15]. We also studied magnetic vortex structures in mesoscopic-scale ferromagnetic systems which are of relevance for current developments in MRAM technology [7]. Magnetic switching phenomena of nano-scale magnetic islands and nanoparticles were studied by time-dependent spin-sensitive STM imaging [16]. It will be shown that granular thin films exhibit a complex magnetic switching behaviour due to the statistical distribution of grain sizes, grain shapes and inter-grain spacings.

Finally, we will discuss the application of spin-sensitive STM measurements to individual atoms and molecules on magnetic substrates [17]. In particular, we will show that both the orbital symmetry as well as the spin character of electronic scattering states around single atomic impurities can be determined from real-space spin-sensitive STM data.

References:

a) Recent review articles:

[1] R. Wiesendanger, Current Opinion in Solid State and Materials Science **4**, 435 (1999): *Surface magnetism at the nanometer and atomic scale.*

[2] R. Wiesendanger and M. Bode, Solid State Commun. **119**, 341 (2001): *Nano- and atomic-scale magnetism studied by spin-polarized scanning tunnelling microscopy and spectroscopy.*

[3] M. Bode and R. Wiesendanger, in: Magnetic Microscopy of Nanostructures (eds. H. Hopster and H.P. Oepen), Springer, Berlin, Heidelberg (2003): *Spin-Polarized Scanning Tunneling Spectroscopy.*

b) Original articles:

[4] R. Wiesendanger, H.-J. Güntherodt, G. Güntherodt, R.J. Gambino, and R. Ruf, Phys. Rev. Lett. **65**, 247 (1990): *Observation of vacuum tunnelling of spin-polarized electrons with the scanning tunnelling microscope.*

[5] M. Bode, O. Pietzsch, A. Kubetzka, S. Heinze, and R. Wiesendanger, Phys. Rev. Lett. **86**, 2142 (2001): *Experimental evidence for intra-atomic non-collinear magnetism at thin film probe tips.*

[6] A. Kubetzka, M. Bode, O. Pietzsch, and R. Wiesendanger, Phys. Rev. Lett. **88**, 057201 (2002): *Spin-polarized scanning tunnelling microscopy with antiferromagnetic probe tips.*

[7] A. Wachowiak, J. Wiebe, M. Bode, O. Pietzsch, M. Morgenstern, and R. Wiesendanger, Science **298**, 577 (2002): *Internal spin structure of magnetic vortex cores observed by spin-polarized scanning tunneling microscopy.*

[8] O. Pietzsch, A. Kubetzka, M. Bode. and R. Wiesendanger, Phys. Rev. Lett. **84**, 5212 (2000): *Real-space observation of dipolar antiferromagnetism in magnetic nanowires by spin-polarized scanning tunneling spectroscopy.*

[9] M. Kleiber, M. Bode, R. Ravli and R. Wiesendanger, Phys. Rev. Lett. **85**, 4606 (2000):

Topology-induced spin frustrations at the Cr(001) surface studied by spin-polarized scanning tunneling spectroscopy.

[10] M. Bode, M. Getzlaff, and R. Wiesendanger, Phys. Rev. Lett. **81**, 4256 (1998): *Spin-polarized vacuum tunneling into the exchange-split surface state of Gd(0001).*

[11] M. Bode, M. Getzlaff, A. Kubetzka, R. Pascal, O. Pietzsch, and R. Wiesendanger, Phys. Rev. Lett. **83**, 3017 (1999): *Temperature-dependent exchange splitting of a surface state on a local-moment magnet: Tb(0001).*

[12] M. Pratzer, H.J. Elmers, M. Bode, O. Pietzsch, A. Kubetzka, and R. Wiesendanger, Phys. Rev. Lett. **87**, 127201 (2001): *Atomic-scale magnetic domain walls in quasi-one-dimensional Fe nanostripes.*

[13] R. Wiesendanger, I.V. Shvets, D. Bürgler, G. Tarrach, H.-J. Güntherodt, J.M.D. Coey, and S. Graeser, Science **255**, 583 (1992): *Topographic and magnetic-sensitive scanning tunnelling microscopy study of magnetite.*

[14] S. Heinze, M. Bode, O. Pietzsch, A. Kubetzka, X. Nie, S. Blügel, and R. Wiesendanger, Science **288**, 1805 (2000): *Real-space imaging of two-dimensional antiferromagnetism on the atomic scale.*

[15] O. Pietzsch, A. Kubetzka, M. Bode, and R. Wiesendanger, Science **292**, 2053 (2001): *Magnetization reversal of Fe nanowires studied by spin-polarized scanning tunnelling spectroscopy.*

[16] M. Bode, O. Pietzsch, A. Kubetzka, and R. Wiesendanger, submitted to Nature: *Shape dependent thermal switching behavior of superparamagnetic nanoislands.*

[17] K. von Bergmann, M. Bode, A. Kubetzka, M. Heide, S. Blügel, and R. Wiesendanger, submitted to Phys. Rev. Lett.: *Spin-polarized electron scattering at single oxygen adsorbates on a magnetic surface.*

NM'03 – ORAL PRESENTATIONS

TEMPERATURE DEPENDENCE OF FMR LINEWIDTH AND FIELD-SHIFT IN EXCHANGE-BIASED BILAYERS

J. Dubowik[a], I. Gościańska[b], A. Paetzold[c], and K. Röll[c]

[a]Institute of Molecular Physics, P.A.Sci, Smoluchowskiego 17, 60-179 Poznań, Poland,
[b]Dept. of Physics, A. Mickiewicz Univ., Umułtowska 85, 61-613 Poznań, Poland,
[c]Department of Physics, Kassel University, H. Plett Str. 40, 34132 Kassel, Germany

Thin ferromagnetic films (FM) in contact with suitably prepared antiferromagnets (AF) can exhibit a hysteresis loop shifted along the field axis. This effect of so-called exchange bias has been found to be practical in various GMR structures (e.g. spin valves). However, many of its aspects including spin dynamics still remain to be resolved. Here results are reported of a detailed investigation of ferromagnetic resonance (FMR) in exchange-biased NiFe/NiO bilayers obtained by sputtering. A striking temperature dependence of negative and nearly isotropic field shift for both in-plane and perpendicular directions of the applied field is accompanied

with pronounced maxima in temperature dependence of FMR linewidth at $\sim 150K$, well below the Neel temperature of NiO. The same structures without any exchange-bias exhibit no such behavior and can serve as reference samples of the "free" FM thin films. It enables us to distinguish spin dynamics phenomena related exclusively to FM/AF interactions. Our results are compared with previous experimental FMR [1-3] and Brillouin light scattering [4] data on various FM/AF structures and suggest that spin dynamics (spin wave damping and anomalous field shift) in the FM/AF structures can be described in a consistent way by a single mechanism of the so-called slow-relaxation [5].

[1] P. Lubitz et al., J. Appl. Phys. **89** (2001) 6901

[2] M. Rubinstein et al., J. Magn. Magn. Mater. **210** (2000) 329

[3] M. Pechan et al., Phys. Rev. B **65** (2002) 064410

[4] W. S. Lew et al., J. Appl. Phys. **89** (2001) 7654

[5] see for example R. W. Teale in *"Physics of magnetic garnets"*, ed. A. Paoletti, North-Holland 1978

MAGNETIC BEHAVIOUR OF CUBIC $(FeNi)_{23}B_6$ PHASE EMBEDDED IN AMORPHOUS MATRIX

<u>B. Idzikowski</u>[a], A. Szajek[a] and J.-M. Greneche[b]

[a] *Institute of Molecular Physics, Polish Academy of Sciences, M. Smoluchowskiego 17, 61-179 Poznań, Poland*

[b] *Laboratoire de Physique de L'Etat Condensé, UMR CNRS 6087, Faculté des Sciences, Université du Maine, 72085 Le Mans, Cedex 9, France*

Due to the magnetic exchange interactions nanocrystalline systems consisting of soft magnetic phase placed in amorphous matrix can reveal a smooth magnetization curve near zero field with extremely small coercive force. Nickel-rich amorphous precursors with chemical composition of $Ni_{64}Fe_{16}Zr_7B_{12}Au_1$ were produced by melt-spinning technique and then heat-treated at temperatures ranged from $420°C$ to $600°C$ for one hour to form nanostructure. The transformation from the amorphous state into the nanocrystalline state was investigated by the DSC, XRD, VSM and Mössbauer techniques. The annealing favours the emergence of cubic $Fe_xNi_{23-x}B_6$ crystalline grains (10-25 nm in diameter), as it was identified by XRD measurements. Magnetic measurements made at 4.2-1100 K reveal rather high value of saturation magnetisation (nearly 60 and 40 Am^2/kg at 4.2 K and room temperature, respectively) in amorphous as well in nanocrystalline states. Those facts are consistent with 300K ^{57}Fe Mössbauer results which are well supported by the calculations of Fe and Ni magnetic moments in not substituted $Ni_{23}B_6$ and $Fe_{23}B_6$ phases, using the spin polarized tight binding linear muffin-tin orbital (TB-LMTO) method. The magnetic moments on Fe and Ni atoms in $Fe_{23}B_6$ and $Ni_{23}B_6$ compounds depend on their local environments. The iron magnetic moments are enhanced up to about $3\mu_B/atom$ and for nickel reduced, even to zero. The present study will be continued for $(Fe_{1-x}Ni_x)_{23}B_6$ systems to establish dependence of magnetization on concentration of Ni impurities and their site

preference. After annealing ribbons became extremely magnetically soft and in a nanocrystalline state show also good mechanical properties, as compared with the FINEMET, NANOPERM or HITPERM. An improved magnetic properties and reduced brittleness of the samples offer attractive possibilities for applications of this novel Ni-rich alloy.

ELECTRONIC, MAGNETIC AND TRANSPORT PROPERTIES OF FERROMAGNET-SEMICONDUCTOR HETEROSTRUCTURE SYSTEMS

Michal Kosuth, **Voicu Popescu, Hubert Ebert**

Department Chemistry / Physical Chemistry University of Munich, Germany

Magneto-electronics receives a lot of interest, because this research field of applied solid state physics allows one to extent the potential of electronic devices by exploiting the spin of the electrons. A very promising effect is the tunneling magnetoresistance (TMR) that denotes the observation that the tunneling current across a tunneling barrier that separates two magnetic layers depends on the relative orientation of the magnetisation of these layers. This effect could be demonstrated several years ago for a ferromagnet-insulator-ferromagnet (FM-I-FM) layer system and first prototypes of a dynamic storage chip could be presented recently. Devices based on ferromagnet-semiconductor-ferromagnet (FM-SC-FM) heterostructures seem to have several advantages compared to insulator-based tunneling junctions. The lecture will give an overview of the achievements in this area. Several examples of experimental results dealing with the magnetic properties of FM-SC systems at the interface and dealing with the spin-polarised injection will be mentioned. Most emphasis, however, will be on theoretical investigations on FM-SC heterostructure systems. The attempt of giving an explanation for the magnetic and transport properties will be followed. Correct treatment of the spin-orbit coupling leads to the possibility of calculating the magneto-crystalline anisotropy and its influence on spin-dependent transport. It will be shown that the magnetic anisotropy strongly depends on the geometry of the interface and correlates with the anisotropy of the orbital moments.

FERROMAGNETICALLY CONTACTED METALLIC CARBON NANOTUBES WITH SPIN-SELECTIVE INTERFACES

S. Krompiewski

Institute of Molecular Physics, Polish Academy of Sciences, M. Smoluchowskiego 17, 60-179 Poznań, Poland

Spin-dependent transport through single-wall armchair carbon nanotubes (SWCNT) is studied theoretically within the single-band tight-binding model, by means of the Green's function partitioning technique. The emphasis is put on the effect of an extra magnetic monolayer at the electrodes on electrical conductance and giant magnetoresistance (GMR). In order to meet the charge neutrality requirement - the so-called extended molecule concept has been used. It has

been shown that in the case when the monolayers have got enhanced magnetic moments and are antiferromagnetically exchange-coupled to the electrodes, the GMR value can approach 100%, i.e. both the spin-dependent conductance channels may become blocked in the anti-aligned electrodes configuration. A remarkable feature of the conductance spectra is that they reveal to a large degree the "finger prints" of the SWCNTs. In particular, the conductance spectra peaks are separated from one another roughly as in isolated nanotubes. It has been also shown that the GMR-effect is very sensitive to the relative band line-up of electrodes and nanotubes, what on the one hand explains a poor reproducibility of experimental results, and on the other hand makes it possible to control the GMR with a gate voltage.

FAST MAGNON RELAXATION

J.A. Morkowski

Institute of Molecular Physics, Polish Academy of Sciences, Poznań, Poland

Magnon relaxation times are usually calculated by solving linearized Boltzmann-type equation for magnon occupation numbers. If in the initial state the occupation number of a particular magnon mode is high, non-linear terms in the Boltzmann equation strongly enhance the short-time relaxation rate for that magnon mode. The problem will be discussed in details for a case of three-magnon confluence processes for degenerate magnon spectrum. The same qualitative features characterize higher order relaxation processes like the four-magnon ones.

AB INITIO SIMULATIONS OF MOLECULAR MAGNETS

Andrei Postnikov

*Universität Osnabrück – Fachbereich Physik, D-49069 Osnabrück, Germany*

A remarkable increase in the number of studies on molecular magnetic systems during the last decade is clearly related to the progress in chemistry of such systems. Different families of molecular magnets have been synthesized, their crystal structure determined, their magnetic properties analyzed.

For the theory, such systems provide an interesting playground accessible from the side of model systems ("exact" diagonalisation within, e.g., Heisenberg model), as well as from the side of of quantitative calculation from first principles. The shortcomings of these two approaches are the neglect of true chemical environment and bonding (in the models) and probably insufficient, or not accurate enough, incorporation of correlation effects (in the density functional theory-related schemes). The chemical complexity of molecular magnets precluded so far their "straightforward" simulation in a calculation approaches of superior accuracy, like quantum Monte Carlo. Therefore it is not *a priori* clear to which extent one or other of "ideologies" now in use will be more valid, or useful – whether an overlap will take place in describing the relevant physics from different point of view, or a gap in between would still leave some essential features unexplored. After a brief introduction to the experimental evidence and the progress with the Heisenberg model for such systems, I'll discuss in detail the situation with

density functional calculations. Here one must note that the advent of molecular magnets did not necessarily demand for the development of essentially new calculation schemes, so that a decades-long progress in quantum-mechanical study of small clusters and molecules could be made use of, and extrapolated further, with the natural rise in computer power. However, molecular magnets turn out to be hard cases for computational treatment – for different reasons in different established calculation approaches.

The openness of crystal structure demands for one or another "full-potential" formalism, leaving traditional muffin-tin- or atomic sphere approximation-based tools out of the market. The presence of transition metals and/or other constituents with important deep semicore states creates problems for pseudopotential planewave methods. Moreover, the need for a large (albeit largely empty) "simulation box" around a molecule makes planewave-related methods expensive. An abundance of hydrogen and hence strong disbalance in atom "sizes" makes it hard for linearized augmented plane wave scheme. The often unusual chemical composition reduces the usefulness of *a priori* tuned basis sets in those tight-binding-type methods which heavily depend on pre-adjusted basis functions for their efficiency. Simultaneously, the options to treat non-collinear spin-density distribution and to have accurate forces on atoms for studying structure relaxation and dynamics may be advantageous and sometimes necessary. As a consequence, flexible, efficient and accurate methods (and codes) are in the demand, of which several have been successfully applied to systems of reasonable complexity. After an overview of situation in this field, a detailed analysis will be given of our recent results.

As an example of a system of practical interest we consider hexanuclear "ferric wheel" $LiFe_6[N(CH_2CH_2O)_3]_6Cl$ (see figure) synthesized at the Institut für Organische Chemie in Erlangen [1], along with other systems with differently bonded Fe atoms. The calculation have been done by the SIESTA method [2], which employs density functional theory and numerical basis orbitals. A large number of electronic states within narrow energy interval and the effective lack of useful crystal symmetry results in a strong nearly-degeneracy of electronic states in the vicinity of the band gap (or, of the Fermi level). This makes the convergence of electronic structure calculation extremely difficult. The imposition of a fixed spin moment constraint help however to improve convergence by suppressing electron density fluctuations between two spin channels.
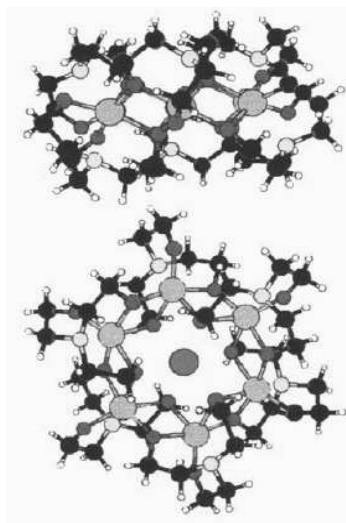
According to both local density (LDA) and generalized gradient (GGA) approximations, local magnetic moments of 4 μ_B persist on Fe sites irrespectively of actual magnetic arrangement – ferromagnetic, inverted spin on one or several atoms, or interchanging antiferromagnetic ordering in the ring, the latter (correctly) turning out to be the ground state. It became commonplace to refer to "ferric wheels" and other related systems as those with $S=5/2$ per Fe atom, on the basis of magnetization measurements, whence the chemical state Fe^{3+} is derived. The calculations indicate that the situation is more complicated than that. In particular, Fe $3d$ states are *not* fully localized but participate in a covalent bonding with neighbouring oxygen atoms (that holds the molecule together). Whereas majority-spin $3d$ states of Fe are fully occupied, minority-spin subband is not empty but contains about one electron on the Fe-O bonds. The description of electronic structure as obtained in the calculation (also, the absence of clearly Fe^{3+} behaviour) is consistent with available experimental data from photoemission and soft X-ray emission.

The magnetic polarization of the triethanolamin group hosting each Fe atom, however, amounts to 1 μ_B, and the resulting spin of, indeed, $S=5/2$, albeit delocalized, behaves nevertheless as a rigid one, experiencing a reversal when a magnetic configuration changes. This behaviour maps well onto the Heisenberg model and allows to estimate exchange parameters from total energies of different magnetic configurations. The estimates of about -80 K are of correct sign and order, but somehow larger magnitude than those derived from neutron scattering data [3]. An inclusion of local correlation effects within the LDA+U scheme or similar doesn't seem probable to change the situation qualitatively, but would tend to reduce the interaction parameters, as the band gap gets larger.

References

[1] R. W. Saalfrank *el al.*, Angew. Chem. **109** (1997) 2596.

[2] J. M. Soler *et al.*, J. Phys. Cond. Matter **14** (2002) 2745.

[3] O. Waldmann *el al.*, Inorg. Chem. **38** (1999) 5879.

Fe-BASED SPIN ALIGNERS GROWN ON SEMICONDUCTING SUBSTRATES

Marek Przybylski

Max-Planck-Institut für Mikrostrukturphysik, Weinberg 2, 06120 Halle, Germany and Solid State Physics Department, Faculty of Physics and Nuclear Technics, AGH University of Science and Technology, Mickiewicza 30, 30-059 Krakow, Poland

The possibility of realizing devices by exploiting the electrons property of possessing a spin has captured physicist attention since the past decade. A variety of Fe-based multilayer structures for a magnetic recording or exchange-biased media have been grown, mostly on MgO substrates. From the point of view of magneto-electronics applications it is preferable to combine the structure with a semiconducting substrate. Recently, an attempt has been made to avoid the formation of "magnetically dead layers" in Fe films epitaxially grown on a number of semiconductors. A variety of phenomena observed for Fe-based spin aligners grown on an atomically flat (4x6)-like reconstructed GaAs(001) surface is reviewed. Antiferromagnetically(AFM)-coupled Fe/Cr/Fe trilayers, epitaxially grown on GaAs(001), reflect magnetic anisotropy of the

GaAs(001)/Fe system characterized by uniaxial anisotropy of the easy-axis of magnetization along the [110] direction. This allows growth of an artificial "layered antiferromagnet" exhibiting uniaxial magnetic anisotropy with minimal material and technological complexities. When such a $(Fe/Cr/Fe)_{AFM}$ structure is completed by another Fe layer separated with another Cr-spacer, the low field magnetization signal from the $(Fe/Cr/Fe)_{AFM}/Cr/Fe$ sample corresponds to the top Fe layer only. A strong increase of coercivity is found at low temperatures and $90°$ interface coupling is detected. In the case of $(Fe/Cr/Fe)_{AFM}$ trilayers of different thickness of the Fe layers, "reversed" minor ellipticity loops are measured with longitudinal MOKE. This behavior is interpreted by depth variation of the MOKE sensitivity. Theoretical work predicts that efficiency of the spin injection from a ferromagnet into a semiconductor can be improved for electrons created by tunneling, since such a process is not affected by the conductivity mismatch and results in conservation of the spin polarization. For single-crystalline Fe/MgO/Fe junctions grown on GaAs(001), magnetization of one of the Fe electrodes is pinned by its AFM-coupling to another Fe layer $((Fe/Cr/Fe)_{AFM})$ over a field range controlled by the thickness relation between both Fe layers in the $(Fe/Cr/Fe)_{AFM}$ structure. Another approach for the independent magnetization switching is realized by differing coercivity of the Fe layers. The coercivity of the top Fe electrode can be increased due to crystallographic defects created e.g. by covering with Ni. We have shown that the interlayer coupling between the Fe electrodes is weak for MgO thicknesses down to about 4ML. It is difficult to reach a structure quality sufficient to detect a pure AFM-exchange interaction expected for the interlayer coupling across a non-metallic spacer. Regardless of the preparation conditions, below 2.5ML of MgO the coupling is dominated by pinholes and "orange peel" effect. Magnetic systems exhibiting perpendicular anisotropy are of particular interest for a potential perpendicular emission of circularly polarized photons resulting from spin injection and electron-hole recombination in a semiconductor. For this purpose, ultrathin Ni films were grown on GaAs(001). Deposition of about 1ML of Fe on the top of GaAs(001)/Ni recovers the LEED pattern which is not visible after deposition of several ML of Ni . The Ni/Fe system exhibits out-of-plane magnetization at low temperature. Another approach for perpendicular magnetization is realized via growth of the L10 ordered alloys by alternating deposition of Fe and Au (or Pt) atomic layers on top of the Au (or Pt) buffer layer.

MAGNETOCRYSTALLINE ANISOTROPY OF STRAINED TRANSITION METALS AND RARE-EARTH INTERMETALLICS: DENSITY FUNCTIONAL CALCULATIONS

Manuel Richter

Dept. of Theoretical Solid State Physics, IFW Dresden, P.O. Box 270016, D-01171 Dresden, Germany

The magnetocrystalline anisotropy (MA) energies of strained hcp Fe and Co, bct Fe, RCo_5 (R = Y, La, Pr, Nd, Sm, Gd) and R_2T_{17} (R = Y, Sm; T = Fe, Co) have been determined by means of relativistic density functional calculations, including orbital polarization corrections. The obtained MA energies agree well with available experimental data. They are found to be strongly affected by changes of the lattice geometry (c/a ratio and volume) and substitutions, as a consequence of band structure and band filling effects.

MAGNETORESISTANCE OF Ni-Fe/Au/Co/Au MULTILAYERS

F. Stobiecki[a], **B. Szymański**[a], **T. Luciński**[a], **J. Dubowik**[a], **M. Urbaniak**[a], and **K. Roell**[b]

[a] *Institute of Molecular Physics, PAS, Smoluchowskiego 17, 60-179 Poznań, Poland*
[b] *Department of Physics, Kassel University, H. Plett Str. 49, 34132 Kassel, Germany*

For particular applications different magnetoresistive elements, i.e., sensors with required R(H) dependence are necessary. Therefore, a large number of artificial thin film structures have been investigated. In result structures such as spin-valves (applied as read heads) or pseudo-spin-valves (optimal for RAM memory cells) were elaborated. For all these structures the giant magnetoresistance (GMR) effect is accompanied by switching from antiparallel to parallel magnetization configuration in ferromagnetic layers. In this contribution the investigations concerning the new type of layered structures, characterized by alternating out-of-plane and in-plane magnetization configurations in ferromagnetic layers in the remanence state, will be demonstrated. To realize such structures the set of $(Py/Au/Co/Au)_{15}$ (Py = Permalloy = $Ni_{83}Fe_{17}$) multilayers were deposited on glass substrates using the UHV magnetron sputtering. Permalloy and Co were chosen since Py posses a pronounced in-plane anisotropy whereas thin Co layers sandwiched between Au have a strong perpendicular anisotropy [1-3]. The exemplary VSM hysteresis loops and GMR(H) (GMR(H) = 100%[R(H)-R(2T)]/R(2T); R(H) and R(2T) are the resistance at magnetic field H and $H = 2T$) dependences are shown in Fig.1. For a thickness of gold layers $t_{Au} > 1.5nm$ the magnetization reversals of the Co and Py layers are independent (the layers are almost completely decoupled) and can be easily recognized in hysteresis loops measured for magnetic field applied in-plane ($H_{\parallel}$) and perpendicular to the plane ($H_{\perp}$) (Fig. 1 a, b). The central portions of hysteresis loops for $H_{\parallel}$ and $H_{\perp}$ correspond to Py and Co reversal, respectively. Neglecting the range of small fields, the magnetization of Py (Co) layer always points in the field direction for $H_{\parallel}$ ($H_{\perp}$) and only magnetization of Co (Py) layer rotates from the perpendicular (in-plane) to the field direction. Thus, the changes of $cos\phi(H)$ (ϕ is the angle between magnetization directions of Py and Co layers) and in consequence the changes of GMR(H) are only related to magnetization reversal of one layer, namely Py for $H_{\perp}$ or Co for $H_{\parallel}$. Due to the uniaxial perpendicular anisotropy of Co layers and in-plane shape anisotropy of Py layers linear GMR(H) dependences are observed both for $H_{\parallel}$ and $H_{\perp}$ (Fig. 1 c, d). This behavior of investigated structures can be applied for quantitative measurements of magnetic field.
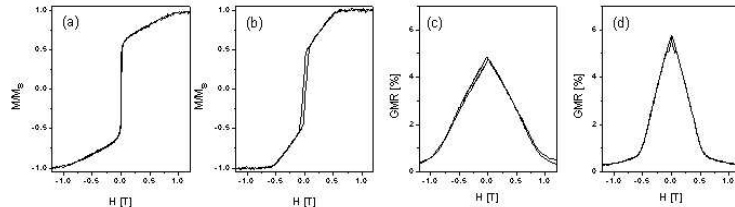

Fig. 1. Hysteresis loops (a, b) and magnetoresistance curves (c, d) of $(Ni_{83}Fe_{17} - 2nm/Au - 3nm/Co - 0.6nm/Au - 3nm)_{15}$ multilayers measured for magnetic field applied in plane $H_{\parallel}$ (a, c) and perpendicular to sample plane $H_{\perp}$ (b, d), respectively.

To optimize the structure and to determine the influence of the thickness (t) of particular layers on GMR(H) dependences the following series of samples were studied:

i) $(Py - 2nm/Au - 3nm/Co - t_{Co}/Au - 3nm)_{15}(0.2 \leq t_{Co} \leq 1.5nm)$,

ii) $(Py - 2nm/Au - t_{Au}/Co - 0.6nm/Au - t_{Au})_{15}(0.5 \leq tAu \leq 3nm)$,

iii) $(Py - t_{Py}/Au - 2nm/Co - 0.6nm/Au - 2nm)_{15}(1 \leq t_{Py} \leq 4nm)$.

The results concerning GMR values as a function of cobalt, gold and Permalloy thickness are demonstrated in Fig. 2 and can be summarized as follows:

• GMR(t_{Co}) (Fig. 2a) - the optimal thickness of Co layers lies in the range $0.4 \leq t_{Co} \leq 1.2nm$, i.e., in the range assuring perpendicular anisotropy and continuous structure of Co layers.

• GMR(t_{Au}) (Fig. 2b) - for $t_{Au} \leq 1.25nm$ the GMR effect strongly decrease due to increasing ferromagnetic coupling between Co and Py layers (in consequence $\phi < \pi/2 at H = 0$), the slow decrease of GMR for $t_{Au} \geq 1.5nm$ is related to the increasing scattering of conduction electrons and to increasing shunting of the curent in Au layers [4].

• GMR(t_{Py}) (Fig. 2c) - the dependence shows a weak maximum for $t_{Py} \approx 3nm$ typical of all GMR structures containing Py [4, 5].
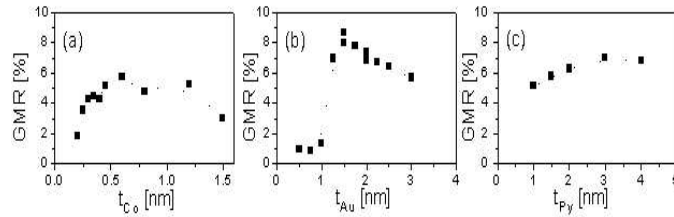

Fig. 2. GMR value of $(Py/1Au/Co/Au)_{15}$ multilayers as a function of cobalt (a), gold (b) and Permalloy (c) layers thickness.

Finally, it should be noted that for the investigated structures the saturation fields of GMR($H_\perp$) and GMR($H_\parallel$) dependences can be tuned by varying thickness of Py and Co layers, respectively. For appropriate layers thickness the magnetoresistance response of the structure can be nearly isotropic (Fig. 3).
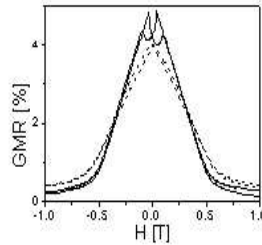

Fig. 3. GMR(H) dependence of $(Py - 2nm/Au - 3nm/Co - 0.8nm/Au - 3nm)_{15}$ for magnetic field applied in-plane (dash line) and perpendicular to the plane.

[1] C. Chappert et al., Phys. Rev. B **34** (1986) 3192.

[2] J. Dubowik et al., phys. stat. sol. (a) **196** (2003) 41.

[3] F. Stobiecki et al., J. Magn. Magn. Mater. **239** (2002) 276.

[4] B. Dieny, J. Magn. Magn. Mater. 136 (1994) 335.

[5] T. Luciski et al. J. Magn. Magn. Mater. **174** (1997) 192.

LARGE INTERFACE SCATTERING FROM FIRST PRINCIPLES

M. Zwierzycki[1,4], M. Talanana[1], K. Xia[5], P.J.Kelly[1], G.E.W. Bauer[2]

[1] *University of Twente, Enschede, The Netherlands*
[2] *Delft University of Technology, The Netherlands*
[4] *Institute of Molecular Physics, Poznan, Poland*
[5] *State Key Laboratory for Surface Physics, Beijing , China*

The open 3d shells of the transition metal atoms used to make magnetic multilayers give rise to complex band structures which have to be taken into account in any quantitative estimation of the interface scattering whose spin-dependence determines the remarkable transport properties of these structures. Using the TB-LMTO surface Green's function method we study a number of metallic and hybrid (metal/semiconductor) interfaces and interpret their transmittivity in terms of the electronic structures of the component materials. The efficiency of the TB-LMTO method allows us to treat disordered layers using large lateral supercells and allows us to unravel the contribution of various factors to the final transmission.

NM'03 – POSTERS

MÖSSBAUER EFFECT STUDY OF ATOMIC DISORDER IN Fe_2TiSn ALLOY

J.E. Frąckowiak, J. Deniszczyk

Institute of Physics and Chemistry of Metals, Silesian University 40-007 Katowice, Bankowa 12, Poland

The recent discovery of Fe_2TiSn alloy has simulated a renewal of interest in studying the effect of the local environment on the electronic and magnetic properties of the Heusler-type compounds. It was shown that Fe_2TiSn alloy belongs to the group of system in which the weakly ferromagnetic and probably heavy fermion behavior is induced by atomic disorder [1-3]. The abnormal change of the slope in the experimental lattice parameter a is observed at 240 K [1]. This anomalies provide evidence of an isostructural phase transition which could be created by an atomic disorder. The band structure calculation [4] predicts that the substitution of Fe atoms onto titanium or tin position in $L2_1$ structure leads to an occurence of magnetic moment in Fe_2TiSn alloy.

The aim of present study was to investigate an effect of local atomic disorder in Fe_2TiSn alloy on the hyperfine parameters of ^{57}Fe and ^{119}Sn nuclei by Mössbauer spectroscopy. An Fe_2TiSn ingot was prepared by arc melting the constituent metals on the water-cooled copper hearth in a high-purity argon atmosphere. The sample was annealed at 1073 K for 10 hours and then

quenched in water. The iron and tin Mössbauer spectra was recorded from 80 to 300 K in a Nitrogen Liquide cryostat. The stability of the sample temperature was about 0.5 K. The Mössbauer spectra were fitted with a least-squares method program using the Gauss-Legendre technique for evaluation of the transmission integral. The direct evidence for crystallographic disorder on an atomic scale comes from Mössbauer measurements. A single broad and asymmetric absorption lines are observed both for Fe and Sn nucleus in the investigated range of temperature. An analysis shows that to fit the ^{57}Fe spectra at least the one magnetic component (sextuplet) and the one paramagnetic component (single line) is required. Figure 1 presents the temperature dependence of the ^{57}Fe isomer shift, IS, for magnetic (M) and paramagnetic (P) components.

The observed at 240 K drop in ISP curve provide evidence of a phase transition in the paramagnetic phase. The ^{119}Sn Mössbauer spectra of Fe_2TiSn measured at room temperature in a longitudinal field of 0.25 T show a Zeeman splitting with the value of magnetic field about 32 kGs. The experimental hyperfine parameters are compared with theoretical ones resulted from the band structure calculation using TB-LMTO method.

References

1. A. Ślebarski, M.B. Maple, E.J. Freeman, C. Sirvent, D. Tworuszka, M. Orzechowska, A. Wrona, A. Jezierski, S. Chiuzbaian, M. Neumann, Phys. Rev. B **62** (2000) 3296.

2. A. Ślebarski, A. Wrona, T. Zawada, A. Jezierski, A. Zygmunt, K. Szot, S. Chiuzbaian, M. Neumann, Phys. Rev. B **65** (2002) 144430.

3. S.V. Dordevic, D.N. Basov, A. lebarski, M.B. Maple, L. Degiorgi, Phys. Rev. B **66** (2002) 75122.

4. A. Jezierski, A. Ślebarski, J. Magn. Magn. Mater. **223** (2001) 33.
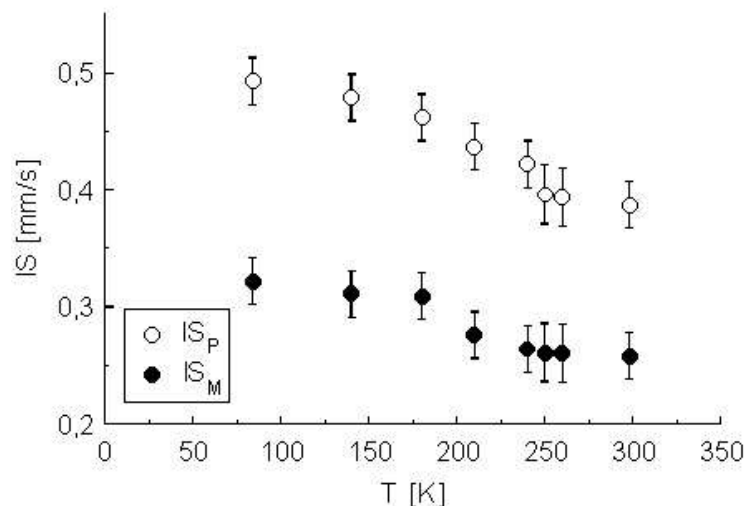
Fig. 1. The temperature dependence of the ^{57}Fe isomer shift for Fe_2TiSn alloy.

EFFECT OF THE LOCAL ENVIRONMENT ON THE ELECTRONIC AND

MAGNETIC PROPERTIES OF $Fe_{3-x}Cr_xAl$ AND $Fe_{3-x}Cr_xSi$

A. Go[a], M. Pugaczowa-Michalska[b] L. Dobrzyński[a,c]

[a]*Institute of Experimental Physics, University of Białystok, Lipowa 41, 15-424 Białystok, Poland*
[b]*Institute of Molecular Physics, Polish Academy of Science, Smoluchowskiego 17, 60-179 Poznań, Poland*
[c]*The Soltan Institute for Nuclear Studies, 05-400 Otwock-Świerk, Poland*

Fe_3Si and Fe_3Al alloys doped with transition metal atoms were investigated many times by different experimental and theoretical techniques. Both Fe_3Si and Fe_3Al crystallise in DO_3-type structure (Fig.1). This structure can be interpreted as four interpenetrating f.c.c. Baravais lattices translated by (1/4,1/4,1/4) vector and abbreviated A, B, C and D. In the perfectly ordered compound aluminium or silicon atoms occupy D positions. There are two non-equivalent types of iron in (A,C) position and in B position. One of them - (A,C) position has eight Fe nearest neighbour in an octahedral configuration, the second one - B site - is surrounded by four Fe and four Si or Al atoms. Transition metal atoms preferentially occupy one type of these sites, depending of their positions in the periodic table of elements. Atoms of elements that are placed on the left-hand side of iron preferentially locate at B-sites, however, atoms which are on the right side of iron demonstrate strong preference for (A,C) positions in DO_3-type structure.
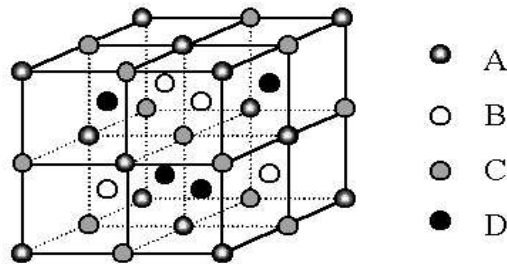

Fig.1. The DO_3-type structure.

The aim of paper is to investigate an influence of the local surrounding of iron on its magnetic moment, hyperfine field and density of states in compounds where iron is substituted by chromium. The chromium concentration in both of alloys changes in range from x=0 to x=0.5. In order to test the influence of the local environment on electronic and magnetic properties in $Fe_{3-x}Cr_xAl$ and $Fe_{3-x}Cr_xSi$ magnetic contribution of all possible configurations in the nearest neighbour's shell for Fe(A,C) and Fe(B) sites are analysed. The presence of chromium atom in the nearest neighbourhood causes strong decrease of the magnetic moment and hyperfine field on iron. The total magnetic moments as well as the magnetic moments of chromium and iron decrease almost linearly with the concentration of chromium in considered alloys. The relationship between magnetic moments and hyperfine fields intensities is studied in detail.

The electronic structure and magnetic properties are calculated method within the framework of the local spin density approximation (LDA) by the spin-polarised self-consistent tight-binding

linearized muffin-tin orbital method (TB-LMTO) in the atomic sphere approximation (ASA) for the experimental values. In present calculation the supercell structure with 32 atoms in the cell was used. The supercell structure can be divided into 32 simple cubic sublattices. Eight of them are occupied by Si or Al atoms (D positions), whereas Fe and Cr randomly occupy the remaining sublattices (A, B, C positions).

SINGLE-ION ANISOTROPY EFFECTS IN THE SUPRAMOLECULAR ASSEMBLY Ni_{12}

Monika Haglauer[1], Grzegorz Kamieniarz[1], Alvaro Caramico D'Auria[2] and Filippo Esposito[2]

[1] *Computational Physics Division, Institute of Physics, A. Mickiewicz University, ul.Umultowska 85, 61-614 Poznań, Poland* [2] *Dipartimento di Scienze Fisiche, Universita di Napoli "Federico II", Piazzale Tecchio, 80125 Napoli and INFM Unita di Napoli, Italy*

gjk@amu.edu.pl (G. Kamieniarz) and filesp@na.infn.it (F. Esposito)

The $Ni_{12}(O_2CMe)_{12}(chp)_{12}(H_2O)_6(THF)_6$ cluster [1] (Ni_{12} in short) is a dodecanuclear metallocyclic complex containing a ring of twelve S=1 Ni ions bridged by intersecting Ni_2O_2 rings. Such clusters are not subject to significant intermolecular interactions. Measurements of the effective magnetic moment for T>4.2 K and a subsequent approximate analysis, have shown that the magnetic properties of Ni_{12} can be explained by a ferromagnetic coupling inside the ring, estimated as J=13.5 K [1].

Characterization of polynuclear magnetic aggregates remains a challenging task. They have well defined molecular weights and crystal structures [2], allowing quantitative comparison of experimental results with theory. Unlike other assemblies of small magnetic particles with size and/or shape distributions, a typical sample of a molecular magnetic compound is composed of nominally identical non-interacting magnets with a unique set of chemically determined parameters. They are complex organometallic systems, too difficult to approach by the *ab initio* methods applicable to simple metal clusters.

To characterize the Ni_{12} cluster, we consider the spin S=1 rings in the framework of the Heisenberg model with the earlier neglected single-ion anisotropy [3] and we apply the diagonalization method exploiting the point-group symmetry. Our diagonalization method, implements the idea of applying the corresponding shift operator to take into account the translational (or rotational) symmetry. This idea and the group-theory arguments enable an effective coding to be achieved and provide a reduction of the corresponding invariant subspaces, even in the presence of anisotropy for the rings size N=12, so that the numerical diagonalization of the Hamiltonian describing Ni_{12} can be accomplished.

We calculate the corresponding energy spectra, and discuss, using the perturbative calculations, the level crossing in the presence of the applied field. A comparison with the experimental data is also performed [3].

References

[1] Blake A.J., Grant C.M., Parsons S., Rawson J.M. and Winpenny R.E.P. 1994 *J. Chem. Soc.*,

Chem. Commun. 2363

[2] Gatteschi D., Caneschi A., Pardi L. and Sessoli R. 1994 *Science* **265** 1054

[3] Kamieniarz G., Matysiak R., Caramico D'Auria, Esposito F. and Benelli C. 2001 *Eur. Phys. J.* B **23**, 183-189

LARGE $CeCu_2Si_2$ SINGLE CRYSTALS FOR MAGNETIC NEUTRON SCATTERING

H. S. Jeevan[1], M. Deppe[1], O. Stockert[1], E. Faulhaber[2] and C. Geibel[1]

[1] *Max-Planck-Inst. for Chem. Physics of Solids, Nothnitzer Str, 40, 01187 Dresden, Germany*
[2] *TU Dresden, IAPD, D-01062 Dresden, Germany*

The discovery of superconductivity in $CeCu_2Si_2$ in 1979 opened the field of unconventional superconductivity in strongly correlated systems. Later on, another unconventional phase, the A-phase, of presumably magnetic character was found to compete with the superconducting phase in $CeCu_2Si_2$. Despite more than 20 years of intensive research, the nature of the superconducting phase and of the A-phase as well as the interaction between both are very far from being understood. A major problem is the lack of large single crystals with well defined physical properties. This prevents e.g. a study of the magnetic structure and magnetic excitations of this compound with neutron scattering, which would allow a much deeper insight into the nature of these unconventional phases. Thus despite several attempts, no magnetic Bragg peaks could yet be observed for the unconventional A-phase. The main problem in obtaining large single crystals of $CeCu_2Si_2$ with well defined physical properties is the peritectic formation of this compound, and the extreme sensitivity of its physical properties to tiny changes in the composition. We have grown large single crystals of $CeCu_2Si_2$ using a self flux method in oxide crucibles. The structure of the single crystals, their composition and their physical properties were investigated by XR-diffraction, microprobe and resistivity as well as specific heat measurements, respectively. We observed correlations between growth parameters, composition of the single crystals, and their physical properties. By tuning the growth parameters, we could grow large ($\sim 1cm^3$) single crystals of $CeCu_2Si_2$ showing either a stable A-phase ground state, a stable superconducting ground state or a competition between both phases. With these single crystals, we were now able to detect the magnetic Bragg peaks of the A-phase in pure $CeCu_2Si_2$. This shall allow a detailed study of this unconventional magnetic phase and of its interaction with the superconducting state.

MAGNETISM AND BAND STRUCTURE OF Co/Ti MULTILAYERS

Andrzej Jezierski and Piotr Napierała

Institute of Molecular Physics, Polish Academy of Sciences, Poznań, Poland

An effect of local atomic disorder on the electronic structure and magnetic moments in $Co_{1-x}Ti_x$ systems is studied by ab-initio methods. Co-Ti alloys belong to the group of the systems in which the magnetic properties dependent strongly on the distribution of atoms in the cell. The band

structure is calculated by the spin-polarised TB LMTO and SPR-KKR-CPA methods. The Co and Ti atoms are distributed in the different crystallographic structures (fcc, hcp, bcc and $L2_1$). We studied the change of the electronic structure of CoTi during the transformation from fcc to bcc structure(Bain path). We found the dependence of the total energy on the ratio of c/a . For BCC structure(c/a=1) energy was the highest and the lowest energy was obtained for FCC structure (c/a=1.41). For each crystallographic structure the electronic and magnetic properties were calculated for the different distributions of Co and Ti atoms in unit cell. The calculations indicate that that magnetic moment of Co decreases about 50% near Ti layer. The density of states on the Fermi level in Co-Ti systems strongly depends on the concentration of Co atoms, as well on the distribution of Co and Ti atoms in the unit cell for the given concentration.
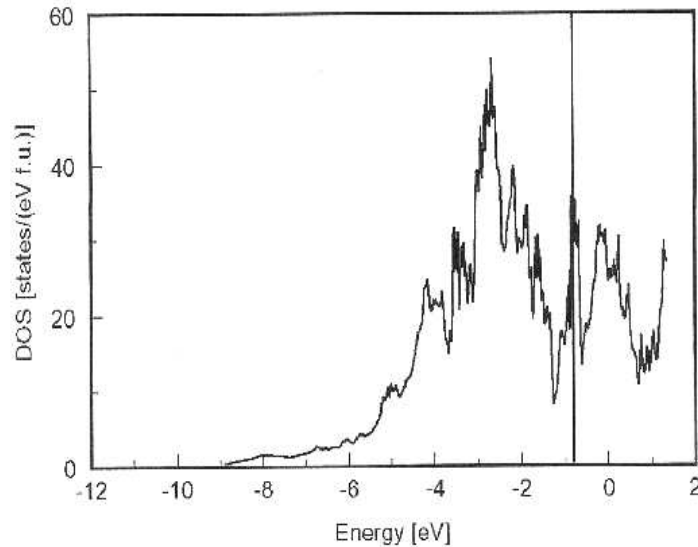
The figure presents the total density of states for $Co_{0.62}Ti_{0.38}$ in $L2_1$ type structure.

AB-INITIO CALCULATIONS OF THE PROPERTIES OF THE HEUSLER ALLOY NiMnSb

Marjana Ležaić, Gustav Bihlmayer, and Stefan Blügel

IFF, Forschungszentrum Jülich, D-52425 Jülich, Germany

Spin-gap materials, presenting 100% spin polarisation at the Fermi level, are presently receiving much of attention because of their potential use in spintronics devices. A class of such materials are the Heusler alloys. Here we present a theoretical study of the Heusler alloy NiMnSb. In particular, we show the complex band structure as a tool for understanding of surface and interface states, and we calculate the properties of the interface with InP. We investigate the influence of the spin-orbit interaction in bulk and at the surfaces. Finally, we calculate the Curie temperature using frozen magnon excitations.

ANTIFERROMAGNETIC EXCHANGE COUPLING IN $FeSi_xFe_{1-X}$ MULTILAYERS

T. Luciński[a], **P. Wandziuk**[a,b], **M. Urbaniak**[a], **B. Andrzejewski**[a]

[a]*Institute of Molecular Physics, PAS, M. Smoluchowskiego 17, 60-179 Poznań, Poland*
[b]*Poznań University of Technology, Nieszawska 13A, 60-965 Poznań, Poland*

Metal-semiconductor multilayers (Mls) are extensively studied because of their potential application in electronics. Recently the investigations have been focused on Fe/Si/Fe coupled heterostructures since they show a very strong antiferromagnetic (AF) interlayer coupling [1]. In spite of many efforts, the origin of the interlayer coupling in Fe/Si system has not been clarified [2-5]. Moreover, it is not well understood how the iron-silicides formation affects the interlayer coupling. Therefore the information about the spacer layer composition and its correlation with magnetic properties of this system is of particular interest.

The $[Fe(3nm)/Si_xFe_{1-x}(dS)]*15$ multilayers, (where Si_xFe_{1-x} alloys for x=1, 0.66, 0.5 and 0.4 simulate Si and $FeSi_2$, $FeSi$, Fe_5Si_3 iron-silicide phases, respectively and dS denotes the spacer layer thickness) were deposited in UHV by d.c. magnetron sputtering at room temperature onto oxidized Si wafers. The crystalline structure of our samples and their multilayer periodicity were examined using the high- and small-angle X-ray diffraction, respectively. Magnetization measurements were performed in the as-deposited state and after sequential annealing at $100°C$ and $220°C$ as a function of temperature ranging from 4.2 K to 300 K.

We have found that the spacer layer with $Si_{40}Fe_{60}$ composition is ferromagnetic at room temperature leading to direct ferromagnetic coupling between Fe layers in $Fe/Si_{40}Fe_{60}$ multilayers (Fig. 1a). The strongest antiferromagnetic coupling $J = -1.94mJ/m^2$ accompanied by saturation field of HS=1.51 T has been found for Fe/Si multilayers with dSi=1.4 nm. We have found (Fig.1a) that both saturation field and so-called FAF parameter (FAF=1-MR/MS, where MR and MS denote remanent and saturation magnetizations, respectively) decline when x decreases. Figure 1b shows that for all examined Fe/Si_xFe_{1-x} multilayers (except $Fe/Si_{40}Fe_{60}$ Mls) only a single saturation field maximum versus spacer layer thickness has been observed however, its position moved toward the thicker spacer layer with decreasing x. Above the HS(dS) maximum for thicker spacer layer its values was found to decay exponentially. The reduction of FAF parameter (FAF indicates fraction of the Ml which is antiferromagneticaly coupled) and HS values below the HS(dS) maximum points out that the neighboring Fe layers become gradually connected through pinholes. It was confirmed by FAF and HS temperature measurements which showed that FAF(T), of the samples with dS representing HS maximum, always decreases with decreasing temperature in spite of continuous HS(T) improvement.

Above results may suggest that the appearance of the observed HS maximum versus spacer layer thickness is not due to RKKY-like coupling mechanism. The observed non-oscillatory but exponentially decaying saturation field values seems to correspond rather to the quantum interference model of exchange coupling [6]. Comparing the results obtained for Fe/Si, $Fe/Si_{66}Fe_{33}$ and $Fe/Si_{50}Fe_{50}$ multilayers we may conclude that for certain dS range the $Si, Si_{66}Fe_{33}$ and $Si_{50}Fe_{50}$ spacer layers mediate antiferromagnetic coupling in $(Fe/Si_xFe_{1-x})*15$ multilayers however, the coupling energy is distinctly stronger for nominally pure Si spacer layer.

[1] R. R. Gareev, D. E. Buergler, M. Buchmeyer, R. Schreiber,and P. Grünberg, J. Magn. Magn. Mater. **240**, 235 (2002)

[2] S. Toscano, B. Briner, H. Hopster, M. Landolt, J. Magn. Magn. Mater. **114**, L6 (1992)

[3] M. Xiao, Z. Li, Phys. Rev. B **54**, 3322 (1996)

[4] E. F. Fullerton, S. D. Bader, Phys. Rev. B **53**, 5112 (1996)

[5] K. Inomata, K. Yusu, Y. Saito, Phys. Rev. Lett. **74**, 1863 (1995
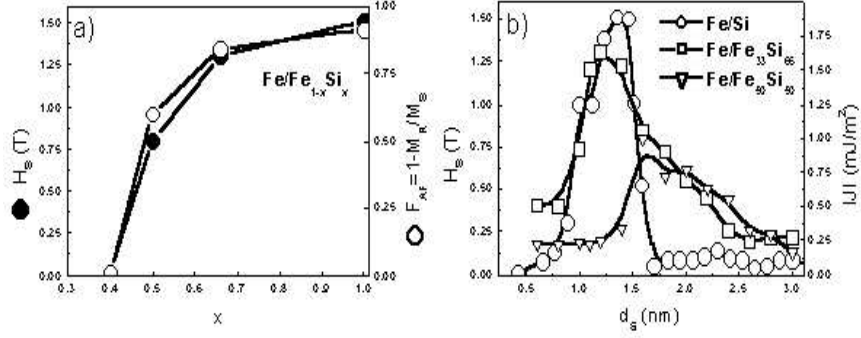
[6] P. Bruno, J. Appl. Phys. **76** 6972 (1994)

Figure 1. Spacer layer composition dependence of the saturation field HS and FAF parameter (a), and the values of HS and coupling energy J versus spacer layer thickness dS for different x in Fe/Si_xFe_{1-x} multilayers (b).

INTERFACE-LOCALIZED MODE AND CRITICAL ANGLE EFFECT IN FMR SPECTRUM OF EXCHANGE-COUPLED BILAYER FILMS

S. MAMICA and H. PUSZKARSKI

Surface Physics Division, Faculty of Physics, Adam Mickiewicz

University,
61-614 Poznań, Umultowska 85, Poland

From the experimental viewpoint, a characteristic feature of ferromagnetic resonance (FMR) in bilayer films is that some specimens show single resonance, whereas others show double resonance. Double resonance can exhibit a regular pattern in which the high-field (HF) line intensity surpasses that of the low-field (LF) line, or it can exhibit an *inverted* pattern with the HF line less intense than the LF line. There is a general agreement that the inverted FMR pattern occurs when the HF line is an 'optic mode', *i.e.* an out-of-phase composition of individual sublayer modes, and the LF line is an 'acoustic mode', or an in-phase mode composition. The existing theoretical explanations of bilayer ferromagnetic resonance are, as a rule, based on phenomenological equation of motion of the magnetization. In this work, we propose a theory of FMR in bilayer film based on an entirely microscopic approach, using the Heisenberg model of localized spins and assuming that the two ferromagnetic sublayers are exchange-coupled through their interface; both the strength and the sign of this interface coupling (J_{int}) is arbitrary (we admit ferromagnetic or antiferromagnetic interface coupling). The Hamiltonian contains an

exchange energy and a Zeeman energy terms; the external field is assumed to be applied obliquely to the film surface. We focus on the effects originating in the interface coupling, though the system is assumed to exhibit also *pinning* effects originating from surface anisotropy on the outer surfaces of the film as well as from intrinsic interface anisotropy present on internal interfaces. The latter is assumed to consist of two components, corresponding to uni-directional ($\vec{K}_{int}$) and uni-axial (D_{int}) anisotropies. We show that the resonance spectrum in symmetric bilayer is completely independent of J_{int}, but depends strongly on the applied static field configuration with respect to the interface normal (angle θ). A critical angle θ_{crit} is found to exist (as in the case of single-layer film) for which the multipeak spectrum reduces to a single-peak spectrum. By applying this rigorous microscopic FMR theory we do show that the inverted pattern of the bilayer FMR spectrum can also be explained if the HF line is assumed to correspond to an *in-phase mode, but of interface-localized nature.* Then, its intensity decreases with growing strength of its localization on the interface and, when the localization becomes sufficiently strong, the intensity of the localized mode becomes lower than that of the other mode (which is of the bulk type). This gives a possibility to explore the HF resonance line corresponding to the interface-localized mode as a potential source of information concerning the bilayer interface.

THEORY OF MAGNETOSTATIC MODES IN THIN PLATES

M. Krawczyk[1], H. Puszkarski[1], S. Mamica[1] and J.-C.S. Lévy[2]

[1] *1Surface Physics Division, Faculty of Physics, A. Mickiewicz University, ul. Umultowska 85, 61-614 Poznan, Poland*
[2] *LPTMC, case 7020, EA 2382 and Pole MPQ FDR CNRS 2437, Université Paris 7 Denis Diderot, 2 Place Jussieu, 75251 Paris cedex 05, France*

The dipolar field static and dynamic components are calculated in thin plates in saturating field applied parallel or perpendicularly to the sample surface. Lattice sums, a generalization of the sums used in theoretical treatment of infinite samples with short-range interactions, are calculated numerically, and found to be in good agreement with our analytical approximations proposed for a confined system. The equations of motion are derived for a system with pure dipolar interactions, and magnetostatic modes propagating perpendicularly to the sample surfaces are calculated. The corresponding frequency spectra and mode profiles are computed numerically with emphasis laid on size effects. The lowest-frequency modes, exhibiting typical antiferromagnetic profile, are identified as surface-localized modes. The profiles of the highest-frequency modes are found to be close to the uniform mode profile. These results are compared with available recent experimental ferromagnetic measurements [1,2] reporting the observation of resonance spectra with well-resolved magnetostatic modes. Consequences for the magnetic reversal dynamics will be discussed as well.

[1] M. Pardavi-Horvath et al. J. Appl. Phys. **87** (2000) 4969. [2] S. Tamaru et al. J. Appl. Phys. **91** (2002) 8034.

HALF-METALLIC ZINC-BLENDE COMPOUNDS AND MULTILAYERS WITH SEMICONDUCTORS

Ph. Mavropoulos, I. Galanakis, and P. H. Dederichs

IFF, Forschungszentrum Jülich, D-52425 Jülich, Germany

Zinc-blende compounds of transition elements with group-V and VI elements, such as CrAs, have been reported to be half-metallic with high Curie temperature. They represent the concentrated limit of magnetic semiconductors. The fabrication of such materials and their multilayers with semiconductors has also been reported [1] In a recent paper [2] we made an extensive theoretical study of the bulk of such materials and found that the half-metallic property depends on the lattice constant. We have identified systems which have equilibrium lattice constants close to the ones of semiconductors, and which are also half-metallic in these lattice constants. In this way we propose possible half-metal semiconductor combinations for coherent growth with small lattice mismatch. These are VAs/GaAs, VSb/InAs, VSb/GaSb, CrAs/GaAs, CrSb/InAs, CrSb/GaSb, MnSb/GaSb. We also extend our calculations to the case of the (001) multilayers CrAs/GaAs, CrSb/InAs, CrAs/ZnSe and CrSb/ZnTe. We find that half-metallicity can be preserved throughout the multilayers.

[1] H. Akinaga *et al.*, Jpn. J. Appl. Phys. **39**, L1118 (2000);

[2] I. Galanakis and Ph. Mavropoulos, Phys. Rev. B **67**, 104417 (2003).

ELECTRONIC STRUCTURE, MAGNETISM AND HYPERFINE PARAMETERS OF $Fe_{3-x}Ti_xAl(0 \leq x \leq 1)$ ALLOYS

T. Michalecki, J. Deniszczyk, J.E Frąckowiak

Institute of Physics and Chemistry of Metals, University of Silesia 40-007 Katowice, Bankowa 12, Poland

In the last decade several representatives of the ternary transition metal intermetallics with the Heusler-type crystal structure have been widely investigated with the aim of explaining the origin of their anomalous heavy-fermion-like behavior. It was discovered that in Heusler compounds $Fe_{2+x}V_{1-x}M(M = Al, Ga, Si)$ the semiconductor-like resistivity behavior accompanies the large value of the low temperature electronic specific coefficient g and the presence of the clear Fermi cutoff in the XPS spectra [1,2]. We did not find detailed information on the properties of $Fe_{2+x}Ti_{1-x}Al$ while the much less anomalous resistivity behavior has been reported for $Fe_{2+x}Ti_{1-x}M(M = Ga, Si)$ [2].

Electronic structure calculations for $Fe_{2+x}V_{1-x}M(M = Al, Ga)$ with low concentration of anti-site defects (Fe at V position - x=0.06, 0.12, and V at Fe position - x=-0.06) have shown that the both types of the anti-site defects give rise to the narrow bands (of d character) located near the Fermi energy (where in the stochiometric Heusler Fe_2VM compounds the quasi gap forms) which may response for the anomalous properties of these compounds [3,4].

The aim of the presented study was to investigate an effect of the alloying on the electronic structure, magnetic and hyperfine properties of Heusler type $Fe_{3-x}Ti_xAl$ alloys. The band structure calculations were performed with the use of the tight-binding linearised muffin tin orbital method in the spin-polarised mode (the spin-orbit interaction was not taken into account). The calculations predict the magnetic ground-state of the Heusler Fe_2TiAl with the half-metallic

density of states (DOS) in the vicinity of Fermi level (ε_F). As Fig. 1 shows, the DOS near ε_F has the quasi-gap in the majority spin channel. The minority spin DOS quasi-gap is shifted above ε_F. For the purpose of the alloying simulations we have performed the calculations with the use of the super-cell including eight formula units. For Ti concentrations x=0, 0.25, 0.5, 0.625, 0.75, 0.875, 1 different configurations of the Fe atoms were tested and the site preference have been established. For each preferred energetically configuration the volume optimization have been done. Figure 2 presents the concentration dependence of the average hyperfine field ($< B_{hf} >$) and related total magnetic moment (per formula unit). The magnetic moment is on the decrease with concentration similar to $< B_{hf} >$. The strong magnetic moment for Heusler concentration Fe_2TiAl is carried by iron atoms.

The calculated hyperfine parameters and their concentration dependence are in good agreement with that resulted from the Mössbauer spectroscopy [5].
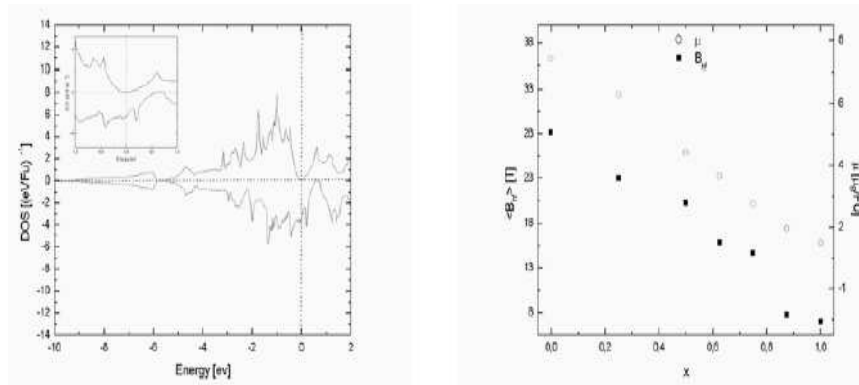

Fig. 1 Total DOS in Fe_2TiAl obtainetd from TB-LMTO calculation. In the insert the total DOS in the vicinity of ε_F is shown.

Fig. 2 Total magnetic moment and the average hyperfine field on Ti concentration (x) for $Fe_{3-x}Ti_xAl$ **References**

[1] M. Kato, Y. Nishino, U. Mizutani, S. Asano, J. Phys.: Condens Matter, **12**, 1769 (2000).

[2] W. Zarek, E. Talik, J. Heimann, M. Kulpa, A. Winiarska, M. Neumann, J. Alloys Comp., **297**, 53 (2000), and references therein.

[3] J. Deniszczyk, Acta Phys. Pol., **B32**, 529 (2001),

[4] J. Deniszczyk, W. Borgieł, phys. stat. sol. (a) **196**, 236-239 (2003).

[5] K. Brząkalik, J.E Frąckowiak, Nukleonika (2003) in press

XPS SPECTRA, ELECTRONIC STRUCTURE AND ELECTRICAL RESISTIVITY OF YNi_4B COMPOUND

M. Pugaczowa-Michalska[1,*], G. Chełkowska[2], T. Toliński[1] and A. Kowalczyk[1]

[1] *Institute of Molecular Physics, Polish Academy of Sciences, Smoluchowskiego 17, 60-179 Poznań, Poland*

[2] *Institute of Physics, Silesian University, Uniwersytecka 4, 40-007 Katowice, Poland*

The electronic structure of the ternary YNi_4B compound, crystallizing in the hexagonal $CeCo_4B$ structure (P_6/mmm space group), was studied by X-ray photoelectron spectroscopy (XPS) and ab-initio calculations. Core levels and the valence band were investigated. The XPS valence band is compared with that obtained from ab-initio calculations. The valence band spectrum at the Fermi level exhibits the domination of the Ni(3d) states, which are hybridized with 4d states of Y and 2p states of B. The total, partial density of states of YNi4B, obtained from electronic structure calculations, reveal the hybridisation d states of Ni with d-states of Y and p-states of B. The self?consistent electronic structure calculations were performed for the experimental lattice constant and for the lattice parameter estimated from the minimum of the total energy. The equilibrium lattice parameters are $a = 5.143\mathring{A}$ and $c = 7.165\mathring{A}$. The theoretical values of lattice parameters are about 3.13% higher than the experimental ones. The calculated electronic specific heat coefficient g derived from $N(E_F)$ is about $11.33mJ/molK^2$ for experimental lattice parameters. The calculated bulk modulus is $B_0 = 1.61632Mbar$. The temperature dependence of electrical resistivity can be described using the modified Bloch-Grüneisen relation. The r(T) curve above the transition temperature can be well fitted using the modified Bloch-Grüneisen relation. The experimental Debye temperature θ_D is 240 K is in good agreement with calculated value ($\theta_D = 273K$).

CRYSTALLOCHEMICAL AND MAGNETIC BEHAVIOUR OF $Sc(FeAl)_{12}$ SAMPLES BY POWDER DIFFRACTION AND MÖSSBAUER TECHNIQUES

K. Rećko[a]**, K. Szymański**[a]**, L. Dobrzyński**[a,b]**, D. Satuł**[a]** and B.C. Hauback**[c]**, W. Suski**[d,e]**, B. Yu. Kotur**[f]

[a] *Institute of Experimental Physics, Univ. of Białystok, Lipowa 41, 15-424 Białystok, Poland*
[b] *The Soltan Institute for Nuclear Studies, 05-400 Otwock-Świerk, Poland*
[c] *Dept. of Physics, Institute for Energy Technology, P.O. Box 40, N-2027 Kjeller, Norway*
[d] *W. Trzebiatowski Institute of Low Temperature and Structure Research, PAS, P.O. Box 1410, 50-950 Wrocław 2, Poland*
[e] *International Lab. of High Magnetic Fields and Low Temperatures, ul. Gajowicka 95, 53-421 Wrocław, Poland*
[f] *Department of Inorganic Chemistry, L'viv State University, bul. Kirila i Mefodiya 6, L'viv 290005, Ukraine*

Chemical ordering and magnetic properties of $ScFe_4Al_8$, $ScFe_5A_{l7}$ and $ScFe_6A_{l6}$ powder samples are presented. These alloys have been measured by means of powder diffraction techniques, namely X-ray and thermal neutron one, conventional Mössbauer effect (ME) method as well as by Monochromatic Circularly Polarized Mössbauer Source (MCPMS). X-ray and neutron powder patterns allowed to determine crystallochemical structure of $Sc(FeAl)_{12}$ alloys with symmetry $I/4mmm$, isostructural with $ThMn_{12}$ - type of structure. Our earlier studies carried out on crystal and magnetic structures of $(U,Th)(FeAl)_{12}$ intermetallic compounds [1-2] indicated large crystallochemical similarity in both series of actinide's alloys. In the case of scandium samples this rule was broken. The latter turned out to exhibit new type of precipitations appearing during annealing procedure as well as a new kind of disordering within their lattices. In the case of scandium alloys the extra phases disclosed much lower symmetry than the ones,

mainly cubic FeAl-type, appearing in U- or Th-samples. In addition, the a-f disordering in the basic phase was observed which contrasts with previously investigated samples where typically f-j disordering took place.

On the magnetic side, with increasing iron content the isostructural UFe_xAl_{12-x} alloys [1-2] exhibited the transition from spin-canted system for x = 4, with the antiferromagnetic interactions as a dominant ones, to the ferromagnetic ordering for x = 6. In the case of $ThFe_4Al_8$ sample in which only iron atoms were responsible for magnetism, the incommensurate magnetic structure was discovered [3]. The same situation was found in scandium sample with x = 4. We note that the magnetic behaviour of $ScFe_4Al_8$ raised already some controversies in the literature [4-5]. The published results indicated presence of a spin glass state or a mixture of antiferromagnetic structure and spin glass. Our unpolarized neutron diffraction pattern, however, leaves no doubts that the modulated magnetic structure is observed in the $ScFe_4Al_8$ compound. The interpretation of the neutron data requires presence of non-zero magnetic propagation vector different from the nuclear one. The iron magnetic moments of $ScFe_4Al_8$ sample create spiral structure with spins rotated in a plane parallel to the wave vector $q = (q_x, q_x, 0)$, with $q_x = 0.136(2)$ which is temperature independent up to 175 K. The value of iron magnetic moment at 8 K is close to 1.08(12) μ_B. The basic magnetic cell has to be purely antiferromagnetic with iron spins directed along a or b axis and rotated in the basal plane by 49(1)0 from cell to cell. The antiferromagnetic nature of $ScFe_4Al_8$ is fully confirmed by Mössbauer measurements. All Mössbauer spectra were measured at the magnetic field of 1 T. The magnetic spectra's components in the ME and MCPMS diagrams show that the angular distribution of iron magnetic moments is independent of the external magnetic field. This is typical for antiferromagnetically ordered sample. In contrast to that, the MCPMS spectra measured for $ScFe_6Al_6$ show that the angular distribution of iron magnetic moments is strongly dependent on the magnetic field that proves in turn a ferromagnetic nature of this alloy. The hyperfine magnetic field of $ScFe_4Al_8$ is equal to 11.20(2) T, very close to 11.5(3) T and 11.0(2) T obtained for $ThFe_4Al_8$ [3] and UFe_4Al_8 [1-2], respectively. The iron magnetic moment in the 1 T field reaches value of 1.24(8) B at 12 K.

Because neither scandium nor thorium bear magnetic moments in the samples of our interest, the iron atoms must play key role in formation of the incommensurate magnetic structures in both, scandium and thorium alloys. In the case of uranium samples, the uranium itself is active ion formation of the magnetic structure, so one faces the necessity of explanation of all additional magnetic interactions, including anisotropic ones.

References [1] K. Rećko, K. Szymański, L. Dobrzyński, J. Waliszewski, D. Satuła, M. Biernacka, K. Perzyńska, W. Suski, K. Wochowski, A. Hoser, G. André, F. Bourée, J. Alloys Comp. **323-324** (2001) 531

[2] K. Rećko, K. Szymański, L. Dobrzyński, D. Satuła, W. Suski, K. Wochowski, G. André, F. Bourée, A. Hoser, J. Alloys Comp. **334** 1-2 (2002) 58

[3] K. Rećko, L. Dobrzyński, K. Szymański, D. Satuła, K. Perzyńska, M. Biernacka, J. Waliszewski, P. Zaleski, W. Suski, K. Wochowski, M. Hofmann and D. Hohlwein, Phys. Stat. Sol. (a) **196** (2003) 344

[4] B.Yu. Kotur, D. Badurski, W. Suski, K. Wochowski, A. Gilewski, T. Mydlarz, Physica B

254 (1998) 107

[5] P. Gaczyński, F.G. Vagizov, W. Suski, B.Yu. Kotur, W. Iwasieczko, H. Drulis, J. Magn. Magn. Mater. **225** (2001) 351

XPS STUDIES OF NANOCRYSTALLINE AND POLYCRYSTALLINE $LaNi_5$ THIN FILMS

L. Smardz[1], K. Smardz[2], M. Nowak[2], M. Jurczyk[2]

[1] *Inst. of Molecular Phys., Polish Acad. of Sci., Smoluchowskiego 17, 60-179 PoznaŃ, Poland*
[2] *Inst. of Materials Sciences and Engineering, Poznań Univ. of Technology, M. Curie 5 Sq., Poznań, Poland*

A large number of experimental investigation on $LaNi_5$ and related compounds have been performed up to now in relation to their exceptional hydrogenation properties [1]. In order to optimise the choice of the intermetallic compounds for a selected application, a better understanding of the role of each alloy constituent on the electronic properties of the material is crucial. Several semi-empirical models [2, 3] have been proposed for the heat of formation and heat of solution of metal hydrides and attempts have been made for justifying the maximum hydrogen absorption capacity of the metallic matrices. These models showed that the energy of the metal - hydrogen interaction depend both on geometric and electronic factors. In this contribution, we study experimentally the electronic properties of polycrystalline and nanocrystalline LaNi5 thin films using X-ray photoelectron spectroscopy (XPS). For a comparison we will also show XPS results for bulk nanocrystalline and polycrystalline $LaNi_{4.2}Al_{0.8}$ alloys. The structure of the samples has been studied by X-ray diffraction (XRD). Their bulk chemical compositions were measured using X-ray fluorescence (XRF) method. The scanning electron microscopy (SEM) technique was used to follow the changes in size and shape of the grains. These measurements may supply useful indirect information about the influence of the electronic structure of polycrystalline and nanocrystalline $LaNi_5$-type alloys on their hydrogenation properties.

$LaNi_5$ alloy thin films were prepared onto glass substrates in the temperature range 285 - 700 K using computer-controlled ultra high vacuum (UHV) magnetron co-sputtering. Ni and La targets were sputtered using DC and RF modes, respectively. The base pressure before the deposition process was lower than $5x10^{-10}$ mbar. The chemical composition and the cleanness of all layers was checked in-situ, immediately after deposition, transferring the samples to an UHV (410^{-11} mbar) analysis chamber equipped with XPS [4]. The XPS spectra were measured with $Al - K_\alpha$ radiation at 1486.6 eV at room temperature using a SPECS EA 10 PLUS energy spectrometer. All emission spectra were measured immediately after sample transfer in a vacuum of $8x10^{-11}$ mbar. The deposition rates of La and Ni and $LaNi_5$ thin films are individually checked by a quartz thickness monitors. Typical deposition rate of $LaNi_5$ thin films was about 0.15 nm/s. The thickness and composition of the deposited films were also determined using X-ray fluorescence analysis (XRF).

The polycrystalline $LaNi_{4.2}Al_{0.8}$ alloy was prepared by arc melting stoichiometric amounts of the constituent elements (purity 99.9% or better) in a high purity argon atmosphere. The as

cast ingot was homogenised at 1170 K for 3 days and then rapidly cooled to room temperature in water. The average grain size of the polycrystalline sample was about 500 nm. The nanocrystalline $LaNi_{4.2}Al_{0.8}$ alloy was prepared using mechanical alloying (MA) followed by annealing. MA was performed under argon atmosphere using a SPEX 8000 Mixer Mill. Results show that the amorphous phase of MA samples forms directly from the starting mixture of the elements, without other phase formation. Heating the MA powders at 1070 K for 1 h resulted in the creation of hexagonal $CaCu_5$-type nanocrystalline compound with mean crystallite size less than 50 nm. Structural studies showed that the LaNi5 thin films deposited at 295 K are nanocrystalline with average grain size $D \sim 15nm$. Thin films deposited at about 700K are polycrystalline with $D \sim 200nm$. The total thickness of the samples was about 1000 nm.

In Fig. 1 we show the XPS valence bands for nanocrystalline (bold solid line) and polycrystalline (thin solid line) $LaNi_5$ films. The shape of the valence band measured for the polycrystalline $LaNi_5$ thin film is practically the same compared to that reported earlier for the single crystalline sample [1]. On the other hand, the XPS valence band of the nanocrystalline $LaNi_5$ thin film (bold solid line) is considerably broader compared to that measured for the polycrystalline sample. This is probably due to a strong deformation of the nanocrystals. Normally the interior of the nanocrystal is constrained and the distances between atoms located at the grain boundaries expanded. Similar broadening of the valence band can be also observed for the MA nanocrystalline $LaNi_{4.2}Al_{0.8}$ bulk alloy (bold broken line) compared to that measured for the polycrystalline bulk sample (thin broken line).
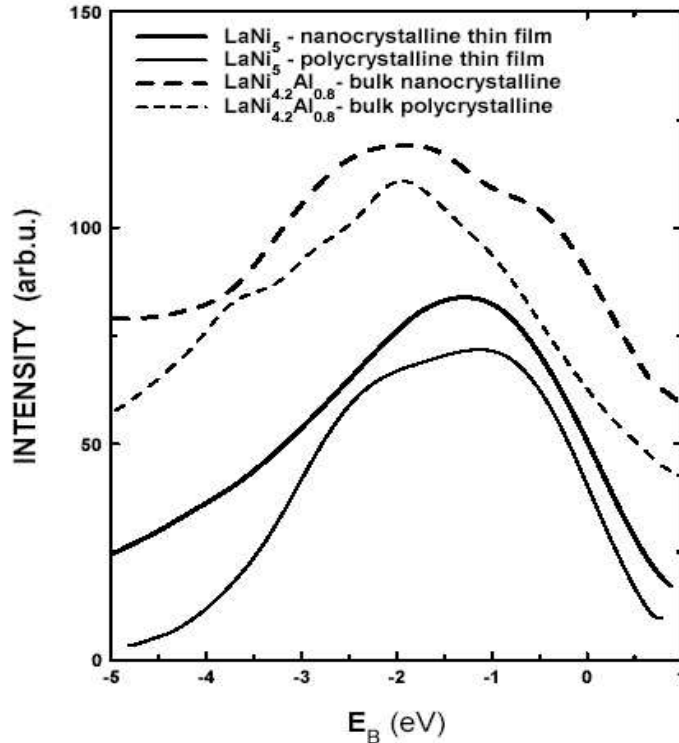

Fig.1. XPS valence band spectra for nanocrystalline (bold solid line) and polycrystalline (thin solid line) $LaNi_5$ thin films using $Al - K_\alpha$ radiation. For a comparison we show results for the nanocrystalline and polycrystalline $LaNi_{4.2}Al_{0.8}$ bulk alloys represented by bold and thin broken lines, respectively. The spectra of the thin films were measured in-situ, immediately

after deposition. The bulk samples were measured immediately after heating in UHV conditions followed by removing of a native oxide and possible impurities layer using ion gun etching system.

In conclusion, the different microstructure observed in polycrystalline and nanocrystalline $LaNi_5$ - type alloys prepared as a bulk material or thin film leads to significant modifications of the electronic structure of the intermetallic. Such a modification of the electronic structure of the nanocrystalline $LaNi_5$ - type alloy compared to that of polycrystalline sample could significantly influence on its hydrogenation properties [4].

REFERENCES

[1] L. Schlapbach, Hydrogen in Intermetallic Compounds, II, Springer, Berlin, 1992, p. 165

[2] P. C. Bouten, A. R. Miedema, J. Less Common Metals, **71** (1980) 147-160.

[3] R Griessen, Phys. Rev. B **38** (1988) 3690-8.

[4] L. Smardz, K. Smardz, M. Jurczyk, J. Jakubowicz, J. Alloy Comp. **313** (2000) 192-200.

0.7 ANOMALY IN QUANTUM POINT CONTACT, MODELLING BASED ON ANDERSON MODEL

Piotr Stefański and Bogdan R. Bułka

Institute of Molecular Physics of the Polish Academy of Sciences ul. Smoluchowskiego 17, 60-179 Poznań, Poland

An unusual temperature behavior of the conductance vs. gate voltage in quantum point contact (QPC) has been observed for years [1, 2] without satisfactory theoretical explanation. Recently it has attracted large interest again and there are strong evidences for the Kondo effect to be responsible for it [3, 4]. We model a QPC by localized spin-degenerate quasi-bound state (QBS) located inside the constriction which forms QPC. Electrons occupying QBS interact with the strength of Coulomb repulsion U, and QBS is hybridized with electrodes (2D-electron baths). Such a system we describe in the frame of the Anderson Hamiltonian:

The hybridization $\Gamma = \pi v^2 \rho_{el,\alpha}$ ($\rho_{el,\alpha}$ is the density of states in the α -electrode) is assumed to have a step-like profile to simulate the potential barrier present inside QPC and increasing transparency of the QPC when the potential of the confining gate increases and the QBS level approaches Fermi surface. Firstly, the non-interacting case is analyzed. Without interactions the Hamiltonian is quadratic in operators and can be solved exactly. The step-like behavior of the experimental first plateau in conductance is reproduced. The hybridization of the bound state with electrodes for the fully transparent QPC is one order of magnitude larger comparing to quantum dots. Interacting case is analyzed within the Interpolative Perturbative Scheme (IPS) [5] which is an extension of the second order perturbation in U to the atomic limit [6]. We have modified the method to be applicable for the case when the hybridization increases in the step-like fashion. The method is applied both for strong (Kondo regime) and weak (Coulomb blockade regime) hybridization. Such crossover from one regime to another indeed takes place in QPC when the hybridization of QBC with electrodes increases while increasing of the gate

voltage. We start our modeling when the bound state inside QPC is initially weakly coupled to electrodes. Even for an infinitesimally small hybridization the level is fully occupied by two electrons with opposite spins when it lies below Fermi surface at T=0. Then, when the bare level is shifted towards Fermi surface it enters the region where the level $\varepsilon_d + n_{-\sigma}U$ is pushed above the Fermi level and starts to be empty. This is a regime when the conductance is mainly enhanced by the Kondo effect. Then, the occupancy of the level ε_d decreases though the hybridization with electrodes increases. Thus, the level occupancy is controlled mainly by the position of the level relative to Fermi surface. The anomaly around the value of 0.7x $(2e^2/h)$ appears in the conductance curves vs. QBS level position when temperature increases. The shape of the curves strongly depends on the energy for which the hybridization step takes place. The 0.7 anomaly arises as a result of the competition between two mechanisms of enhancing the conductance up to the unitary limit: the Kondo effect and the increase of hybridization.

[1] N.K. Patel et al., Phys. Rev. B **44**, 13549 (1991).

[2] K.J. Thomas et al., Phys. Rev. Lett. **77**, 135 (1996).

[3] S.M. Cronenwett et al., Phys. Rev. Lett. **88**, 226805 (2002).

[4] Y. Meir et al., Phys. Rev. Lett. **89**, 196802 (2002).

[5] A. Levy-Yeyati et al., Phys. Rev. Lett. **71**, (1993) 2991.

[6] K. Yoshida et al., Prog. Theor. Phys. **46**, (1970) 244.

ELECTRONIC STRUCTURE AND PHOTOEMISSION SPECTRA OF USn_2 COMPOUND

A. Szajek

Institute of Molecular Physics, Polish Academy of Sciences, Poznań, Poland

The $ab - initio$ self-consistent calculations have been performed for USn2 compound, which crystallizes in the $ZrGa_2$-type structure ($Cmmm$ space group). The tight binding linear muffin-tin orbital method ($TBLMTO$) in the atomic sphere approximation (ASA) was used in the calculations. The spin-polarized calculations have confirmed the antiferromagnetic order in the USn_2 system. The magnetic moment is predominantly located on the uranium atoms and is formed mainly by the f electrons. The three types of Sn atoms may be treated as nonmagnetic. The calculated X-ray photoemission spectra are presented.

Ni/Cu/Co TRILAYERS WITH OUT-OF-PLANE Ni MAGNETIZATION: $in - situ$ MOKE INVESTIGATIONS

T. Toliński*, K. Lenz, E. Kosubek, J. Lindner, K. Baberschke

Institute fuer Experimentalphysik, Freie Universität Berlin, Arnimallee 14, D-14195 Berlin-Dahlem, Germany

We have prepared $Ni/Cu_x/Co/Cu(001)$ films in ultrahigh-vacuum (base pressure of about $5x10^{-11}$ mbar) with variable spacer thickness ($4ML < x < 50ML$) and constant thickness of Ni(9ML), Co(2ML) and capping Cu(4ML) layers. The films growth was monitored by MEED (medium energy electron diffraction) oscillations and the AES (Auger electron spectroscopy).

Usually trilayers characterized by in-plane or perpendicular anisotropy of *both* ferromagnetic (FM) films are studied. The thicknesses of FM films we have used lead to the exceptional case of perpendicular Ni and in-plane Co magnetization orientation, which is a result of the different out-of-plane anisotropies. Co is in-plane in the whole thickness range and Ni undergoes a transition to perpendicular direction above 7ML [1]. Additionally, this Co thickness enables room temperature studies because T_C of 2ML Co is about 340 K. Thinner Co films exhibit lower anisotropy (better for magnetic measurements), which already for 2ML is $M_{eff} = 37.6$ kG ($M_{eff} = 4\pi M - 2K^2/M$), but below 1.8ML of Co T_C jumps down to 200 K [2]. For comparison the effective magnetization of 9ML of Ni is equal to $M_{eff} = $ -2.18 kG.

We have measured in-situ polar dc-MOKE (magneto-optical Kerr effect) hysteresis loops. The polar geometry is sensitive only to the perpendicular component of magnetization, therefore the Ni film contribution has been measured. Fig. 1 presents the calculated hysteresis loop assuming either coherent rotation of moments (solid line) or magnetization by domain wall movement (dotted line) [3,4]. The experimental loop shown in the inset is measured for an uncoupled film with a spacer thickness of 50ML. It is visible that the coercive field is strongly reduced compared to the rotational model. The domain nucleation is favoured in polar measurements, however, the coercivity is not zero, which supports the prediction that intermediate behaviour is observed [3,4].

Our investigations concern the influence of the interlayer exchange coupling on the measured polar MOKE loops with the coupling modified by changing the spacer Cu thickness. The question of the temperature dependence of the magnetization curves is also addressed. The experimental results are supported by model calculations of the hysteresis loops.

References

[1] K. Baberschke and M. Farle, J. Appl. Phys. **81** (1997) 5038.

[2] P. Poulopoulos, P.J. Jensen, A. Ney, J. Lindner and K. Baberschke, Phys. Rev. B **65** (2002) 064431.

[3] B. Dieny and J.P. Gavigan, J. Phys.: Condensed Matter **2** (1990) 187.

[4] T. Toliński and J. Baszyński, phys. stat. sol. (a) **169** (1998) 139.

_____

* permanent address: Institute of Molecular Physics, PAS, Smoluchowskiego 17, 60-179 Poznań, Poland

Fig. 1. Calculated magnetization curve of uncoupled $Cu_5/Ni_9/Cu_{50}/Co_2/Cu(001)$ trilayer (solid line - coherent rotation model, dotted line - domain wall movement model). Inset: Experimental polar MOKE hysteresis loop of the Ni component. One should note that the experimental coercive field is close to zero in the scale of the main figure.
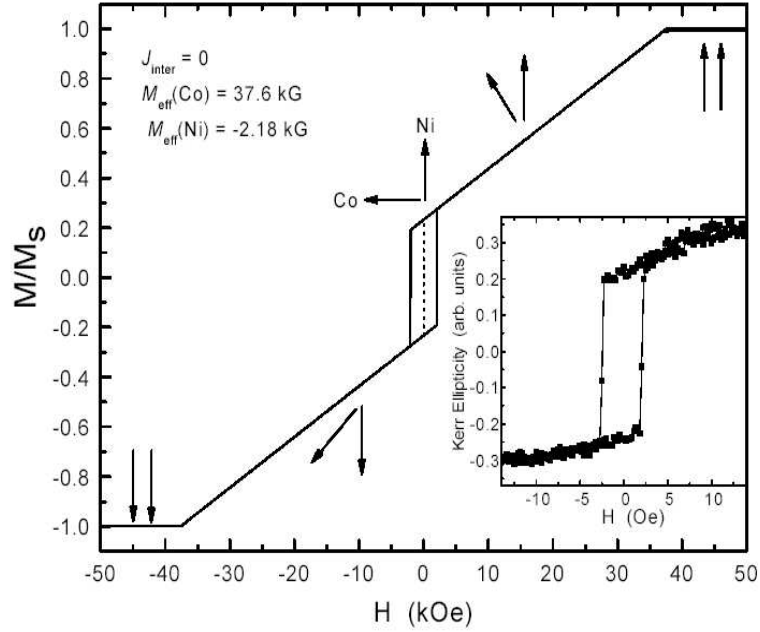
COMPARATIVE STUDIES OF STRUCTURAL, MAGNETIC AND ELECTRONIC PROPERTIES OF $NdNi_4Al$ AND $NdNi_4B$ COMPOUNDS

T. Toliński[1*], W. Schaefer[2], G. Chełkowska[3], W. Kockelmann[4], A. Hoser[5], B. Andrzejewski[1], A. Szlaferek[1] and A. Kowalczyk[1]

[1] *Institute of Molecular Physics, Polish Academy of Sciences, M. Smoluchowskiego 17, 60-179 Poznań, Poland*

[2] *Mineralogisches Institut, Univ. Bonn, in Forschungszentrum Juelich, 52425 Juelich, Germany*

[3] *Institute of Physics, Silesian University, Uniwersytecka 4, 40-007 Katowice, Poland*

[4] *Mineralogisches Institut, Univ. of Bonn, at ISIS Facility, Rutherford Appleton Laboratory, Chilton OX11 0QX, U.K.*

[5] *Institut fuer Kristallographie, RWTH-Aachen, Germany*

We present our results on magnetic and structural studies of the hexagonal rare-earth based $NdNi_4Al$ and $NdNi_4B$ compounds. The samples were prepared by the induction melting of stoichiometric amounts of the constituent elements in a water-cooled boat, under an argon atmosphere. $NdNi_4Al$ crystallizes in the hexagonal $CaCu_5$-type structure, space group P_6/mmm, whereas $NdNi_4B$ crystallizes in the hexagonal $CeCo_4B$-type structure, space group P_6/mmm. The room temperature lattice constants are a = 5.0103 Å, c = 4.0601 Åfor $NdNi_4Al$ and a = 5.053 Å, c = 6.954 Åfor $NdNi_4B$.

In spite of different crystallographic structures $NdNi_4Al$ and $NdNi_4B$ compounds exhibit many similarities in their magnetic and transport properties. The ferromagnetic ordering temperature TC and magnetic moments at 6 T for these compounds are 6 K, 1.52 $\mu_B/f.u.$ and 11.7 K, 1.68 $\mu_B/f.u.$ [1], respectively. The magnetization curves are displayed in Fig. 1. The phase transitions are confirmed both by our ac/dc magnetic susceptibility (Fig.1) measurements and electrical resistivity studies [2].

In the case of the $NdNi_4Al$ samples we have performed also neutron diffraction studies, which are not possible for compounds containing natural boron due to large absorption. Hence, the magnetic order of $NdNi_4Al$ has been established with the magnetic moments ordered in the hexagonal basis plane. Besides, a negligible magnetic contribution of Ni atoms was observed. This condition simplifies the interpretation of the magnetic, transport and electronic properties of RNi_4Al or RNi_4B (R = rare earth or Y) compounds. The photoemission spectra (XPS) of the valence band region at the Fermi level exhibits the dominance of the Ni(3d) states (1.5 eV) [3].
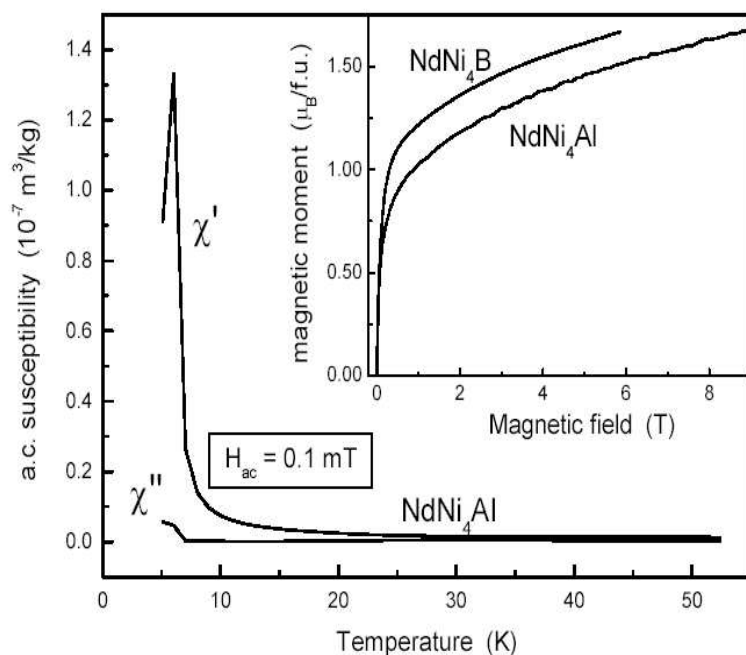

Fig. 1. The real, $\chi^{'}$, and the imaginary, $\chi^{''}$, part of the a.c. susceptibility for $NdNi_4Al$ compound. Inset: The magnetization curve of $NdNi_4Al$ and $NdNi_4B$ compounds.

References

[1] T. Toliński, A. Kowalczyk, A. Szlaferek, M. Timko and J. Ková č, Solid State Commun. **122** (2002) 363.

[2] T. Toliński, A. Kowalczyk, V. Ivanov, phys. status sol. (b), accepted for publication

[3] T. Toliński, G. Chełkowska and A. Kowalczyk, Solid State Commun. **122** (2002) 145.

—————————————————————————————

* permanent address: Institute of Molecular Physics, PAS, Smoluchowskiego 17, 60-179 Poznań, Poland

KONDO EFFECT AND MIXED VALENCE IN $CeNi_4X$ (X=B and Al) COMPOUNDS

T. Toliński[1*], G. Chełkowska[2], A. Szlaferek[1] V. Ivanov[3], M. Falkowski[4] and A. Kowalczyk[1]

[1]*Institute of Molecular Physics PAS, Smoluchowskiego 17, 60-179 Poznań, Poland*

[2] *Institute of Physics, Silesian University, Uniwersytecka 4, 40-007 Katowice, Poland*
[3] *General Physics Institute, RAS, Vavilov 38, Moscow, Russia*
[4]*Faculty of Technical Physics, Poznań University of Technology, Nieszawska 13a, Poland*

Despite the increased interest in the metallic systems with electronic instability of 4f-states known as systems with intermediate valence, heavy fermions or Kondo-lattices, the nature of 4f-states of Ce in the considered phases is still unclear at the microscopic level. In the Ce-based compounds, depending on the position of the Fermi level E_F compared to that of the 4f state the following electronic states of cerium are expected: magnetic 3+ state, 3+ state with Kondo effect and intermediate (3+/4+) valence state. The cerium- transition metal compounds are attractive for studies of these diverse Ce states because of the strong dependence of the Fermi level position on the amount of the contributing elements. The behavior of Ce changes in various Ce-Ni systems also due to the different crystallographic structures.

The series RNi_4B, where R stands for rare-earth element or Y is attracting attention developed owing to its interesting magnetic, structural and electronic behavior. The materials belonging to the RNi_4B series create a hexagonal structure of $CeCo_4B$ with space group P_6/mmm. The Ni atoms occupy the crystallographic sites (2c) and (6c), rare earth is also located in two sites (1a) (1b) and boron atoms are located in the (2d) positions. For comparision, in the case of RNi_4Al compounds ($CaCu_5$ -type structure) R occupies the 1a site and Ni (1) the 2c site. Ni(2) and Al are statisically distributed on the 3g site.

The X-ray photoemission spectra were obtained for the radiation of the photon energy equal to 1487.6 eV, $Al - K_\alpha$ source using a PHI 5700/660 Physical Electronics Spectrometer. The energy spectra of the electrons were analyzed by a hemispherical mirror analyzer with the energy resolution of about 0.3 eV. The Fermi level $E_F = 0$ was referred to the gold 4f-level binding energy at 84 eV. All photoemission spectra were measured immediately after breaking the sample in a vacuum of 10^{-10} Torr.

X-ray photoelectron spectroscopy is not an ideal tool to probe the Ce 4f valence bands because of relatively small cross sections. The XPS spectra of the 3d core levels give more information about the 4f configuration and hybridization. The Ce-based intermetallic compounds show different final states depending on the occupation of the f shell: f^0, f^1 and f^2 [1]. The spin-orbit coupling $\Delta = (3d^94f^1)_{3/2} - (3d^94f^1)_{5/2} = 18.4eV$ for $CeNi_4B$ and $CeNi_4Al$. The appearance of the f^0 components is a clear evidence of a mixed valence. In $\alpha - Ce$ there is also evidence of the $3d^94f^0$ peaks for both $3d_{3/2}$ and $3d_{5/2}$ multiplets, which are not present in $\gamma - Ce$ [2], however, the $3d_{5/2}f^0$ peak overlaps with the $3d_{3/2}f^2$ peak and only the $3d_{3/2}f^0$ peak can be accurately estimated [2]. The f-occupation in the initial state of $\alpha - Ce$ is connected with the intensity of the $3d^9f^0$ satellite. The XPS of Ce(3d) spectra are usually interpreted in terms of the Gunnarsson-Schönhammer theory [1]. Based on this model the intensity ratio $r = I(f^0)/(I(f^0) + I(f^0) + I(f^2))$ is directly related to the f-occupation. The separation of the overlapping peaks in the Ce(3d) XPS spectra was made basing on the Donaich- Šunjić theory [3]. The hybridization energy $\Delta = \pi V \rho_m ax$ describes the hybridization part of the Anderson impurity Hamiltonian, where ρ_{max} rmax is the maximum DOS and V is the hybridization matrix element. Assuming the dependence of the intensity ratio r on the D parameter like in the case of Ce [1, 2] the D value is about 85 meV for $3d_{3/2}$ band and the f occupancy, $n_f \approx 0.83$ [4]. The

hybridization for $\alpha - Ce$ estimated by this way from XPS 3d spectra is $\Delta = 60 meV$. For Ce intermetallic compounds with strong f shell instabilities Δ is of the order of 150 meV [1, 2].

The effective magnetic moment derived from the Curie constant C is lower than the magnetic moment of free Ce^{3+} ion ($\approx 2.4\mu_B$). Since the magnetic moment of Ce^{4+} is zero, the reduction of the moment in $CeNi_4B$ and $CeNi_4Al$ may be due to the intermediate or fluctuating Ce valence state. The magnetic contribution $\rho_{mag}(T)$ of the $CeNi_4B$ [5] and $CeNi_4Al$ resistivity was obtained by subtracting the temperature dependent part of $\rho(T)$ for the non-f-electron reference compound $YNi_4X(X = B, Al)$ [5]. Below 15 K a shallow minimum typical of the Kondo systems is observed for $CeNi_4B$. At low temperature ($T < 12K$) $\rho_{mag}(T)$ was analyzed in terms of the Kondo theory and the data were fitted with the standard formula:

$$\rho_{mag}(T) = \rho_0^\infty - \rho_K lnT$$

yielding a value of $\rho_0^\infty = 88.4 m\Omega cm$ for the spin disorder resistivity and $\rho_K = 0.29 m\Omega cm$ for the Kondo coefficient. The value of the later confirms that this effect is very small. The minimum may also be induced be a Kondo-like effect originating from the intermediate or fluctuating Ce valence state. Summarizing the results, one may conclude both from the susceptibility measurements and the XPS spectra that Ce ions in $CeNi_4B$ and $CeNi_4Al$ are in the intermediate valence state. These compounds are paramagnetic and follow the Curie-Weiss law. However, the derived effective magnetic moment is much lower in comparison with free Ce^{3+} ions value equal to $2.54\mu_B$. Since magnetic moment of tetravalent cerium is zero, the observed reduction of the magnetic moment can be explained in a natural way by contribution of both the $4f^0$ (Ce^{4+}) and $4f^1$ (Ce^{3+}) configurations. The magnetic contribution to the electrical resistivity reveals in the paramagnetic region at low temperatures (below 12 K) a logarithmic slope characteristic of the Kondo-like systems.

[1] O. Gunnarsson, K. Schönhammer, Phys. Rev B **28** (1983) 4315.

[2] J.C. Fuggle, F.U. Hillebrecht, Z. Zolnierek, R. Laesser, Ch. Freiburg, O. Gunnarsson, K. Schönhammer, Phys. Rev. B **27** (1983) 7330.

[3] S. Doniach and M. Šunjić, J. Phys. C **3** (1970) 285.

[4] T. Toliński, A. Kowalczyk, G. Chełkowska, Phys. Lett. A **308** (2003) 75.

[5] T. Toliński, A. Kowalczyk, M. Pugaczowa-Michalska, G. Chełkowska, J.Phys.: Condens. Matter **15** (2003) 1397.

―――――――――――――――――――――――――――――

* permanent address: Institute of Molecular Physics, PAS, Smoluchowskiego 17, 60-179 Poznań, Poland

MAGNETISM AND ELECTRONIC STRUCTURE OF GdMnGe

B. Tyszka[a], J. Szade[a], J. Deniszczyk[b]

[a] *A. Chełkowski Inst. of Physics, Univ. of Silesia, Uniwersytecka 4, 40-007 Katowice, Poland*
[b] *Inst. of Phys. and Chem. of Metals, Univ. of Silesia, Bankowa 12, 40-007 Katowice, Poland*

Rare-earth-transition metal germanides have been intensively studied in recent years because of the variety of interesting magnetic and crystallographic properties. GdTiGe and compounds obtained by Mn substitution of Ti (up to 60% at.) show ferromagnetic behaviour with T_C in the temperature range 374 K - 430 K [1]. The electronic structure of GdTiGe determined from photoemission spectra appeared to be in good agreement with the TB-LMTO calculations [2]. Among the known RTX system only the Mn compounds have essential magnetic moments in the 3d sublattice [3].

GdMnGe crystallizes in the orthorhombic TiNiSi type of structure (Pnma) (a=7.14, b=4.17, c=8.20 Å). The Néel temperature of 490 K has been reported by Klosek et al. [4] whereas we have found two additional transitions of the antiferromagnetic like character at 337 and 102 K. The antiferromagnetic character of ordering is confirmed by the magnetic field dependence of magnetization obtained at 1.9 K.

The nearest Mn-Mn distance has been found to be a factor determining the magnetic moment and coupling. For dMn-Mn¿2.89 A an antiferromagnetic coupling has been found, whereas for lower distances ferromagnetic or mixed interaction have been reported [1]. The antiferromagnetic coupling within the Mn sublattice is in agreement with the shortest Mn-Mn distance within the TiNiSi-type of structure (3.147 Å).

Calculations using the TB-LMTO method have shown that Mn and Gd d bands are strongly polarized what leads to the Mn moment of about $3.22 mu_B$. Antiparallel polarization of Gd and Mn d states has been found. It leads to the ferrimagnetic character of magnetic ordering in GdMnGe.

[1] B. Tyszka, J. Szade, J. Alloys Comp.,in press

[2] G. Skorek, J. Deniszczyk, J. Szade, B. Tyszka, J. Phys.: Cond. Matter **13** (2000) 6397

[3] A. Szytłua, Crystal Structure and Magnetic Properties of RTX Rare Earth Intermetallics, Jagiellonian University, Cracow, 1998

[4] V. Klosek, A. Verniere, B. Ouladdiaf, B. Malaman, J. Magn. Magn. Mater. **256** (2003) 69

LIST OF PARTICIPANTS

the full addresses are available on the NM'03 WWW page:
http://www.ifmpan.poznan.pl/zp2/nm03/main02.htm

K. Baberschke, Berlin, Germany, bab@physik.fu-berlin.de

M. Bąk, Poznań, Poland, karen@amu.edu.pl

J. Baszyński, Poznań, Poland, Janusz.Baszynski@ifmpan.poznan.pl

S. Blügel, Juelich, Germany, S.Bluegel@fz-juelich.de

G. Chełkowska, Katowice, Poland, gchelkow@us.edu.pl

J. Deniszczyk, Katowice, Poland, jdeni@us.edu.pl

E. Długaszewska, Poznań, Poland, ewa@ifmpan.poznan.pl

J. Dubowik, Poznań, Poland, Janusz.Dubowik@ifmpan.poznan.pl

K. Dziatkowski, Warszawa, Poland, Konrad.Dziatkowski@fuw.edu.pl

H. Ebert, München, Germany, Hubert.Ebert@cup.uni-muenchen.de

O. Eriksson, Uppsala, Sweden, Olle.Eriksson@fysik.uu.se

H. Eschrig, Dresden, Germany, h.eschrig@ifw-dresden.de

V. Eyert, Augsburg, Germany, eyert@physik.uni-augsburg.de

J.E. Frąckowiak, Katowice, Poland, jfrack@us.edu.pl

A. Go, Białystok, Poland, annago@alpha.uwb.edu.pl

J. Goraus, Katowice, Poland, jgoraus@o2.pl

J.-M. Greneche, Le Mans, France, greneche@univ-lemans.fr

J. Hafner, Wien, Austria, juergen.hafner@univie.ac.at

M. Haglauer, Poznań, Poland, monika@amu.edu.pl

B. Idzikowski, Poznań, Poland, idzi@ifmpan.poznan.pl

K. Jaśniewicz, Poznań, Poland, kja6@wp.pl

H.S. Jeevan, Dresden, Germany, jeevan@cpfs.mpg.de

A. Jezierski, Poznań, Poland, Andrzej.Jezierski@ifmpan.poznan.pl

T. Jungwirth, Prague, Czech Republic, jungw@fzu.cz

J. Kirschner, Halle, Germany, sekrki@mpi-halle.mpg.de

M. Košuth, Münichen, Germany, Michal.Kosuth@cup.uni-muenchen.de

A. Kowalczyk, Poznań, Poland, ankow@ifmpan.poznan.pl

M. Krawczyk, Poznań, Poland, krawczyk@amu.edu.pl

S. Krompiewski, Poznań, Poland, stefan@ifmpan.poznan.pl

H. Kroha, Bonn, Germany, kroha@th.physik.uni-bonn.de

M. Ležaić, Juelich, Germany, m.lezaic@fz-juelich.de

H. von Löhneysen, Karlsruhe, Germany, h.vL@ifp.fzk.de

T. Luciński, Poznań, Poland, Tadeusz.Lucinski@ifmpan.poznan.pl

S. Mamica, Poznań, Poland, mamica@main.amu.edu.pl

Ph. Mavropoulos, Juelich, Germany, ph.mavropoulos@fz-juelich.de

T. Michalecki, Katowice, Poland, tomek@beta.ifichm.us.edu.pl

G. Michałek, Poznań, Poland, Grzegorz.Michalek@ifmpan.poznan.pl

J.A. Morkowski, Poznań, Poland, Janusz.Morkowski@ifmpan.poznan.pl

K.-H. Mueller, Dresden, Germany, K.H.Mueller@ifw-dresden.de

P. Napierała, Poznań, Poland, Piotr.Napierala@ifmpan.poznan.pl

M. Nogala, Poznań, Poland, mnogala@amu.edu.pl

L. Nordström, Uppsala, Sweden, Lars.Nordstrom@fysik.uu.se

F. Petroff, Orsay, France, frederic.petroff@thalesgroup.com

A. Postnikov, Osnabrueck, Germany, apostnik@uos.de

H. Puszkarski, Poznań, Poland, henpusz@amu.edu.pl

M. Przybylski, Halle, Germany, mprzybyl@mpi-halle.de

M. Pugaczowa-Michalska, Poznań, Poland, maria@ifmpan.poznan.pl

K. Rećko, Białystok, Poland, karo@alpha.uwb.edu.pl

M. Richter, Dresden, Germany, email m.richter@ifw-dresden.de

A. Ślebarski, Katowice, Poland, slebar@us.edu.pl

L. Smardz, Poznań, Poland, smardz@ifmpan.poznan.pl

P. Stefański, Poznań, Poland, Piotr.Stefanski@ifmpan.poznan.pl

F. Stobiecki, Poznań, Poland, Feliks.Stobiecki@ifmpan.poznan.pl

A. Szajek, Poznań, Poland, szajek@ifmpan.poznan.pl

Z. Szotek, Daresbury, U.K., z.szotek@dl.ac.uk

W. Temmerman, Daresbury, U.K., w.m.temmerman@dl.ac.uk

T. Toliński, Berlin, Germany, tomtol@ifmpan.poznan.pl or babgroup@physik.fu-berlin.de

B. Tyszka, Katowice, Poland, beata@kulpa.zfcst.us.edu.pl

R. Wiesendanger, Hamburg, Germany, wiesendanger@physnet.uni-hamburg.de

T. Zawada, Katowice, Poland, tomekz@polbox.com

M. Zwierzycki, Enschede, The Netherlands, M.Zwierzycki@tn.utwente.nl

5 News from UK's CCP9 Programme

UK's Collaborative Computational Project 9 on "Computational Studies of the Electronic Structure of Solids"

5.1 Reports on CCP9 Workshops

5.1.1 Report on Satellite Meeting of SRS User Meeting

International Workshop on Ferromagnetic Semiconductors and Synchrotron Radiation

Thursday 11th Friday 12th September 2003

Venue: Tower Seminar Room, SRS Daresbury Laboratory

Scientific Chair: Gerrit van der Laan

Organisation: Physics College, Synchrotron Radiation Source, Daresbury Laboratory, UK with support from CCP9.

Conference Office: Sue Waller

Web pages: `http://www.srs.ac.uk/srum/satellite_1.htm`

Diluted magnetic semiconductors (DMS) are expected to play an important role in interdisciplinary materials science and future spintronics because the integration of charge and spin degrees of freedom will deliver new types of devices for information storage and processing. This workshop is to introduce these new materials as well as to report on state-of-art results (both experiment and theory). The emphasis will be on the exploitation of powerful techniques derived from magnetic x-ray dichroism using synchrotron radiation, offering vector magnetometry which is site, element and chemical specific.

Programme

Thursday, 11th September 2003

Time	Speakers	Title
14:00	G. van der Laan (Daresbury)	Opening remarks
14:10	Tomas Jungwirth (Prague)	Ferromagnetic III,V semiconductors
15:10	Oliver Rader (Bessy)	Photoemission on diluted magnetic semiconductors
15:40	Tea/Coffee break and posters	
16:10	Bryan Gallagher (Nottingham)	GaMnAs: improved materials
17:10	Tomasz Story (Warsaw)	Ferromagnetic EuS-PbS semiconductor heterostructures
18:10	End of session	
	Posters and SR Facility Tour	
19:00	Buffet meal provided in Science Centre	

Friday, 12th September 2003

Time	Speakers	Title
09:00	Russell Cowburn (Durham)	Magnetic nanostructures for digital logic
10:00	Ulrich Hillebrecht (Karlsruhe)	Antiferromagnetic domains imaged by photoemission microscopy
10:30	Coffee break and posters	
11:00	Hermann Dürr (Bessy)	Femto second spin dynamics in magnetic materials
12:00	Thomas Schulthess (ORNL)	Electronic Structure and Valence of Mn impurities in III-V semiconductors
13:00	Closing Remarks	

Participants:

Prof James Annett (Physics, Bristol)

Dr Russell Cowburn (Physics, Durham)

Mr Mark de Vries (Chemistry, Edinburgh

Dr Sarnjeet Dhesi (Diamond Light Source)

Dr Hermann Dürr (BESSY, Berlin)

Dr Kevin Edmonds (Physics, Nottingham)

Dr Nicola Farley (Physics, Nottingham)

Miss Sam Foster (Elsevie,r Oxford)

Dr Bryan Gallagher (Physics, Nottingham)

Prof Nicholas Harrison (Chemistry, Imperial College London)

Prof Ulrich Hillebrecht (Förschüngszentrum Karlsruhe, Germany)

Dr Tarnjit Johal (Daresbury Laboratory)

Prof Tomas Jungwirth (Physics, ASCR Praha, Czech Republic)

Mr James Neal (Physics, Sheffield)

Dr Sergey Okatov (KU Nijmegen, Netherlands)

Dr Oliver Rader (BESSY, Berlin)

Dr Thomas Schulthess (Oak Ridge National Lab, US)

Dr Tomasz Story (Polish Academy of Sciences, Warsaw)
Mr Dave Teehan (Daresbury Laboratory)
Dr Neil Telling (Daresbury Laboratory)
Dr Tracy Turner (Daresbury Laboratory)
Prof Gerrit van der Laan (Daresbury Laboratory)
Dr Sam Warren (Daresbury Laboratory)

ABSTRACTS

Thursday 11th September 2003

14:00 Prof Gerrit van der Laan
Daresbury Laboratory
Opening remarks

14:10 Prof Tomas Jungwirth

Univ Texas, Dept Phys, Austin, TX 78712 USA
Inst Phys ASCR, Prague 16253 6, Czech Republic

Ferromagnetic (III,Mn)V semiconductors

The basic microscopic origins of ferromagnetism in the (III,Mn)As and
(III,Mn)Sb compounds appear to be well understood within a model of
valence-band holes induced magnetic interactions between Mn local moments.
Efficient computation methods have been developed, based on the effective
Hamiltonian description of the system, which are able to model their
magnetic, transport, and optical properties on a semi-quantitative level. In
this presentation we discuss possibilities for achieving high Curie
temperatures in (III,Mn)V semiconductors and then focus on magnetic and
transport properties of these new ferromagnetic materials. In particular, we
summarize our understanding of anisotropic magnetoresistance effects, the
anomalous Hall effect, and magneto-optical properties. We also introduce a
microscopic theory of the Gilbert damping of magnetization precession and
make predictions for the current-induced magnetization switching in diluted
magnetic semiconductor multilayers.

15:10 Dr Oliver Rader

BESSY, Berlin

Photoemission on diluted magnetic semiconductors

Our electron spectroscopy activities on ferromagnetic diluted III-V
semiconductors started out with x-ray photoelectron spectroscopy of the Mn
$2p$ core level in Ga$_{1-x}$MnxAs [1]. The spectrum with its strong
satellite has been analyzed using configuration-interaction calculations
taking into consideration the local surrounding of the Mn impurity in a
cluster model. The exchange constant Nb has been determined as -1.2$\pm$0.2
eV meaning antiferromagnetic Mn$3d$-As$4p$ interaction in the case of the
half-occupied Mn^{2+} ion. The Mn d electron number was determined to be
$\sim>$5 and both Mn^{2+} and Mn^{3+} states were found to be in
agreement with the experimental data. Because of the strong magnetic
coupling between Mn^{3+} and an As $4p$ hole, the hole will be responsible
for the long-range magnetic interaction.
The possibility to distinguish Mn-$3d$ derived states by resonant
photoemission is particularly important for the region near the Fermi
energy. Substantial Mn-$3d$ derived intensity at E_F had been prediced by
all local density theory calculations [2] with the interesting consequence
that these systems would belong to the class of half metals. Angle-resolved
photoemission of a p(1$\times$1) surface of GaAs6.9\%Mn(100) showed very
similar band dispersions along Γ-X as in pure GaAs(100), however,
shifted by 100-200 meV for large portions of the Δ_1 band. More
importantly, the experiments permitted the direct observation of the
acceptor states induced by Mn doping near E_F by comparison to pure GaAs
spectra for various photon energies [3].

Recently, photoemission spectra have been studied in dependence of the Mn
concentration [4]. The data of Ref. 4 confirm the shift [3] of the
Δ_1 band near the X point with Mn concentration. The position of the
Mn $3d$ contribution is in agreement with previous work. As no satellite
emission was seen, it was concluded that local-density theory gives a proper
description of the Mn contribution to the spectra [4]. We conducted resonant
valence band photoemission and find a 20-fold enhancement of the Mn $3d$
contribution at the L_3-edge [5]. The difference spectrum is similar to
previously obtained resonant photoemission at the Mn M-edge [6] with
concomitant lower probing depth, in particular a strong satellite appears
and no clear Fermi edge ruling out strong Mn $3d$ weight at the valence-band
maximum. A resonant photoemission calculation based on a
configuration-interaction cluster model reproduces the L_3-on-resonance
spectrum for model parameters Δ, U, and (pdσ) consistent with
previous work.

In spite of these important contributions from electron spectroscopy,

understanding the electronic structure has been hampered by an indistinguishability of Mn atoms. This holds also for published x-ray magnetic circular dichroism (XMCD) data [7]. We combined sensitivity to atomic number, chemical shifts, and to magnetic order in a field-dependent magnetic circular x-ray dichroism (XMCD) study at the Mn L-edge and observe three constituents with distinct magnetic behavior. We find that ferromagnetic Mn deviates more strongly from a $3d^5$ configuration than believed previously and that interstitial Mn does not contribute to the ferromagnetism.

In order to extend to large-band gap hosts, we studied the $3d$ density of states for Mn in GaN and Cr in GaN by photoemission. In agreement with theoretical expectations, the $3d$ density of states extends into the band gap region in these systems. This work was supported by BMBF under contract no. 05 KS1IPA/0.

1. J. Okabayashi, A. Kimura, O. Rader, T. Mizokawa, A. Fujimori, T. Hayashi, and M. Tanaka, Phys. Rev. B 58, R4211 (1998).

2. M. Shirai, T. Ogawa, I. Kitagawa, and N. Suzuki, J. Magn. Magn. Mat. 177-181, 1383 (1998); H. Akai, Phys. Rev. Lett. 81, 3002 (1998); S. Sanvito and N. A. Hill, Phys. Rev. B 62, 15553 (2000); S. Sanvito, P. Ordejon, and N. A. Hill, Phys. Rev. B 63, 165206 (2001); M. van Schilfgaarde and O. N. Mryasov, Phys. Rev. B 63, 233205 (2001).

3. J. Okabayashi, A. Kimura, O. Rader, T. Mizokawa, A. Fujimori, T. Hayashi, and M. Tanaka, Phys. Rev. B 64, 125304 (2001).

4. H. Asklund, L. Ilver, J. Kanski, J. Sadowski, and R. Mathieu, Phys. Rev. B 66, 115319 (2002).

5. O. Rader, C. Pampuch, A. M. Shikin, W. Gudat, J. Okabayashi, T. Mizokawa, A. Fujimori, T. Hayashi, M. Tanaka, A. Tanaka, and A. Kimura, Phys. Rev. B, submitted.

6. J. Okabayashi, A. Kimura, T. Mizokawa, A. Fujimori, T. Hayashi, and M. Tanaka, Phys. Rev. B 59, R2486 (1999).

7. H. Ohldag, V. Solinas, F. U. Hillebrecht, J. B. Goedkoop, M. Finazzi, F. Matsukura, and H. Ohno, Appl. Phys. Lett. 76, 2928 (2000); S. Ueda, S. Imada, T. Muro, Y. Saitoh, S. Suga, F. Matsukura, and H. Ohno, Physica E 10, 210 (2001).

15:40 Tea/Coffee break and posters

16:10 Dr Bryan Gallagher

School of Physics & Astronomy, University of Nottingham

GaMnAs: improved materials and the emerging understanding of magnetic and magnetotransport properties.

By careful control of MBE growth conditions and post growth annealing procedures we have produced GaMnAs epilayers which high conductivities and Curie temperature up to 159 K. We demonstrate that the improvement in material properties resulting from annealing is due to the out diffusion of interstitial Mn. The high conductivies of our material makes it possible to obtain accurate hole densities for a range of Mn compositions. We find that compensation is very low in best samples. We show that our measured Curie Temperatures, Hall conductivities and AMR are in good agreement with the mean field theory. We also find that there is no evidence of a fundamental magnetisation deficit in our material. Time permitting we will also discuss the room temperature ferromagnetism we observe GaMnN, transition metal doped oxides.

17:10 Dr Tomasz Story

Institute of Physics, Polish Academy of Sciences
Al. Lotnikw 32/46, 02-668 Warsaw, Poland

Ferromagnetic EuS-PbS semiconductor heterostructures

EuS-PbS ferromagnetic multilayers constitute all-semiconductor ferromagnetic-nonmagnetic structures with magnetic layers of EuS (a model nonmetallic Heisenberg ferromagnet) and diamagnetic layers of PbS (IV-VI semiconductor compound well known for its infrared optoelectronic applications). Both EuS and PbS crystallise in the same rock salt structure and their lattice parameters differ only by 0.5\%. Therefore, employing various high vacuum deposition techniques epitaxial quality EuS-PbS multilayers can be grown.
Ferromagnetic transition temperature in EuS-PbS multilayers depends on the thickness of the magnetic layer as well as on the thermal strain brought about by the difference between the thermal expansion coefficients of the

substrate and the multilayer structure [1]. For EuS-PbS trilayers and superlattices with ultrathin PbS spacer layers one observes (in neutron diffraction, neutron reflectivity and magnetic hysteresis measurements) pronounced magnetic effects related to the antiferromagnetic interlayer coupling between ferromagnetic layers of EuS via nomagnetic PbS spacer [2,3]. These effects are discussed for the variety of EuS-PbS layered structures grown epitaxially on KCl, BaF2 and n-PbS monocrystalline substrates.

Due to the large spontaneous exchange splitting of the conduction band states observed in EuS below its ferromagnetic transition temperature, the EuS-PbS heterostructures form an intriguing spintronic and spin optoelectronic system with nonmagnetic PbS quantum wells and ferromagnetic EuS electron barriers of easily (temperature and magnetic field) controlled height [3]. Recent photoluminescence, magnetotransport and electron tunnelling studies of the spin dependent effects in EuS-PbS structures are discussed together with the analysis of photoemission spectroscopy investigations of the key spintronic features of the EuS-PbS multilayers electron structure, i.e. the contribution of Eu $5d$ and $4f$ electron states to the density of states of EuS-PbS multilayers.

[1] A. Stachow-Wjcik, T. Story, W. Dobrowolski, M. Arciszewska, R.R. Ga__zka, M.W. Kreiveld, C.H.W. Swuste, H.J.M. Swagten, W.J.M. de Jonge, A. Twardowski, A.Yu. Sipatov, Phys. Rev. B 60, 15220 (1999).

[2] H. K_pa, J. Kutner-Pielaszek, J. Blinowski, A. Twardowski, C.F. Majkrzak, T. Story, P. Kacman, R.R. Ga__zka, K. Ha, H.J.M. Swagten, W.J.M. de Jonge, A.Yu. Sipatov, V.V. Volobuev, T. Giebultowicz, Europhys. Lett. 56, 54 (2001).

[3] T. Story, Physica Status Solidi (b) 236, 310 (2003).

18:10 End of session

Posters and SRS Facility tour

19:00 Buffet provided in Science Centre

Friday 12th September 2003

09:00 Dr Russell P. Cowburn (Durham University Physics Department)

Magnetic nanostructures for digital logic

Spintronic devices such as magnetic random access memory (MRAM) have to-date
only been able to store magnetic information. We have made a ferromagnetic
device which is able to process magnetic information as well as store it.
As in MRAM, we represent information by the ferromagnetic magnetization
direction. Information is transported from one point to another by the
motion of a domain wall through a nanoscale track of ferromagnetic material.
In order to process information, 4 different circuit architecture elements
are required: a NOT gate, a comparison gate (e.g. AND or OR), a fan-out
element and a track-crossing element. We have demonstrated experimentally
designs for all of these.

As an example, Fig. 1 shows a micrograph of the element that performs the
logical NOT operation [1]. When this two-terminal ferromagnetic structure
is incorporated into a magnetic feedback loop made from 200nm wide Permalloy
tracks, the junction performs a frequency division operation on an applied
oscillating magnetic field. Up to 11 of these junctions are then directly
linked together to create a magnetic serial shift register (Fig. 2).   This
shows how functions usually only associated with microelectronics, i.e. NOT
logic functions, digital frequency division and shift register operation,
can also be performed in all-metallic ferromagnetic devices. The devices
are non-volatile, radiation-hard and, being all-metallic, have excellent
potential for scaling deep into the nanoscale regime.

[1] Allwood et al. Science 296, 2003 (2002).

Figures can be found at http://www.srs.ac.uk/srum/satellite_1.htm

10:00 Prof Ulrich Hillebrecht

Forschungszentrum Karlsruhe, Institut f\"ur Festk\"orperphysik, P.O. Box
3640, 76021 Karlsruhe, Germany.

Antiferromagnetic domains imaged by photoemission microscopy

To achieve an adequate understanding of the micromagnetism of antiferromagnets, information about the antiferromagnetic domains and how they are influenced by various experimental parameters is required. Spatially resolved polarization dependent x-ray absorption as provided by photoemission microscopy [1] can yield this information with high resolution and chemical sensitivity. Contrast between differently oriented antiferromagnetic domains is generated by linear magnetic dichroism when the excitation energy is tuned to the core level excitation threshold. On NiO (100) surfaces, one finds usually stripe-shaped T domains with domain boundaries running along in-plane [10] or [11] directions. The width of the stripe domains amounts up to a few tens of microns. The domain contrast disappears on heating above the Nel temperature, and re-appears with the same domain shapes on cooling.

By exploiting the inherent polarization dependence of the antiferromagnetic contrast, we obtain images showing the antiferromagnetic domain walls, while the contrast between the domains themselves is suppressed [3]. The width of the walls between T domains is typically 150 nm. We also observe walls within T domains where the orientation of the AF vector (i.e. the difference of the two sublattice magnetization vectors) is identical on both sides of the wall. These walls can be characterized as s-like, with a rotation of the AF vector by 180°. The width of these walls is of the order of 200 nm. A model taking into account the rather large magnetostrictive strains occurring in antiferromagnetic NiO, the wall properties can be well reproduced. For ferromagnetic Co or Fe deposits on NiO we find a collinear coupling between the Ni and Co/Fe moments [3], in contrast to a SEMPA study [4] and a theoretical modelling [5] of for a compensated interface.

1. F.U. Hillebrecht, H. Ohldag, N. Weber, C. Bethke, U. Mick, M. Weiss, and J. Bahrdt, Phys. Rev. Lett. 86, 3419-3422 (2001).

2. N.B. Weber, H. Ohldag, H. Gomonaj, and F.U. Hillebrecht, in print.

3. H. Ohldag, A. Scholl, F. Nolting, S. Anders, F.U. Hillebrecht, and J. Sthr, Phys. Rev. Lett. 86, 2878-2881 (2001).

4. H. Matsuyama, C. Haginoya, and K. Koike, Phys. Rev. Lett. 85, 646 (2000).

5. N.C. Koon, Phys. Rev. Lett. 78, 4865 (1997).

10:30 Coffee break and posters

11:00 Dr Hermann A. D\"urr

BESSY, Berlin

Femtosecond Spin Dynamic in Magnetic Materials

Magnetism is a collective phenomenon involving correlated electrons. The
relevant interactions in magnetic solids such as exchange, spin-orbit and
electron-phonon coupling are of various strength and lead to different
characteristic time scales for energy transfer between orbital, spin and
lattice degrees of freedom. In this talk an overview will be given how
pump-probe experiments using optical fs-lasers offer unique possibilities to
investigate the ultra fast spin dynamics following a fs excitation of the
electronic system. Such studies are of direct relevance for establishing
the ultimate time scale for magnetic switching in future data storage
devices. The availability in the near future of fs soft x-ray pulses
offering elemental and orbital sensitivity is expected to revolutionize this
field. Applications for probing element resolved the magnetization dynamics
in magnetic semiconductors will be discussed.

12:00 Dr Thomas Schulthess

Electronic Structure and Valence of Mn impurities in III-V semiconductors

T. C. Schulthess and G. M. Stocks
Center for Computational Sciences, Oak Ridge National Laboratory

W. Temmerman and Z. Szotek
Daresbury Laboratory, UK

W. H. Butler
MINT Center, University of Alabama

Substitutional Mn impurities in III-V semiconductors can acquire either
a divalent or a trivalent configuration. For example, it is generally
accepted that Mn in GaAs is in a ($\it d^5+h$) configuration with five
occupied Mn $\it d$-orbitals and a delocalized hole in the valence
band. In contrast, Mn in GaN is believed to be in a $\it d^4$
configuration with a deep impurity state that has $\it d$-character. But
there have recently been some discussions about the possibility of
having some Mn ion in GaN assuming a divalent ($\it d^5+h$) type

configuration.

In order to achieve carrier induced ferromagnetism, the desired state of the Mn ions in III-V semiconductors is the ($\ti d^5+h$) configuration. We have therefore performed ab-initio calculations of the Mn valence when it substitutes Ga in various III-V semiconductor hosts. We use the self-interaction corrected local spin density (SIC-LSD) method which is able to treat localized impurity orbitals properly. In particular we find that the method is capable of predicting the ($\ti d^5+h$) state of Mn in GaAs. For Mn in GaP and GaN the calculations predict a trivalent $\it d^4$ state in the idealized system. The energy differences between $\it d^4$ and ($\ti d^5+h$) configurations in GaP are, however, very small. Introduction of defects or donors doe change the valence of Mn in GaP, favoring the divalent state under certain circumstances.

Posters (submitted abstracts) Dr Sergey Okatov

Correlation effects in electronic structure of diluted magnetic semiconductors

L. Choincel (1), S.Okatov(1), I.A. Abrikosov (2), M.I. Katsnelson (2), and A.I. Lichtenstein (1)

1 Katholieke Univesiteit Nijmegen, NL-6525ED Nijmegen, The Netherlands

2 Uppsala University, P.O.Box 530, S-751 21 Uppsala, Sweden

We investigate the role of the correlation effects in the electronic structure of diluted magnetic semiconductors MnGaAs in the framework of the ab-initio LDA, LDA+U and LDA+DMFT methods. Two hypothetical situations containing (6\%, 12.5\%) and respectively a realistic case (6.25\%) of Mn impurities are investigated.

According to our calculations LDA fails in the proper prediction of the electronic structure of these compounds. Using a static self-energy (LDA+U) with the physically reasonable value of U=4eV is sufficient to describe the unoccupied part of the spectral function (DOS). On the

other hand for the occupied part, the LDA+U produce too narrow bands and fails in describing the position of experimentally found XPS main peak (3.4eV). Choosing a lower value for the on-site Colulomb correlations (U=2) we succeed in reproducing the main peak positions in the occupied as well as unoccupied part of DOS. Even thought this calculation reproduce fairly well the low and high energy scales, it is not sufficient to describe the situation in the vicinity of the Fermi level. This motivated us to use an energy dependent self-energy in the framework of LDA+DMFT in order to clarify the nature of carriers at E_F.

6   General Workshop/Conference Announcements

6.1   First Workshop on Predictive Capabilities for Strongly Correlated Systems

7-9 November, 2003

Knoxville, Tennessee, U.S.A.

The First Workshop on Predictive Capabilities for Strongly Correlated Systems will be held on November 7-9, 2003 on the Knoxville campus of the University of Tennessee. This workshop is part of the Computational Material Science Network (CMSN)of the U.S. Department of Energy. The goal is to bring together all participants of the network, students, postdocs as well as experimentalists and theorists working in the area of strong correlations to discuss science, research plans, current and future collaborations as well as various issues of organization of the CMSN. We plan to have: (i) talks related to the research proposals from the lead investigators of the CMSN (ii) talks from non-CMSN speakers who are lead experts of the experiment and theory of strongly correlated systems (iii) overviews of recent research from participants of the network. The workshop will start on Friday afternoon, November 7, 2003 and will end on Sunday afternoon, November 9, 2003. Further details on the workshop and information for participants is available on the web site:

`http://cst-www.nrl.navy.mil/~singh/pcscs-workshop`

or by contacting one of the organizers: (1) Adolfo Eguiluz, eguiluz@utk.edu (2) Sergej Savrasov, savrasov@oak.njit.edu (3) David J. Singh, singh@dave.nrl.navy.mil (4) Shiwei Zhang, shiwei@spiffy.physics.wm.edu.

Limited funding is available to support participants, including some outside participants.

6.2 Hands-on Course on QMC

"Joint DEMOCRITOS - ICTP School on Continuum Quantum Monte Carlo Methods"

12-23 January, 2004, Miramare-Trieste, Italy

Organized by: D. Ceperley, S. Baroni and S. Moroni
Funded by: ICTP and DEMOCRITOS

`http://agenda.ictp.trieste.it/agenda/current/fullAgenda.php?ida=a0332`

An international course on quantum Monte Carlo simulations will be held at the Abdus Salam International Centre for Theoretical Physics (ICTP). For details check the above website of the school.

6.3 CECAM Tutorial

Linear-scaling density-functional calculations with local orbitals

CECAM - Lyon, 9-13 December 2003

Organized by Emilio Artacho (emilio@esc.cam.ac.uk) and Pablo Ordejon (ordejon@icmab.es)

The fundamentals for the use of linear-scaling DFT methods based on localised orbitals will be taught, as well as the practicalities for the use of two different methods:

* The Siesta method, based on atomic orbitals as basis sets,
The Conquest method, based on B-splines (finite-element approach).

Morning sessions with lectures will be followed by hands-on afternoon sessions for the practice in the use of Siesta, Conquest, and auxiliary programs for the generation of pseudopotentials and bases.

For more information and registration:

http://www.uam.es/departamentos/ciencias/fismateriac/siesta/tutlyon.html

and

http://www.cecam.fr/activities/tutorials2003.html

7 General Job Announcements

Postdoctoral Position
Department of Physics, New Jersey Institute of Technology

Applications are invited for post-doctoral research positions in theoretical condensed matter physics. The initial appointments are for one year, with renewal possible upon mutual agreement and availability of funding up to total of three years. The successful candidates will carry out development of methods, algorithms and computer programs based on many-body dynamical mean field theories as well as their applications for calculating properties of realistic strongly correlated systems. These include, but are not restricted to, transition metal oxides, f-electron systems, high-temperature superconducting materials and so on. Developments will be carried out at Department of Physics, New Jersey Institute of Technology in close collaboration with Center for Materials Theory at Rutgers University. Applicants with a strong background in electronic structure and many-body theories are particularly encouraged to apply. Knowledge of computer languages such as C++ and Fortran 90 is a big plus. Review of applicants will begin immediately and continue until the positions are filled.

Candidates must have a PhD in physics, materials science, chemistry or a related field. Please send applications including a vita, list of publications, and e-mail addresses of at least two references by e-mail (preferable) to savrasov@oak.njit.edu or by paper mail to

Prof. S. Y. Savrasov
Department of Physics
New Jersey Institute of Technology
University Heights
323 Martin Luther King Blvd.
Newark, NJ 07102-1982
USA

More information about the research can be found on

```
http://physics.njit.edu/~savrasov
```

Postdoctoral Position

Theory Department, Max-Planck-Institute of Microstructure Physics
Halle, Germany

A postdoctoral position is available at the Theory Department of the Max-Planck-Institute of Microstructure Physics in Halle.

The project deals with the development of new calculational techniques for first-principles studies of magnetic excitations in complex systems. The density functional theory provides the mathematical basis for this project.

An intensive experience in scientific programming and strong background in mathematics and solid state physics are requested for this project and should be reflected in the application.

The Max Planck Institute is one of the leading research institutions in Germany. We offer excellent working conditions in an international and interdisciplinary environment.

Interested candidates should send a detailed curriculum vitae and the names of two referees to:

L. Sandratskii
Max-Planck-Institute of Microstructure Physics
Weinberg 2
D-06120 Halle
Germany

email: lsandr@mpi-halle.de

One Postdoctoral- and two Ph. D. positions

Max Planck Institute for Chemical Physics of Solids; MPI CPfS

Dresden, Germany

In the framework of a recently established "Emmy Noether" group, the Max-Planck-Institut fuer Chemische Physik fester Stoffe (Max Planck Institute for Chemical Physics of Solids; MPI CPfS) in Dresden has an opening for a Postdoc position and for two PhD candidates in the field of theoretical solid state physics.

The scientific scope of the research is the description of phase transitions in physically complex behaving compounds with competing interactions. The goal of the research project is the improvement of the description of real systems with strong electron correlations starting from density functional theory. This band structure approach shall be joined by a subsequent description in terms of many body model Hamiltonians. The results shall be applied to compounds recently synthesized at our institute. The work will be in close collaboration with the related chemistry research fields of the MPI CPFS.

Experience with numerical work (especially Fortran) and Linux is desirable.

Candidates with interdisciplinary research interests and a degree (MSc, Diplom) in the fields of solid state physics and/or chemistry are welcome to apply. Applications including a CV, a short statement of research interests and a list of publications should be send to the address below. Applications will be accepted until positions are filled.

Helge Rosner

Max-Planck Institute for Chemical Physics of Solids

Noethnitzer Str. 40

D-01187 Dresden

Germany

email: rosner@cpfs.mpg.de

Phone: +49 351 4646.4211

Fax: +49 351 4646.4002

Home page: `http://www.cpfs.mpg.de/index_en.html`

 `http://maugre.ucdavis.edu`

POSTDOCTORAL POSITIONS IN COMPUTATIONAL NANOSCIENCE

LAWRENCE BERKELEY NATIONAL LABORATORY

Lawrence Berkeley National Laboratory has multiple postdoctoral openings in the development of methods for electronic structure calculations of nanosystems. Positions are available for methodology development for large nanosystem atomistic calculations; the development of mathematical/computational methods for large nanosystems and possibly another position for high level many body electronic methods. The hired persons will work with Lin-Wang Wang, Andrew Canning and Osni Marques of the scientific computing group of the Computational Research Division at LBNL. The positions are funded by different sources and will involve collaborations with other researchers in these fields, such as Alex Zunger (NREL), Jack Dongarra (University of Tennesse) and Steven Louie, Martin Head-Gordon (LBNL, UC Berkeley), Juan Meza (LBNL). A Ph.D degree in physics, chemistry, maths or a related field is required and experience in ab initio electronic structure calculations is desired. Interest in algorithmic/mathematical development and ability for scientific code writting is highly desired.

The position is initially for one year with the possibility of renewal for up to three years. A highly competitive salary will be offered. Our division is closely affiliated with NERSC at LBNL which is the largest civilian research computer center in the United States with a 6656 processor IBM SP computer. The scientific computing group is a diverse group working on various aspects of scientific computation. More information about our research activities can be found at

http://www.nersc.gov/research/SCG.

Interested persons should send a curriculum vitae to:

Andrew Canning acanning@lbl.gov
Lin-Wang Wang lwwang@lbl.gov
Osni Marques OAMarques@lbl.gov

POSTDOCTORAL POSITION IN NANOSCIENCE
NATIONAL RENEWABLE ENERGY LABORATORY

A postdoctoral research position in the area of inverse solutions for electronic properties of nanostructures is available in the National Renewable Energy Laboratory's (NREL) Computational Sciences Center in Golden, CO. The work involves developing new mathematical and computational methodologies capable of designing materials with relevant properties using electronic structure methods for million atom nanostructures.

The hired person will primarily work with Kwiseon Kim and Wesley Jones in computational sciences center at NREL. The position is funded by Theory, Modeling and Simulation in Nanoscience initiative from DOE and will involve close collaboration with Alex Zunger (Basic Sciences Center, NREL), Lin-Wang Wang (Lawrence Berkeley National Lab) and Jack Dongarra (University of Tennessee). Significant use of supercomputing resources at the National Energy Research Scientific Computing Center (NERSC) and at NREL is expected.

A Ph.D. degree in physics, material science, chemistry, math or related field is required. Experience in electronic structure calculations and in global optimization methods is desired. Interest in algorithmic/mathematical development and ability for scientific programming including parallel programming is highly desired and should be reflected in the application.

The position is initially for one year with the possibility of renewal for up to three years. The start date is during the fall of 2003 or early 2004.

Interested candidates should send curriculum vitae, list of publications (including preprints of unpublished papers if possible), and arrange reference letters addressed to:

Kwiseon Kim
Mail Stop 1608
Computational Sciences Center
National Renewable Energy Laboratory
1617 Cole Blvd.
Golden, CO 80401
`kwiseon_kim@nrel.gov`

NREL is an equal opportunity employer and proud of its commitment to diversity. Women and minorities are encouraged to apply.

Postdoctoral Openings

Theoretical Condensed Matter Physics, Computational Physics, Quantum Computing

The Frontier Research System, RIKEN, near Tokyo, Japan

and

University of Michigan at Ann Arbor, USA

Recently, four linked groups working on nanoscience (quantum computing, quantum nano-magnetism, next-generation coherent electron-wave microscopy, and our condensed matter theory group) were established at the Frontier Research System (FRS), The Institute of Physical and Chemical Research (RIKEN), near Tokyo, Japan.

Applications are invited for several postdoctoral and visiting researcher positions in computational and theoretical condensed matter physics.

Our research focuses on several aspects of complex systems research and theoretical condensed matter physics, with special emphasis on quantum computing, superconducting qubits, and vortex dynamics.

RIKEN offers competitive salaries, and outstanding computational facilities. More information on RIKEN can be found at:

http://www.riken.go.jp/

Information on the Frontier Research System can be found at:

`http://www.riken.go.jp/engn/r-world/research/lab/frontier/index.html`

`http://www.riken.go.jp/engn/r-world/research/lab/frontier/quantum/digital/index.html`

Information on our previous research projects can be found at:

`http://www-personal.engin.umich.edu/~nori/`

Recent preprints from our group can be obtained upon request from fnori@riken.jp

Complete applications in PDF format (CV, list of publications, selected recent publications, and letters of reference) should be sent electronically to:

Prof. Franco Nori
Frontier Research Program
RIKEN, Hirosawa 2-1,
Wako-shi, Saitama, 351-01
Japan

+81-48-465-8048 fax

email: fnori@riken.jp

Permanent address:

Professor Franco Nori

Department of Physics

The University of Michigan

Ann Arbor, MI 48109-1120, USA.

Postdoc Position in Theoretical Solid State Physics
IFW Dresden, Germany

We would like to announce an open postdoc position at the Institute for Solid State and Materials Research Dresden (http://www.ifw-dresden.de).

The project includes

(1) density functional studies of magnetism on transition metal, lanthanide, and actinide elements and compounds, using the recently developed FPLO code (http://www.ifw-dresden.de/FPLO/);

(2) code development with respect to non-collinear magnetic structures.

Close contact with related experimental work at IFW Dresden, University of Technology Dresden (http://www.tu-dresden.de), and the Max-Planck Institute for the Chemical Physics of Solids Dresden (http://www.cpfs.mpg.de) is envisaged, as well as collaboration with several Dresden groups active in solid state theory.

The applicant should preferably have a safe background in solid state physics, good knowledge of density functional theory, and experience in the understanding and development of extended code for numerical purposes (FORTRAN 90 and C).

We offer a one-year position, extendable up to 3 years, at the level BAT IIa-O (annual net income about kEUR 20, depending on age and family status).

The Department of Theoretical Solid State Physics at IFW Dresden consists of thirteen PhDs in solid state theory, four PhD students, and several guest scientists, see http://www.ifw-dresden.de/agtheo/eagtheo1.htm. The group has up-to-date computer facilities, daily coffee meetings, and a lively exchange with a number of other groups inside and outside of Dresden (theoretical and experimental, physics and chemistry). The city of Dresden is situated mid-way between Berlin and Prague, in the valley of river Elbe. With a population of about 500,000, it is known for a rich cultural live and for its baroque silhouette.

Interested candidates should send their application together with a curriculum vitae, a list of publications or current research activities, and other relevant material to:

Dr. Manuel Richter
Dept. of Theoretical Solid State Physics
IFW Dresden e.V.
P.O. Box 270016
D-01171 Dresden, Germany

Tel. +49-351-4659-360
Fax. +49-351-4659-490
email m.richter@ifw-dresden.de
http://www.ifw-dresden.de/~manuel

Two post-doctoral- and two postgraduate student-positions
Physics Department and NMRC, University College Cork, Ireland

Two post-doctoral positions and two postgraduate student positions, available in a joint project between the Physics Department and NMRC, University College Cork, funded by Science Foundation Ireland. Funding is available for up to four years and the positions can start any time after October 1, 2003.

The focus of the project is the development and application of ab-initio electronic structure calculations and other electronic structure methods to calculate the scattering of charge carriers by defects and phonons in semiconductor alloys, with particular reference to dilute nitride and Si/Ge systems. Related work is ongoing at University College Cork, in the groups of Dr. James Greer (on transport in nanostructures and on electronic and structural properties of high-K dielectric layers) and Prof. Eoin O'Reilly (on optoelectronic applications of dilute nitride alloys and physics of laser systems) and a close collaboration between this project and their work is anticipated. Large-scale computing facilities (Beowulf cluster with over 100 dual-processor nodes) will be available locally for computational work on this project.

Enquiries should be made to Prof. Stephen Fahy at s.fahy@ucc.ie.

Postdoctoral position in Computer Simulation of Nanostructures

Materials Simulation Center
Penn State

The Materials Simulation Center at Penn State is looking to fill one postdoctoral position in the area of atomistic simulation of materials. Applicants are expected to have a strong background in condensed matter physics or chemistry and experience with electronic structure and/or molecular dynamics codes. The Center is a University-wide facility of the Materials Research Institute (MRI) promoting interdisciplinary research in the computer simulation of materials. The Center supports collaborations with several departments including Chemistry, Chemical Engineering, Energy and Geo-Environmental Engineering, Geosciences, Materials Science and Engineering, and Physics. Current projects include the study of structural and optical properties of small ionic clusters, phonons in nanostructures, water interaction with crystalline and amorphous ionic surfaces, epitaxial growth of metallic thin films, and nanostructure precipitates in alloys. The successful candidate will have the opportunity to contribute to any of these ongoing projects, in addition to contributing to the initiation of new research thrusts. The candidate is expected to assist in the installation and development of our simulation codes. The Center operates excellent computer facilities including a 352 CPU Beowulf cluster.

This two-year position is available immediately. Further details can be obtained by e-mail to sofo@psu.edu. Please email a cover letter with your resume and list of publications, and 2-3 reference letters, to Jorge O. Sofo at sofo@psu.edu, or fax them to 814-865-3604.

Penn State is committed to affirmative action, equal opportunity and the diversity of its workforce.

Jorge O. Sofo
Director
Materials Simulation Center
104 Davey Lab PMB #68
University Park, PA 16802
USA

PhD Studentship in Computational Nanotechnology
University College London, United Kingdom

We have money from the Interdisciplinary Reserach Collaboration in Nanotechnology for a PhD student at UCL in the Condensed Matter and Materials Physics group. Below is a description of the project we have in mind. If you think you might be interested in this project please contact either one of:

Andrew Horsfield a.horsfield@ucl.ac.uk
David Bowler david.bowler@ucl.ac.uk

This project will be a computational study of nanowires both isolated and on semiconductor substrates. We will investigate their structure, both atomic and electronic, at the level of density functional theory, and will study electrical conduction and heat generation in the nanowires using our recently developed time dependent conduction formalism.

The student will be exposed to the phenomenology of nanowires, and more generally to the world of nanotechnology. A very solid grounding in electronic structure methods, notably density functional theory and tight binding, will be provided. Further, the student will be working with state-of-the-art conduction formalisms, and will have the opportunity to contribute new computer code. Links with experiment will be actively sought at all points through the project, both in terms of the conduction properties of nanowires, and their structure and nature on semiconductor surfaces.

Marie Curie Host Fellowships for PhD Students

"Ab initio calculations of many-body effects in electronic spectra"

Laboratoire des Solides Irradies, Ecole Polytechnique, Palaiseau, Paris, France

Several Marie Curie host fellowships for PhD students will be available at the Laboratoire des Solides Irradies, Ecole Polytechnique, Palaiseau (Paris, France), in collaboration with the group of Dr. Lucia Reining. The fellowships are for 6 to 12 months. The research will be inserted in the framework of ongoing collaborations within the EU Research Training Network network "NANOPHASE: Nanoscale photon absorption and spectroscopy with electrons." The overall topic of the network research is the theory of nanometer-scale structures and the spectroscopic processes that can be used to characterise those structures, their electronic and optical properties, and their growth. These are studied using fundamental theory and state-of the-art ab initio computer simulations. (Please see also http://www-users.york.ac.uk/~rwg3/nanophase.html). In particular, the group in Palaiseau has been working during the last years in the field of one - and two-particles Green's functions calculations (GW, excitons in optical absorption), and Time-Dependent Density Functional Theory. These topics should be developed further, concerning both theory and numerics, preferably towards applications to nanostructures and oxides including defects. The work will include the determination, within DFT-LDA, of structural relaxations, the calculation of the corresponding quasiparticle levels using the GW method, and absorption and luminescence spectra including local field and excitonic effects. Computer codes are already available in Palaiseau. Computational facilities include locally several Compaq DS-25 Workstations, and national supercomputer time.

Candidates should be working on a thesis subject close to these topics, preferentially about the optical properties of amorphous systems. He/she should have a strong background in theoretical condensed matter physics and like to perform both analytical and numerical work.

The position is for about one year, starting from the middle of November, 2003. The deadline for applying for this position is Saturday, September 20.

The topic is ab initio calculations of phase change media which have a high potential for rewritable optical and electronic data storage. Applications are based on the significant change of the optical properties of these materials upon structural phase transition, from amorphous to crystalline state. In particular, the proposed study will focus on crystalline and amorphous chalcogenide alloys, investigating the link between the atomic structure and the optical contrast. The calculation of the dynamical dielectric matrix will be performed as a first step within Time-Dependent Density Functional Theory. The induced exchange-correlation contribution will be evaluated in the adiabatic local density approximation (TDLDA), and by an improved scheme, taking into account long-range correlations, which has been recently developed in Palaiseau [1-3].

[1] L. Reining, V. Olevano, A. Rubio, and G. Onida, Phys. Rev. Lett. 88, 066404 (2002). \\
[2] Francesco Sottile, Valerio Olevano, and Lucia Reining, Phys. Rev. Lett. 91, 056402 (2003). \\
[3] G. Onida, L. Reining, and A. Rubio, Reviews of Modern Physics 74, 601 (2002). \\

If you are interested in this or upcoming possibilities, please do not hesitate to contact

Silvana Botti e-mail: Silvana.Botti@polytechnique.fr

Silvana Botti
Laboratoire des Solides Irradies
Ecole Polytechnique
91128 Palaiseau, France
Tel. 0033-(0)1-6933-4682
Fax. 0033-(0)1-6933-3022

PHD STUDENTSHIPS IN NANOSCALE TRANSPORT THEORY

Two PhD studentships are available for the study of "Current Induced Effects in Nanoscale Conductors". The project is sponsored by the Irish High Education Autority within the North-South Programme for Collaborative Research, and is a collaboration between the Computational Spintronics group at Trinity College Dublin and the Atomistic Simulation Group at Queen's University Belfast. The project will be supervised jointly by Dr. Stefano Sanvito in Dublin and Dr. Tchavdar Todorov in Belfast.

The overall aim of the project is to develop a combined computational framework for quantum transport in nanoscale systems, capable of describing both current induced mechanical effects and the interplay between spin transport and microscopic magnetic properties. We wish to make extensions to our existing formalism for the description of current induced forces and the interplay between electronic current and vibrational degrees of freedom, and to apply this formalism to magnetic materials in order to investigate the effects of a spin-polarised current on the magnetic state of a nanoconductor. Spin pressure, Bloch wall movement and current induced magnetization flips will be modelled.

Both PhD projects will involve the development and the numerical implementation of quantum transport techniques combined with density functional or other electronic structure methods, in strong collaborations with other groups both in Europe and the USA. One of the students will be based in Dublin and the other in Belfast, with frequent visits to the partner institution.

The studentships will commence on the 1st November 2003. The Physics Departments at both Trinity College and Queen's University have a long and distinguished history. Currently the department in Dublin is host to the prestigious first phase of Science Foundation of Ireland Nanotechnology projects, attracting world class researchers and establishing internationally competitive facilities.

Candidates are invited to send a CV together with the full addresses of two potential referees, before 15 October 2003, by post or e-mail to BOTH:

Dr. Stefano Sanvito
Department of Physics
Trinity College
Dublin 2, Ireland
Tel: +353-1-6083065
Fax: +353-1-6711759
E-mail: sanvitos@tcd.ie

and

Dr. Tchavdar Todorov

School of Mathematics and Physics

Queen's University of Belfast

Belfast, UK

Tel: +44-28-90335293

Fax: +44-28-90241958

E-mail: T.Todorov@qub.ac.uk

Information about our research activity may be found at:
http://www.tcd.ie/Physics/People/Stefano.Sanvito/ and

http://titus.phy.qub.ac.uk/group/Tchavdar/

Further particulars regarding the Studentships are avaliable on request from Dr. Sanvito.

PhD Studentship

Institute for Theoretical Physics, Free University Berlin, Germany

A position for a PhD student is available immediately at the Free University Berlin. The position is funded through a priority program of the Deutsche Forschungsgemeinschaft (DFG) and is available for two years with a possible extension.

The project will be performed in collaboration with Dr. Stefan Kurth and Prof. E.K.U. Gross. It will focus on the construction and implementation of approximate functionals in current-density functional theory (CDFT), both in the static and the time-dependent case. In the static case, the aim is an improved description of open-shell systems by using orbital functionals in CDFT. In the time-dependent case the construction of an approximate functional in the linear-response regime is planned.

The successful candidate should hold a university degree in physics (masters, diploma, or equivalent). The position requires a good background knowledge on the foundations of density functional theory. Previous experience with electronic structure calculations as well as programming experience is welcome. Applications including a CV, a list of publications and the contact addresses of two potential references should be addressed to (preferably by e-mail)

Dr. Stefan Kurth
Institute for Theoretical Physics
Free University Berlin
Arnimallee 14
D-14195 Berlin
Germany
e-mail: kurth@physik.fu-berlin.de

Postdoctoral Research Position in Computational Materials Physics/Chemistry

National Renewable Energy Laboratory, Golden, Colorado

We at the National Renewable Energy Laboratory invite applications for a total of three theoretical postdoctoral positions, available immediately. Initial assignment is for a year, but renewable upon funding availability, performance, and mutual agreement up to a total of three years. The research direction can be one of the followings: to apply and develop first-principles theories for (1) a new program on hydrogen storage in carbon based nanotubes and organic materials, (2) doping and defect control in next-generation optoelectronic semiconductors, and (3) surface-related growth phenomena such as spontaneous ordering, solubility enhancement, and quantum-dot array formation. The starting salary is US\$43-50K/year depending on the qualification. Candidate should send curriculum vitae, a list of publications (including preprints of unpublished papers, if possible) and arrange three reference letters to

Dr. Shengbai Zhang
National Renewable Energy Laboratory
1617 Cole Blvd.
Golden, CO 80401, USA
Email:szhang@nrel.gov

NREL, in the vicinity of Denver, is one of DOE's prestige National Laboratories, a gate to the beautiful Rocky Mountains and ski resorts, and an equal opportunity/affirmative action employer.

RESEARCH SCIENTIST

CCLRC Daresbury Laboratory, Cheshire or,

Rutherford Appleton Laboratory, Oxfordshire, U.K.

The Computational Materials Science group at CCLRC is seeking to fill a staff position concerned with the first principles simulation of materials. The successful candidate will work within an internationally recognised team of scientists to develop the theoretical framework and computational tools for the simulation of material properties. This work will be performed in collaboration with leading academic research groups in the United Kingdom. There will also be an opportunity to work closely with researchers performing experiments on the synchrotron radiation source at Daresbury and the spallation neutron source at Rutherford Appleton Laboratory. The location of the post is flexible; it may be based at the Daresbury or Rutherford Laboratories.

Candidates should have a good degree at Ph.D. level and a strong research track record in theoretical physics, chemistry or a related discipline. A strong background in advanced scientific computing and experience of collaborative software development is also desirable.

For further information contact: Professor Nicholas M Harrison at n.harrison@dl.ac.uk or http://www.cse.dl.a

The salary range for a band 4 is up to 32740 on a salary range from GBP 26190 to GBP 36010 and for a Band 5 it is up to GBP 25790 on a salary range from GBP 20630 to GBP 28370 (pay award pending). Progression within the salary range is dependent upon performance. A non-contributory pension scheme, flexible working hours and a generous leave allowance are also offered.

Application forms can be obtained from:

Recruitment Office,
Human Resources Division,
Daresbury Laboratory,
Daresbury,
Warrington,
Cheshire,
WA4 4AD.

Telephone (01925) 603114 quoting reference VND189/03.

More information about CCLRC is available from CCLRC's World Wide Web pages at http://www.cclrc.ac.uk

All applications must be returned by 10th October 2003.

The CCLRC is committed to Equal Opportunities. CCLRC is a recognised Investor in People. A no smoking policy is in operation.

RESEARCH OPPORTUNITIES AT COMP

Laboratory of Physics, Helsinki University of Technology (HUT)

COMP is a research unit at Laboratory of Physics, Helsinki University of Technology (HUT), specialising in computational materials science and condensed-matter physics (see www.fyslab.hut.fi). It has been designated a Center of Excellence by the Academy of Finland for the period 2000-2006. HUT is the leading university of technology in Finland.

COMP is anticipating several appointment opportunities for qualified candidates, both at the Ph.D. student and post-doctoral levels. The Ph.D. studentships are usually funded for a four-year period, and the post-doctoral appointments are typically for two years. The starting remuneration (taxable) for Ph.D. students is around 1800 euro and for post-doctoral research associates around 2700 euro per month.

COMP has excellent facilities for theoretical and computational research, including access to high-performance computing resources. It has more than 50 researchers (including M.Sc. students):

The present research activities cover wide areas of condensed-matter and materials physics as well as statistical physics of complex systems, including those of biological relevance.

For further details and application procedures, interested candidates are encouraged to contact one of the senior researchers at COMP:

Profs. Risto Nieminen , Martti Puska, Juhani von Boehm (electronic properties of materials),

Prof. Tapio Ala-Nissilä, Dr. Mikko Alava (statistical physics and nonequilibrium dynamics),

Dr. Ilpo Vattulainen (biological physics).

The e-mail addresses are avalailable at the website

http://www.fyslab.hut.fi

Postdoctoral Position in Computational Surface Physics

Institute of Solid State Theory at the University of Muenster, Germany

A postdoctoral position is available in the Surface Physics Group of the Institute of Solid State Theory at the University of Muenster. The group develops and applies methods for ab-initio calculations of atomic, elec- tronic, vibrational and optical properties of semiconductors and their sur- faces. For recent publications of the group, see

http://www.uni-muenster.de/Physik/FT.

The successfull applicant will study hydrogen adsorption at cubic SiC surfaces using state-of-the-art ab-initio techniques. In particular, hydrogen-induced metallization of SiC(001) surfaces, as observed recently in experiment, will be analysed in detail. Available computer codes of proved methods can be used. Experience with density functional theory calculations would be advantageous. The successful applicant holds a PhD in Solid State Physics or Theoretical Quantum Chemistry.

If you are interested in this position, contact either one of:

Peter Krueger (kruger@uni-muenster.de)

Johannes Pollmann (pollman@uni-muenster.de)

or send your application with the usual material to

Prof. Dr. Johannes Pollmann
Institut fuer Festkoerpertheorie
Westf. Wilhelms-Universitaet Muenster
Wilhelm-Klemm-Str. 10
D-48149 Muenster
Tel.: (0251)83-36311 (33581)
Fax: (0251)83-33669

Postdoctoral Position in Surface Science at Extreme Conditions
Theoretical Chemistry, Ruhr-Universitaet Bochum, Germany

Applications are invited for a research associate position. The preferred starting date would be December 2003.

The ideal candidate would have significant experience in electronic structure theory, DFT/MD calculations, surface science, and heterogeneous catalysis. She or he would work primarily on using dynamical (Car-Parrinello) electronic structure methods in order to understand the complex processes involved in chemical reactions occurring at surfaces in contact with dense/hot water. In addition, he/she can also be involved in other challenging research projects including both method development and large-scale applications.

Information on the techniques used and developed are accessible via

http://www.theochem.ruhr-uni-bochum.de/go/cprev.html.

The Theoretical Chemistry Group at RUB offers an exciting interdisciplinary environment with excellent working conditions (including several in house parallel platforms and a 500 GFlop/s SCI machine).

Candidates should send a detailed resume including an outline of their research achievements and interests as well as contact information for academic references as one pdf/ps file to office@theochem.ruhr-uni-bochum.de.

Consideration of candidates will begin immediately and continue until the position is filled. The University particularly welcomes applications from women.

Professor Dominik Marx
Lehrstuhl fuer Theoretische Chemie
Ruhr-Universitaet Bochum
D-44780 Bochum
Germany
Phone : ++49 234 322 6485
Fax : ++49 234 321 4045
office@theochem.ruhr-uni-bochum.de
http://www.theochem.ruhr-uni-bochum.de/

PhD/Postdoc Position at CAMP
Technical University of Denmark

A theoretical PhD or postdoc project in the field of molecular electronics is open at Center for Atomic-scale Materials Physics (CAMP) at the Technical University of Denmark. The focus of the project is mechanical and transport properties of molecule-surface contacts. Recent experimental developments have made it possible to study the transport and mechanical response of individual molecules suspended between surfaces and it is the purpose of the present project to perform theoretical investigations of structure and dynamics of such molecular contacts. The project will involve the use of electronic structure and molecular dynamics techniques. It will be carried out at the Technical University of Denmark in close contact with experimental and theoretical activities at the University of Copenhagen.

Interested students and postdocs are encouraged to submit an expression of interest including a full CV and publication list preferably before September 26, 2003 to Prof. Karsten W. Jacobsen (kwj@fysik.dtu.dk).

Additional information about CAMP at http://www.fysik.dtu.dk. Additional information about the Nano Science Center at University of Copenhagen: http://www.nano.ku.dk

Contact information:

Prof. Karsten W. Jacobsen
CAMP, Dept. of Physics, DTU
DK-2800 Kongens Lyngby
Denmark
ph: +45 45 25 31 86
fax: +45 45 93 23 99
email: kwj@fysik.dtu.dk
www: `http://www.fysik.dtu.dk/~kwj`

Postdoctoral Positions and Ph.D. Positions in Computational Materials Science

Institut fuer Materialphysik, Universitaet Wien, Austria
http://cms.mpi.univie.ac.at

Two postdoctoral and two Ph.D. positions are available, to begin in Jannuary 2004, associated with Prof. Georg Kresse, Computational Materials Science Group at the Institute for Materials Science, University Vienna. The Group has developed and maintains the Vienna ab initio package (VASP), that is used world wide by 400 academic and industrial groups. An outstanding environment for acquiring first hand knowledge on density functional computations and program development is offered with special graduate courses for PhD students and a total of 40 scientists and PhD's working in this field.

The research will be performed in the domain of DFT and will involve methodological developments as well as applications of these developments to oxides, oxide growth, and chemical reactions on metal and oxidic substrates. A background in quantum mechanics and previous experience in FORTRAN programming are recommended.

Interested applicants should send (1) a CV including a publication list, (2) one or two reprints representative of previous research, and (3) two confidential letters of recommendation or contact information for references to:

Ao. Univ.-Prof. Georg Kresse
Institut fuer Materialphysik
Universitaet Wien
Sensengasse 8/12
A-1090 Wien, AUSTRIA

or

Georg.Kresse@univie.ac.at

When send by email, the application should include the CV and reprints as pdf files as well as a short cover letter in the email body.

Consideration of candidates will begin shortly and will continue until the positions are filled.

POST-DOCTORAL POSITION

Materials Design

Le Mans, France

A post-doctoral position is available at Materials Design in Le Mans, France within the European Research and Training Network "Ab-initio Computation of Electronic Properties of f-electron Materials". The research focuses on the optical properties of materials containing rare earth elements, such as optoelectronic devices and pigments. As a leading software technology company in the field of computational materials science, Materials Design offers an exciting environment, which combines advanced research with challenging industrial applications.

The candidate is expected to have experience in electronic structure methods, should be younger than 35 years, and should be a national of a Member State of the European Community (other than France) or of an Associated State or residing in the Community for at least five years prior to the present appointment.

Please send your applications by email to

Erich Wimmer

ewimmer@materialsdesign.com

Assistant Professor

IPCMS-GEMM, Strasbourg, France

Applications are invited for a permanent position at the Assistant Professor level. The starting date is October, 2004. Applicants must have a Ph.D degree, or equivalent experience, and preferably with a postdoc experience. The appointee will value effective teaching at the undergraduate and graduate levels, will have demonstrated excellence in research and can initiate and maintain a research program on ab initio electronic transport. The position is targeted to a materials theorist who has a good experience on condensed matter and electronic structure calculations. The appointee will teach at the University of Strasbourg and perform his/her research at the Institute of Physics and Chemistry of Materials of Strasbourg (http://www-ipcms.u-strasbg.fr).

In France, to apply for any assistant professor or professor position, the candidate should first submit a file to the ministry of education to be qualified at the national level. To know further about this procedure, the candidate should consult the following web page:

http://www.education.gouv.fr/personnel/enssup/antares/default.htm

The application deadline for the qualification is October 20, 2003. After this procedure, applicants should submit by email or regular mail a curriculum vitae, list of publications, a research plan, and the names and full addresses of three possible referees who are familiar with his/her work to M. Alouani or H. Dreysse, IPCMS-GEMM, BP 43, 23 rue du Loess, 67234 Strasbourg, France.

8 Abstracts

Magnetic circular dichroism and spin polarization in $3d \rightarrow 4f$ resonant photoemission in perpendicular geometry from Tb metal

M. Taguchi, G. van der Laan

Magnetic Spectroscopy, Daresbury Laboratory, Warrington WA4 4AD, UK

RIKEN/SPring-8, 1-1-1, Mikazuki-cho, Sayo-gun, Hyogo 679-5148, Japan

G. van der Laan

Magnetic Spectroscopy, Daresbury Laboratory, Warrington WA4 4AD, UK

E. Arenholz

Advanced Light Source, Lawrence Berkeley National Laboratory,

Berkeley, California 94720

S.S. Dhesi

Magnetic Spectroscopy, Daresbury Laboratory, Warrington WA4 4AD, UK

European Synchrotron Radiation Facility, BP 220, F-38043 Grenoble, France

E. Dudzik

Magnetic Spectroscopy, Daresbury Laboratory, Warrington WA4 4AD, UK

Hahn-Meitner-Institut, Glienicker Str. 100, D-14109, Berlin, Germany

Abstract

We present combined experimental and theoretical results for the magnetic circular dichroism in resonant $4f$ photoemission (MCD-RPE) from Tb metal in the perpendicular geometry (PG) at different photon energies across the whole of the $M_{4,5}$ resonance. The atomic calculations, which take into account the full multiplet structure and the coherent second-order optical process, give excellent agreement with new experimental results for the resonant photoemission decay. The angular dependence of the MCD-RPE and its strong spin polarization in the M_5 region are also reported. For a single-configuration state the variations in the spectral shape are found to be stronger as a function of angle than as a function of photon energy. Due to the presence of the multiplet structure in the intermediate state $3d^9 4f^9$ the coherent second-order optical process is essential for a correct description of the RPE. While the analysis of the spectra in parallel geometry yields accurate values of the spin-orbit, Coulomb and exchange interactions, only the angle dependent RPE provides the phase factors of the emitted photoelectron.

Resonant Photoemission in f electron Systems: Pu and Gd

J.G. Tobin, B.W. Chung

Lawrence Livermore National Laboratory, Livermore, CA

R.K. Schulze, J. Terry, J.D. Farr

Los Alamos National Laboratory, Los Alamos, NM

D.K. Shuh, K. Heinzelman, E. Rotenberg

Lawrence Berkeley National Laboratory, Berkeley, CA

G.D. Waddill

University of Missouri-Rolla, Rolla, MO

G. van der Laan

Magnetic Spectroscopy, Daresbury Laboratory, Warrington WA4 4AD, UK

Abstract

Resonant photoemission in the Pu 5f and Pu 6p states is compared to that in the Gd 4f and Gd 5p states. Spectral simulations, based upon and atomic model with angular momentum coupling, are compared to the Gd and Pu results. Additional spectroscopic measurements of Pu, including core level photoemission and X-ray absorption, are also presented.

Contact person: g.vanderlaan@dl.ac.uk

The Spintronic Properties of Rare Earth Nitrides

C.M. Aerts[1], P. Strange[1], M. Horne[1], W. M. Temmerman[2], Z. Szotek[2], and A. Svane[3]

[1]*Department of Physics, Keele University, Staffordshire, ST5 5DY, UK*
[2]*Daresbury Laboratory, Daresbury, Warrington WA4 4AD, UK*
[3]*Institute of Physics and Astronomy, University of Aarhus,*
DK-8000, Aarhus C, Denmark

Abstract

The electronic structure of the rare earth nitrides is studied systematically using the *ab-initio* self-interaction corrected local-spin-density approximation (SIC-LSD). This approach allows both a localised description of the rare earth $f-$electrons and an itinerant description of the valence electrons. Localising different numbers of f-electrons on the rare earth atom corresponds to different valencies, and the total energies can be compared, providing a first-principles description of valence. CeN is found to be tetravalent while the remaining rare earth nitrides are found to be trivalent. We show that these materials have a broad range of electronic properties including forming a new class of half-metallic magnets with high magnetic moments and are strong candidates for applications in spintronic and spin-filtering devices.

Half-Metallicity of LSMO

G. Banach[1,2] and W.M. Temmerman[1]

[1] *Daresbury Laboratory, Daresbury, Warrington WA4 4AD, UK*

[2] *Institute of Low Temperature and Structure Research,*
Polish Academy of Science, Wroclaw, Poland

Abstract

Self-interaction corrected local spin density approximation calculations were performed for $La_{(1-x)}Sr_xMnO_3$ (LSMO) ($0.0 < x < 0.5$). The influence and inter-relationship of Sr doping, magnetic structure, O displacements and phase segregation on the Mn charge state were studied. A half-metallic state was obtained for LSMO with manganese configuration Mn^{3+}, whilst Mn^{4+} gave rise to a metallic state with a negligible spin polarisation at the Fermi level. Elongating the MnO_6 octahedron led to a static mixed valence Mn^{3+}/Mn^{4+} configuration. In the mixed valence state the total energy was minimized by an ordered array of Mn^{4+} and Mn^{3+} MnO_2 planes which showed charge ordered stripes.

Nuclear quadrupole moment determination of ^{35}Cl, ^{79}Br and ^{127}I

R.E. Alonso[1], A. Svane[2], C.O. Rodríguez[3], and N.E. Christensen[2]

[1] *Departamento de Física de Cs. Exactas,*
Universidad Nacional de La Plata,
CC67, CP 1900 La Plata, Argentina
[2] *Department of Physics and Astronomy, University of Aarhus,*
DK–8000 Aarhus C, Denmark
[3] *IFLYSIB, Grupo de Física del Sólido, CC565,*
CP 1900 La Plata, Argentina

Abstract

The electric-field gradient at the halide site is calculated in several compounds of Cl, Br and I. The ab–initio full–potential linear–augmented plane wave method is employed with the generalized gradient approximation for exchange and correlation effects. The nuclear quadrupole moments of ^{35}Cl, ^{79}Br and ^{127}I are obtained by comparison of available experimental nuclear quadrupolar resonance data to the calculated electric-field gradients. The values of $|Q(^{35}\text{Cl})| = 0.0825$ b, $|Q(^{79}\text{Br})| = 0.333$ b and $|Q(^{127}\text{I})| = 0.721$ b are derived with ~ 3 % statistical uncertainty. These new values are in agreement with recent values derived by other methods, and thus confirm the validity of the present methodology for the determination of electric-field gradients in solids.

Charge Distributions in Metallic Alloys:
a Charge Excess Functional Theory Approach

Ezio Bruno and Leon Zingales

Dipartimento di Fisica and Unità INFM, Università di Messina,

Salita Sperone 31, 98166 Messina, Italy

Yang Wang

Pittsburgh Supercomputing Center, Pittsburgh, PA 15213 USA

Abstract

The distribution of local charge excesses (DLC) in metallic alloys, previously obtained as a result of the analysis of order N electronic structure calculations, is derived from a variational principle. A phenomenological Charge Excess Functional (CEF) theory is obtained which is determined by three concentration dependent, material specific, parameters that can be obtained from *ab initio* calculations. The theory requires modest computational efforts and reproduces with an excellent accuracy the DLC and the electrostatic energies of ordered, substitutionally disordered or segregating metallic alloys and, hence, can be considered an efficient approach alternative to conventional electronic structure calculations. The substantial reduction of computing time opens new perspectives for the understanding of metallic systems and their mechanical properties.

Reconstruction and de-reconstruction of the Ir(100) surface and ultrathin Fe/Ir(100) films

D. Spišák and J. Hafner

Institut für Materialphysik and Center for Computational Materials Science,

Universität Wien, Sensengasse 8, A-1090 Vienna, Austria

Abstract

The structure, energetics and magnetic properties of the quasihexagonal reconstruction of the Ir(100) surface and nanostructures formed by Fe atoms on this surface have been investigated using first-principles density functional theory with generalized gradient corrections. We find the reconstructed (1×5) surface to be 0.10 eV/(1×1) area lower in energy than the unreconstructed surface and we demonstrate that first-principles calculations can achieve quantitative agreement with experiment even for such long-period and deep-going reconstructions. For Fe coverage of 0.4 monolayers (ML) we have studied the stripe-like structure with biatomic Fe rows placed in the troughs of the (1×5) reconstructed surface. Results of nonmagnetic calculations agree well with the structure inferred from STM data. Higher Fe coverages lead to a de-reconstruction of the Ir substrate. At 0.8 ML coverage a surface compound with composition Fe_4Ir is formed, which shows an appreciable buckling. In this case, a ferromagnetic calculation leads to good agreement with the low-temperature LEED data. We predict that the (1×5) periodicity of the mixed interface layer will persist also in thicker films with a pure Fe surface. Films with one to four ML Fe are predicted to be tetragonally distorted and ferromagnetic, with an axial ratio corresponding well to an elastic distortion of the Fe lattice.

Density functional study of Ni bulk, surfaces and the adsorbate systems Ni(111) $(\sqrt{3} \times \sqrt{3})$R30°-Cl, and Ni(111)$(2 \times 2)$-K

K. Doll

Institut für Mathematische Physik, TU Braunschweig,
Mendelssohnstrasse 3, D-38106 Braunschweig

Abstract

Nickel bulk, the low index surfaces and the adsorbate systems Ni(111) $(\sqrt{3} \times \sqrt{3})$R30°-Cl, and Ni(111)$(2 \times 2)$-K are studied with gradient corrected density functional calculations. It is demonstrated that an approach based on Gaussian type orbitals is capable of describing these systems. The preferred adsorption sites and geometries are in good agreement with the experiments. Compared to non-magnetic substrates, there does not appear to be a huge difference concerning the structural data and charge distribution. The magnetic moment of the nickel atoms closest to the adsorbate is reduced, and oscillations of the magnetic moments within the first few layers are observed in the case of chlorine as an adsorbate. The trends observed for the Mulliken populations of the adsorbates are consistent with changes in the core levels.

Latex-file available from k.doll@tu-bs.de

Exchange interactions, spin waves, and transition temperatures in itinerant magnets

I. Turek,[1,2,5] J. Kudrnovský,[3] V. Drchal,[3] and P. Bruno[4]

[1] *Institute of Physics of Materials, Academy of Sciences of the Czech Republic,*
Žižkova 22, CZ-61662 Brno, Czech Republic
[2] *Department of Electronic Structures, Charles University in Prague,*
Ke Karlovu 5, CZ-12116 Prague 2, Czech Republic
[3] *Institute of Physics, Academy of Sciences of the Czech Republic,*
Na Slovance 2, CZ-18221 Prague 8, Czech Republic
[4] *Max-Planck-Institut für Mikrostrukturphysik, Weinberg 2, D-06120 Halle, Germany*
[5] *Center for Computational Materials Science, Technical University of Vienna,*
Getreidemarkt 9/158, A-1060 Vienna, Austria

Abstract

The contribution reviews an *ab initio* two-step procedure to determine exchange inter-
actions, spin-wave spectra, and thermodynamic properties of itinerant magnets. In the
first step, the selfconsistent electronic structure of a system is calculated for a collinear spin
structure at zero temperature. In the second step, parameters of an effective classical Heisen-
berg Hamiltonian are determined using the magnetic force theorem and the one-electron
Green functions. The Heisenberg Hamiltonian and methods of statistical physics are em-
ployed in subsequent evaluation of magnon dispersion laws, spin-wave stiffness constants,
and Curie/Néel temperatures. Applicability of the developed scheme is illustrated by se-
lected properties of various systems like transition and rare-earth metals, disordered alloys
including diluted magnetic semiconductors, ultrathin films, and surfaces.

1   Introduction

The quantitative description of ground-state and finite-temperature properties of metallic sys-
tems represents a long-term challenge for solid state theory. Practical implementation of density
functional theory (DFT) [1, 2, 3] led to excellent parameter-free description of ground-state

properties of metallic magnets, including traditional bulk metals and ordered alloys as well as systems without the perfect three-dimensional periodicity, like, e.g., disordered alloys, surfaces and thin films. On the other hand, an accurate quantitative treatment of excited states and finite-temperature properties of these systems remains an unsolved problem for *ab initio* theory [4, 5, 6, 7] despite the formal extension of the DFT to time-dependent phenomena [8] and finite temperatures [9]. The usual local spin-density approximation (LSDA) [3] fails to capture important features of excited states, in particular the magnetic excitations responsible for the decrease of the magnetization with temperature and for the magnetic phase transition.

In developing a practical parameter-free scheme for the finite-temperature magnetism, one has to rely on additional assumptions and approximations the validity of which has to be chosen on the basis of physical arguments. The purpose of this contribution is to review theoretical backgrounds, numerical aspects, and selected results of an approach formulated nearly two decades ago [10, 11] (see Ref. [12] for a recent review), and applied by the present authors to a number of qualitatively different systems [13, 14, 15, 16, 17, 18, 19, 20], including also yet unpublished results. The review is organized as follows: Section 2 lists the underlying physical concepts and approximations of the scheme and Section 3 deals with computational details and specific problems related to its numerical implementation. Examples of applications are given in Section 4: bulk transition metals (Section 4.1), rare-earth metals (Section 4.2), disordered alloys (Section 4.3), diluted magnetic semiconductors (Section 4.4), two-dimensional ferromagnets (Section 4.5), and surfaces of bulk ferromagnets (Section 4.6). Comparisons to other authors using the same (or similar) approach are made throughout Section 4, while a critical discussion of the scheme and a brief comparison to alternative approaches are left to the last section (Section 5).

2   Formalism

It is well known that magnetic excitations in itinerant ferromagnets are basically of two different types, namely, the Stoner excitations, in which an electron is excited from an occupied state of the majority-spin band to an empty state of the minority-spin band and creates an electron-hole pair of triplet spin, and the spin-waves, or magnons, which correspond to collective transverse fluctuations of the magnetization direction. Near the bottom of the excitation spectrum, the density of states of magnons is considerably larger than that of corresponding Stoner excitations (associated with longitudinal fluctuations of the magnetization), so that the thermodynamics in the low-temperature regime is completely dominated by magnons and Stoner excitations can be neglected. Therefore it seems reasonable to extend this approximation up to the Curie temperature and to derive an *ab initio* technique of finite-temperature magnetism by neglecting systematically the Stoner excitations.

With thermodynamic properties in mind, we are primarily interested in the long-wavelength magnons with the lowest energy. We adopt the *adiabatic approximation* [21] in which the precession of the magnetization due to a spin-wave is neglected when calculating the associated change of electronic energy. The condition of validity of this approximation is that the precession time of the magnetization should be large as compared to characteristic times of electronic

motion, i.e., the hopping time of an electron from a given site to a neighboring one and the precession time of the spin of an electron subject to the exchange field. In other words, the spin-wave energies should be small as compared to the band width and to the exchange splitting. This approximation becomes exact in the limit of long wavelength magnons, so that the spin-wave stiffness constants calculated in this way are in principle exact.

This procedure corresponds to evaluation of changes of the total energy of a ferromagnet due to infinitesimal changes of the directions of its local magnetic moments associated with individual lattice sites $\mathbf{R}$. The directions of the moments are specified by unit vectors $\mathbf{e_R}$. An exact calculation of the total energy $\mathcal{E}\{\mathbf{e_R}\}$ of a prescribed spin configuration leads to the constrained density functional theory [22], which allows to obtain the ground state energy for a system subject to certain constraints. The latter are naturally incorporated into the DFT in terms of Lagrange multipliers. In the present case, the constraint consists in imposing a given configuration of spin-polarization directions, namely, along $\mathbf{e_R}$ within the atomic (Wigner-Seitz) cell $\mathbf{R}$. The Lagrange multipliers can be interpreted as magnetic fields $\mathbf{B_R^\perp}$ constant inside the cells with directions perpendicular to the unit vectors $\mathbf{e_R}$. Note that *intracell* non-collinearity of the spin-polarization is neglected since we are primarily interested in low-energy excitations due to *intercell* non-collinearity. In the so-called frozen-magnon approach, one chooses the constrained spin-polarization configuration to be the one of a spin-wave with the wave vector $\mathbf{q}$ and computes the spin-wave energy $E(\mathbf{q})$ directly by employing the generalized Bloch theorem for a spin-spiral configuration [23].

In a real-space approach, adopted here, one calculates directly the energy change associated with a constrained rotation of the spin-polarization axes in two cells $\mathbf{e_R}$ and $\mathbf{e_{R'}}$. This represents a highly non-trivial task which requires selfconsistent electronic structure calculations for non-collinear spin-polarized systems without translational periodicity. Restriction to infinitesimal changes of the moment directions, $\delta\mathbf{u_R} = \mathbf{e_R} - \mathbf{e}^0$, perpendicular to the direction of the ground-state magnetization $\mathbf{e}^0$, leads to an expansion of $\mathcal{E}\{\mathbf{e_R}\}$ to second order in $\delta\mathbf{u_R}$ of the form [11, 24]

$$\Delta\mathcal{E}\{\delta\mathbf{u_R}\} = \sum_{\mathbf{RR'}} A_{\mathbf{RR'}} \, \delta\mathbf{u_R} \cdot \delta\mathbf{u_{R'}} \, . \tag{1}$$

This expression can be extended to finite changes of the moment directions using an effective Heisenberg Hamiltonian (EHH)

$$H_{\text{eff}}\{\mathbf{e_R}\} = -\sum_{\mathbf{RR'}} J_{\mathbf{RR'}} \, \mathbf{e_R} \cdot \mathbf{e_{R'}} \, . \tag{2}$$

The constants $J_{\mathbf{RR'}}$ in Eq. (2), the pair exchange interactions, are parameters of the EHH which satisfy $J_{\mathbf{RR'}} = J_{\mathbf{R'R}}$ and $J_{\mathbf{RR}} = 0$. They are related to the coupling constants $A_{\mathbf{RR'}}$ of Eq. (1) by

$$A_{\mathbf{RR'}} = -J_{\mathbf{RR'}} + \delta_{\mathbf{RR'}} \left(\sum_{\mathbf{R''}} J_{\mathbf{R''R}} \right) \tag{3}$$

so that an important sum rule

$$\sum_{\mathbf{R}} A_{\mathbf{RR'}} = \sum_{\mathbf{R'}} A_{\mathbf{RR'}} = 0 \tag{4}$$

is satisfied which guarantees that the total energy remains invariant upon a uniform rotation of the magnetization.

The practical calculations of the exchange interactions $J_{\mathbf{RR'}}$ in ferromagnets are greatly simplified by using the magnetic force theorem [10, 11] (a similar approach was also suggested for magnetic impurities in a non-magnetic host [25]). The infinitesimal changes of the total energy, Eq. (1), can be expressed using changes in one-particle eigenvalues due to non-selfconsistent changes of the effective one-electron potential accompanying the infinitesimal rotations of spin quantization axes, i.e., without any additional selfconsistent calculations besides that for the collinear ground state. The resulting pair exchange interactions are given by [11, 24]

$$J_{\mathbf{RR'}} = \frac{1}{\pi} \operatorname{Im} \int_{-\infty}^{E_{\mathrm{F}}} dE \int_{\Omega_{\mathbf{R}}} d\mathbf{r} \int_{\Omega_{\mathbf{R'}}} d\mathbf{r'} \, B_{\mathrm{xc}}(\mathbf{r}) \, G^{\uparrow}(\mathbf{r}, \mathbf{r'}; E + \mathrm{i}0) \, B_{\mathrm{xc}}(\mathbf{r'}) \, G^{\downarrow}(\mathbf{r'}, \mathbf{r}; E + \mathrm{i}0) \ , \quad (5)$$

where E_{F} denotes the Fermi level, $\Omega_{\mathbf{R}}$ denotes the $\mathbf{R}$-th atomic cell, $B_{\mathrm{xc}}(\mathbf{r})$ is the exchange-correlation magnetic field, $2B_{\mathrm{xc}}(\mathbf{r}) = V^{\downarrow}(\mathbf{r}) - V^{\uparrow}(\mathbf{r})$, where $V^{\sigma}(\mathbf{r})$ ($\sigma = \uparrow, \downarrow$) is the selfconsistent LSDA potential, and $G^{\sigma}(\mathbf{r}, \mathbf{r'}; E + \mathrm{i}0)$ is the one-electron retarded Green function for the same potential. It should be noted that the parameters $J_{\mathbf{RR'}}$ determined by Eq. (5) do not contain contributions due to constraining magnetic fields necessary to keep a frozen non-collinear spin structure a stationary state of the Kohn-Sham equation. It can be expected that these contributions can be neglected in systems with large local magnetic moments. Validity of this approximation have been put on a more quantitative level in recent studies [24, 26].

Once the exchange parameters $J_{\mathbf{RR'}}$ are obtained, the adiabatic spin-dynamics [27, 28, 29, 30, 31] can be easily determined from the EHH, Eq. (2). One obtains the result known from spin-wave theories of localized ferromagnets: for ferromagnetic crystals with one atom in the primitive cell, the energy $E(\mathbf{q})$ of a zero-temperature magnon is related to the lattice Fourier transform $J(\mathbf{q})$ of the exchange interactions $J_{\mathbf{RR'}}$ by

$$E(\mathbf{q}) = \frac{4}{M} \left[J(\mathbf{0}) - J(\mathbf{q}) \right] \ , \quad J(\mathbf{q}) = \sum_{\mathbf{R}} J_{\mathbf{0R}} \, \exp(\mathrm{i}\mathbf{q} \cdot \mathbf{R}) \ , \quad (6)$$

where $\mathbf{q}$ denotes a vector in the Brillouin zone (BZ) of the lattice, M denotes the local moment magnitude in units of μ_{B} (μ_{B} is the Bohr magneton). For cubic systems and for small $\mathbf{q}$-vectors, $E(\mathbf{q}) \approx D|\mathbf{q}|^2$ with the spin-wave stiffness constant equal to

$$D = \frac{2}{3M} \sum_{\mathbf{R}} |\mathbf{R}|^2 \, J_{\mathbf{0R}} \ . \quad (7)$$

Finally, to obtain thermodynamic quantities such as the Curie temperature, methods of statistical mechanics have to be applied to the EHH, Eq. (2). The simplest estimate of the Curie temperature is based on a mean-field approximation (MFA) which leads to

$$k_{\mathrm{B}} T_{\mathrm{C}}^{\mathrm{MFA}} = \frac{2}{3} J^0 \ , \quad J^0 = \sum_{\mathbf{R}} J_{\mathbf{0R}} = J(\mathbf{0}) \ , \quad (8)$$

where k_{B} is the Boltzmann constant. The quantity J^0 (on-site exchange parameter) reflects the molecular field experienced by a single moment in the ferromagnet. The limitations of the MFA are well known: it is correct only in the limit of high temperatures (above T_{C}) and it fails to describe the low-temperature collective excitations (spin-waves). An improved description of finite-temperature properties is provided by the Green function method within the random phase approximation (RPA) [32, 33]. The RPA is valid not only for high temperatures, but

also at low temperatures, and it describes correctly the spin-waves. In the intermediate regime (around T_C), it represents a rather good approximation which may be viewed as an interpolation between the high and low temperature regimes. The RPA formula for the Curie temperature is given by

$$\left(k_{\mathrm{B}}T_{\mathrm{C}}^{\mathrm{RPA}}\right)^{-1} = \frac{3}{2}\frac{1}{N}\sum_{\mathbf{q}}\left[J^0 - J(\mathbf{q})\right]^{-1} , \tag{9}$$

where N denotes the number of $\mathbf{q}$-vectors used in the BZ-average. It can be shown that $T_{\mathrm{C}}^{\mathrm{RPA}}$ is always smaller than $T_{\mathrm{C}}^{\mathrm{MFA}}$. It should be noted, however, that both the MFA and the RPA fail to describe correctly the critical behavior and yield in particular incorrect critical exponents. Finally, the Curie temperature can also be estimated purely numerically by employing the method of Monte Carlo simulations applied to the EHH. This approach is in principle exact but its application to real itinerant systems requires inclusion of a sufficient number of neighboring shells due to long-ranged interactions $J_{\mathbf{RR'}}$ (see Section 3.2).

3 Numerical implementation

3.1 Selfconsistent electronic structure

Efficient evaluations of the pair exchange interactions, Eq. (5), require a first-principle technique which provides the one-electron Green function in the real space. The results reported here are based on selfconsistent LSDA calculations using the all-electron non-relativistic (scalar-relativistic) tight-binding linear muffin-tin orbital (TB-LMTO) method and the atomic-sphere approximation (ASA) [34, 35, 36], with the exchange-correlation potential parametrized according to Ref. [37]. The energy integrals over the occupied part of the valence band were expressed as integrals over an energy variable along a closed path C starting and ending at the Fermi energy (with the occupied part of the valence band lying inside C). The integrals were numerically evaluated using the Gaussian quadrature method [35, 36]. Other Green function techniques, especially the the Korringa-Kohn-Rostoker (KKR) method [38, 39], are equally suitable in the present context.

Within the ASA, the Green function for a closely packed solid can be written in the form [35, 40] (the spin index σ is omitted for brevity in Section 3.1)

$$
\begin{aligned}
G(\mathbf{r}+\mathbf{R}, \mathbf{r}'+\mathbf{R}'; z) \quad = \quad & -\delta_{\mathbf{RR'}}\sum_{L}\varphi_{\mathbf{R}L}(\mathbf{r}^<, z)\,\tilde{\varphi}_{\mathbf{R}L}(\mathbf{r}^>, z) \\
& + \sum_{LL'}\varphi_{\mathbf{R}L}(\mathbf{r}, z)\,G_{\mathbf{R}L,\mathbf{R}'L'}(z)\,\varphi_{\mathbf{R}'L'}(\mathbf{r}', z) .
\end{aligned}
\tag{10}
$$

In Eq. (10), the variables $\mathbf{r}, \mathbf{r}'$ refer to positions of points inside the individual atomic spheres, z denotes a complex energy variable, the symbol $\mathbf{r}^<$ ($\mathbf{r}^>$) denotes that of the vectors $\mathbf{r}, \mathbf{r}'$ with the smaller (larger) modulus, and L, L' are the angular momentum indices, $L = (\ell, m)$. The functions $\varphi_{\mathbf{R}L}(\mathbf{r}, z)$ and $\tilde{\varphi}_{\mathbf{R}L}(\mathbf{r}, z)$ denote, respectively, properly normalized regular and irregular solutions of the Schrödinger equation for the spherically symmetric potential inside the $\mathbf{R}$-th atomic sphere. All multiple-scattering effects are contained in the Green function matrix $G_{\mathbf{R}L,\mathbf{R}'L'}(z)$ which is given in terms of the potential functions $P_{\mathbf{R}\ell}(z)$ and the structure constants

$S_{\mathbf{R}L,\mathbf{R}'L'}$ of the LMTO method by

$$G_{\mathbf{R}L,\mathbf{R}'L'}(z) = \lambda_{\mathbf{R}\ell}(z)\,\delta_{\mathbf{R}L,\mathbf{R}'L'} + \mu_{\mathbf{R}\ell}(z)\,g_{\mathbf{R}L,\mathbf{R}'L'}(z)\,\mu_{\mathbf{R}'\ell'}(z)\,, \tag{11}$$

where the quantities on the r.h.s. are defined as

$$\mu_{\mathbf{R}\ell}(z) = \sqrt{\dot{P}_{\mathbf{R}\ell}(z)}\,, \qquad\qquad \lambda_{\mathbf{R}\ell}(z) = -\frac{1}{2}\frac{\ddot{P}_{\mathbf{R}\ell}(z)}{\dot{P}_{\mathbf{R}\ell}(z)}\,,$$

$$g_{\mathbf{R}L,\mathbf{R}'L'}(z) = \left\{[P(z) - S]^{-1}\right\}_{\mathbf{R}L,\mathbf{R}'L'}\,. \tag{12}$$

In the last equation, the symbol $P(z)$ denotes a diagonal matrix of potential functions defined as $P_{\mathbf{R}L,\mathbf{R}'L'}(z) = P_{\mathbf{R}\ell}(z)\,\delta_{\mathbf{R}L,\mathbf{R}'L'}$ and an overdot means energy derivative. The matrix $g_{\mathbf{R}L,\mathbf{R}'L'}(z)$ will be referred to as the auxiliary (or KKR-ASA) Green function. The quantities $P_{\mathbf{R}\ell}(z)$, $\mu_{\mathbf{R}\ell}(z)$, $\lambda_{\mathbf{R}\ell}(z)$, $S_{\mathbf{R}L,\mathbf{R}'L'}$, and $g_{\mathbf{R}L,\mathbf{R}'L'}(z)$ can be expressed in any particular LMTO representation (canonical, screened); the resulting Green function matrix, Eq. (11), the Green function, Eq. (10), and all derived physical quantities are invariant with respect to this choice. However, the most screened (tight-binding) representation is the best suited for most calculations and it has been employed in the present implementation. The energy dependence of the potential functions $P_{\mathbf{R}\ell}(z)$ is parametrized in terms of three standard potential parameters, i.e., with the second-order accuracy [34, 35].

3.2 Parameters of the classical Heisenberg Hamiltonian

Substitution of the Green function $G^{\sigma}(\mathbf{r},\mathbf{r}';z)$ in the ASA (Section 3.1) into Eq. (5) yields an expression suitable for computations [11, 12, 14], namely,

$$J_{\mathbf{R}\mathbf{R}'} = -\frac{1}{8\pi\mathrm{i}}\int_C \mathrm{tr}_L\left[\Delta_{\mathbf{R}}(z)\,g^{\uparrow}_{\mathbf{R}\mathbf{R}'}(z)\,\Delta_{\mathbf{R}'}(z)\,g^{\downarrow}_{\mathbf{R}'\mathbf{R}}(z)\right]\,\mathrm{d}z\,,$$

$$\Delta_{\mathbf{R}}(z) = P^{\uparrow}_{\mathbf{R}}(z) - P^{\downarrow}_{\mathbf{R}}(z)\,, \tag{13}$$

where tr_L denotes the trace over the angular momentum index L and energy integration is performed along the contour C described in Section 3.1. The quantities $g^{\sigma}_{\mathbf{R}\mathbf{R}'}(z)$ $(\sigma = \uparrow,\downarrow)$ denote site-off-diagonal blocks of the auxiliary Green-function matrices with elements $g^{\sigma}_{\mathbf{R}L,\mathbf{R}'L'}(z)$ while $\Delta_{\mathbf{R}}(z)$ are diagonal matrices related to the potential functions $P^{\sigma}_{\mathbf{R}\ell}(z)$. The diagonal elements of $\Delta_{\mathbf{R}}(z)$ play a role of energy- and ℓ-dependent exchange splittings on individual atoms while the expression (13) for the exchange interactions $J_{\mathbf{R}\mathbf{R}'}$ has a form of a bare static transversal susceptibility.

Well converged calculations of the exchange interactions $J_{\mathbf{R}\mathbf{R}'}$ for bulk metals with perfect translational symmetry for distances $d = |\mathbf{R} - \mathbf{R}'|$ up to ten lattice constants a require high accuracy of the full BZ-averages (inverse lattice Fourier transforms) defining the site-off-diagonal blocks $g^{\sigma}_{\mathbf{R}\mathbf{R}'}(z)$ [35, 36]. In particular, we have used typically a few millions of $\mathbf{k}$-points in the full BZ for the energy point on the contour C closest to the Fermi energy, and the number of $\mathbf{k}$-points then progressively decreased for more distant energy points [14, 17]. A typical evaluation of exchange interactions requires about two hours on P4-based personal computers.

The calculated Heisenberg exchange parameters for bcc Fe (with experimental value of its lattice constant) are shown in Fig. 1. One can see dominating ferromagnetic interactions for the first

and second nearest-neighbor shells followed by weaker interactions of both signs and decreasing magnitudes for bigger distances $d = |\mathbf{R} - \mathbf{R}'|$ (Fig. 1, left panel). The same qualitative features were found for other $3d$ ferromagnets: fcc Co, fcc Ni [14] and hcp Co [18].
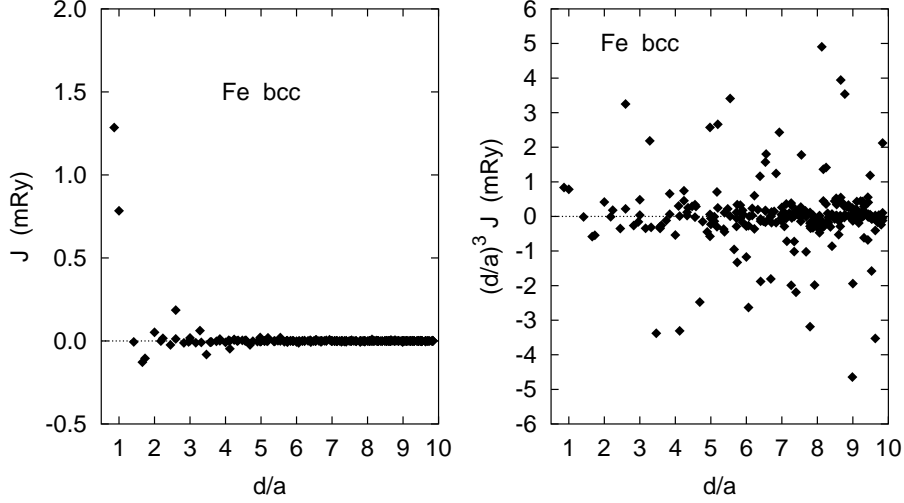

Figure 1: Exchange interactions $J_{\mathbf{RR}'}$ for bcc Fe as a function of the distance $|\mathbf{R} - \mathbf{R}'| = d$ without (left panel) and with (right panel) a prefactor d^3.

An analysis of the exchange interactions $J_{\mathbf{RR}'}$, Eq. (13), in the limit of large distances $d = |\mathbf{R} - \mathbf{R}'|$ has been given in Ref. [14] for a a single-band model using the stationary-phase approximation [41]. For a weak ferromagnet, one reveals a characteristic Ruderman-Kittel-Kasuya-Yoshida (RKKY) asymptotic behavior

$$ J_{\mathbf{RR}'} \propto \frac{\sin\left[\left(\mathbf{k}_{\mathrm{F}}^{\uparrow} + \mathbf{k}_{\mathrm{F}}^{\downarrow}\right) \cdot (\mathbf{R} - \mathbf{R}') + \Phi\right]}{|\mathbf{R} - \mathbf{R}'|^3} \, , \tag{14} $$

where $\mathbf{k}_{\mathrm{F}}^{\sigma}$ is a Fermi wave vector in a direction such that the associated group velocity is parallel to $\mathbf{R} - \mathbf{R}'$, and Φ denotes a phase factor. The exchange interaction according to Eq. (14) has an oscillatory character with an envelope decaying as $|\mathbf{R} - \mathbf{R}'|^{-3}$. On the other hand, for a strong ferromagnet with a fully occupied majority band the corresponding Fermi wave vector is imaginary, namely, $\mathbf{k}_{\mathrm{F}}^{\uparrow} = i\,\mathbf{K}_{\mathrm{F}}^{\uparrow}$, and one obtains an exponentially damped RKKY behavior

$$ J_{\mathbf{RR}'} \propto \frac{\sin\left[\mathbf{k}_{\mathrm{F}}^{\downarrow} \cdot (\mathbf{R} - \mathbf{R}') + \Phi\right] \exp\left[-\mathbf{K}_{\mathrm{F}}^{\uparrow} \cdot (\mathbf{R} - \mathbf{R}')\right]}{|\mathbf{R} - \mathbf{R}'|^3} \, . \tag{15} $$

The qualitative features of these RKKY-type oscillations will not be changed in realistic ferromagnets. This is illustrated for bcc Fe (weak ferromagnet) in Fig. 1 (right panel) which proves undamped oscillations of the quantity $|\mathbf{R} - \mathbf{R}'|^3 J_{\mathbf{RR}'}$. It should be noted that due to the sp-d hybridization no itinerant ferromagnet is a truly strong ferromagnet – the only exceptions are half-metallic ferromagnets.

3.3   Magnetic properties from the Heisenberg Hamiltonian

The RKKY-like asymptotic behavior, Eq. (14), leads to numerical difficulties in calculations of the magnon spectra and the spin-wave stiffness constants. The lattice Fourier transform of the

exchange interactions, Eq. (6), is not an absolutely convergent sum and its convergence with respect to the number of shells included has to be carefully checked (see Section 4.1). Note, however, that the lattice sum over $|J_{0R}|^2$ does converge so that $J(\mathbf{q})$ is defined unambiguously in the L^2 sense.

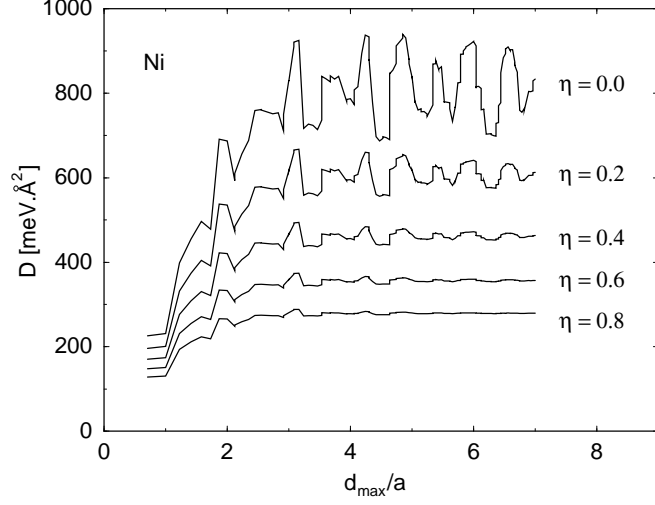Figure 2: Spin-wave stiffness of fcc Ni as a function of d_{max} (in units of lattice constant) for various values of the damping factor η.

The lattice sum for the spin-wave stiffness constant, Eq. (7), is not convergent at all, and the values of D as functions of a cut-off distance d_{max} exhibit undamped oscillations for all three cubic $3d$ ferromagnets [14]. To resolve this difficulty we suggested to regularize the original expression, Eq. (7), by replacing it by the formally equivalent expression which is, however, numerically convergent

$$
\begin{aligned}
D(\eta) &= \frac{2}{3M} \lim_{d_{max} \to \infty} \sum_{|\mathbf{R}| < d_{max}} |\mathbf{R}|^2 \, J_{0R} \, \exp(-\eta|\mathbf{R}|/a) \;, \\
D &= \lim_{\eta \to 0} D(\eta) \;,
\end{aligned}
\tag{16}
$$

where a is the lattice constant. The quantity η plays a role of a damping parameter which makes the lattice sum absolutely convergent as it is seen from Fig. 2 for the case of fcc Ni.

It can be shown that the quantity $D(\eta)$ is an analytical function of the variable η for any value $\eta > 0$ and it can be extrapolated to the value $\eta = 0$. We therefore perform calculations for a set of values $\eta \in (\eta_{min}, \eta_{max})$ for which $D(\eta)$ is a smooth function with a well defined limit for large d_{max}. The limit $\eta \to 0$ is then determined at the end of calculations by a quadratic least-square extrapolation method. The procedure is illustrated in Fig. 3 for the cubic Fe, Co and Ni. Note that these convergence problems are less serious in half-metallic magnets due to the exponential damping described by Eq. (15).

Direct calculations of the Curie temperatures in the MFA according to Eq. (8) face convergence problems similar to the magnon spectra. Alternatively, one can evaluate the on-site exchange parameter J^0 using a sum rule valid also for systems without translational periodicity [11]:

$$
J_{\mathbf{R}}^0 = \sum_{\mathbf{R}'} J_{\mathbf{R}\mathbf{R}'} = \frac{1}{8\pi i} \int_C \mathrm{tr}_L \left[\Delta_{\mathbf{R}}(z) \left(g_{\mathbf{R}\mathbf{R}}^{\uparrow}(z) - g_{\mathbf{R}\mathbf{R}}^{\downarrow}(z) \right) \right.
$$

119
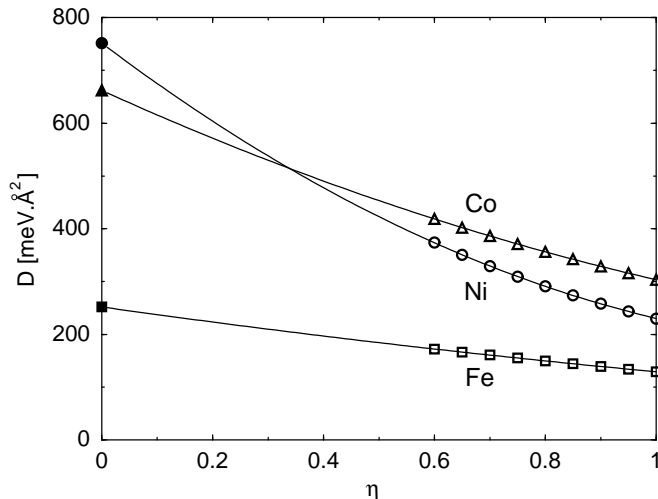
Figure 3: Spin-wave stiffness coefficients $D(\eta)$ for bcc Fe, fcc Co, and fcc Ni as a function of the parameter η (open symbols) and extrapolated values for $\eta = 0$ (filled symbols). The solid line indicates the quadratic fit function used for extrapolation.

$$+ \Delta_{\mathbf{R}}(z)\, g^{\uparrow}_{\mathbf{RR}}(z)\, \Delta_{\mathbf{R}}(z)\, g^{\downarrow}_{\mathbf{RR}}(z) \Big]\; \mathrm{d}z \; . \tag{17}$$

This sum rule involves only the site-diagonal blocks of the auxiliary Green functions and its reliable evaluation for perfect crystals requires only a few thousands of $\mathbf{k}$-points in the irreducible part of the BZ, i.e., accuracy usual in most selfconsistent LSDA calculations.

Another numerical problem is encountered in computations of the Curie temperature in the RPA due to the singularity of the averaged function in Eq. (9) for $|\mathbf{q}| \to 0$. We have therefore calculated $T_{\mathrm{C}}^{\mathrm{RPA}}$ using the expression

$$\left(k_{\mathrm{B}} T_{\mathrm{C}}^{\mathrm{RPA}}\right)^{-1} = -\frac{3}{2}\, \lim_{z \to 0} G^{\mathrm{m}}(z) \; , \qquad G^{\mathrm{m}}(z) = \frac{1}{N} \sum_{\mathbf{q}} \left[z - J^{0} + J(\mathbf{q}) \right]^{-1} \; , \tag{18}$$

where z is a complex energy variable and the quantity $G^{\mathrm{m}}(z)$ is a magnon Green function corresponding (up to the prefactor $4/M$) to the magnon dispersion law, Eq. (6). The magnon Green function was evaluated for energies z in the complex energy plane and its value for $z = 0$ was obtained using an analytical continuation technique [42].

4 Applications

4.1 Transition metals

Calculated magnon energy spectra $E(\mathbf{q})$ for bcc Fe are presented in Fig. 4. Corresponding plots of $E(\mathbf{q})$ for fcc Co and Ni [14] exhibit parabolic, almost isotropic behavior for long wavelengths. On the contrary, in bcc Fe we observe some anisotropy of $E(\mathbf{q})$, i.e., $E(\mathbf{q})$ increases faster along the $\Gamma - N$ direction and more slowly along the $\Gamma - P$ direction. In agreement with Refs. [27, 43, 44] we observe a local minima around the point H along $\Gamma - H$ and $H - N$ directions in the range of short wavelengths. They are indications of the so-called Kohn anomalies which are due to long-range interactions mediated by the RKKY interactions similarly like Kohn-Migdal anomalies in

phonon spectra are due to long-range interactions mediated by Friedel oscillations. It should be mentioned that minima in dispersion curve of bcc Fe appear only if the summation in Eq. (6) is done over a sufficiently large number of shells, in the present case for more than 45 shells.
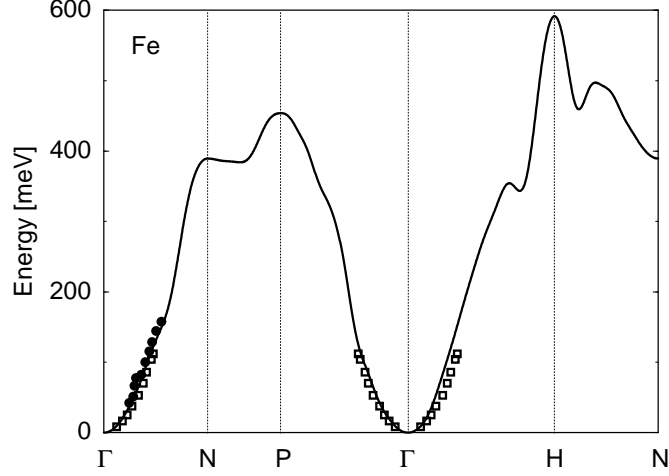

Figure 4: Magnon dispersion law along high-symmetry lines in the Brillouin zone of bcc Fe compared to experiment (filled circles: pure Fe at 10 K [45], empty squares: Fe(12% Si) at room temperature [46]).

Present results for dispersion relations compare well with available experimental data of measured spin-wave spectra for Fe and Ni [45, 46, 47]. For low-lying part of spectra there is also a good agreement of present results for dispersion relations with those of Refs. [27, 44] obtained using the frozen-magnon approach. There are, however, differences for a higher part of spectra, in particular for the magnon bandwidth of bcc Fe which can be identified with the value of $E(\mathbf{q})$ evaluated at the high-symmetry point $\mathbf{q} = H$ in the bcc BZ. The origin of this disagreement is unclear. We have carefully checked the convergence of the magnon dispersion laws $E(\mathbf{q})$, see Fig. 5, with the number of shells included in Eq. (6) and it was found to be weak for $50 - 70$ shells and more, i.e., for the cut-off distance $d_{\max} \geq 6a$.

The results for spin stiffness coefficient D calculated for the three cubic ferromagnetic metals are summarized in Tab. 1 together with available experimental data [48, 49, 50]. There is a reasonable agreement between theory and experiment for bcc Fe and fcc Co but the theoretical values of D are considerably overestimated for fcc Ni. It should be noted that measurements refer to the hcp Co while the present calculations were performed for fcc Co. A similar agreement between calculated and measured spin-wave stiffness constants was obtained by Halilov et al. [27] using the frozen-magnon approach. Our results are also in accordance with those obtained by van Schilfgaarde and Antropov [44] who used the spin-spiral calculations to overcome the problem of evaluation of D from Eq. (7). On the other hand, this problem was overlooked in Refs. [11, 51, 52] so that a good agreement of D, calculated for a small number of coordination shells, with experimental data seems to be fortuitous. Finally, the results of Brown et al. [53] obtained by the layer KKR method in the frozen potential approximation are underestimated for all metals and the best agreement is obtained for Ni.

Calculated values of Curie temperatures for both the MFA and RPA as well as corresponding
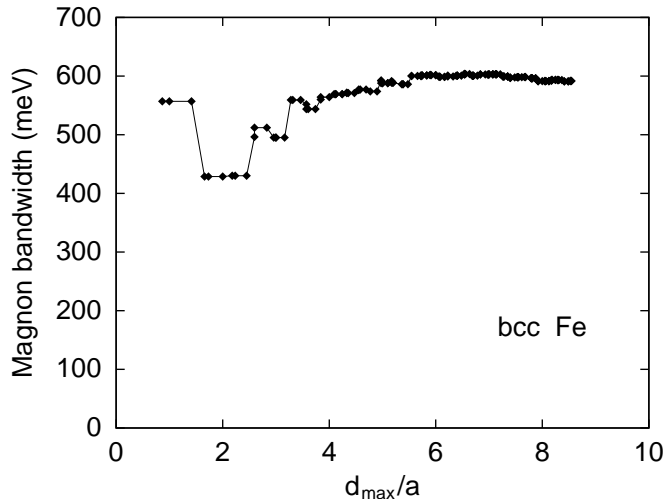
Figure 5: The magnon bandwidth for bcc Fe as a function of the cut-off distance $d_{\max}$. The bandwidth is identified with the magnon energy at the high-symmetry point H in the bcc Brillouin zone.

Table 1: Calculated spin-wave stiffness constants (D_{th}) and Curie temperatures (T_C^{MFA} and T_C^{RPA}) and their comparison with experimental values ($D_{\exp}$ and $T_{C,\exp}$).

Metal	$D_{\text{th}}[\text{meV·Å}^2]$	$D_{\exp}[\text{meV·Å}^2]$	$T_C^{\text{MFA}}[\text{K}]$	$T_C^{\text{RPA}}[\text{K}]$	$T_{C,\exp}[\text{K}]$
Fe bcc	250 ± 7	$280, 330$	1414	950 ± 2	$1044 - 1045$
Co fcc	663 ± 6	$580, 510$	1645	1311 ± 4	$1388 - 1398$
Ni fcc	756 ± 29	$555, 422$	397	350 ± 2	$624 - 631$

experimental data are summarized in Tab. 1. MFA-values of Curie temperatures are overestimated for Fe and Co, but underestimated for Ni in agreement with other calculations [27, 44]. On the other hand, the results obtained using the RPA are in a good agreement with experiment for both fcc Co and bcc Fe, while the results for fcc Ni are even more underestimated. This is in agreement with the fact mentioned in Section 2, namely that $T_C^{\text{RPA}} < T_C^{\text{MFA}}$. The present results for Fe and Ni agree reasonably with results of Ref. [54] using the spin-fluctuation theory and an improved statistical treatment in the framework of the Onsager cavity-field method.

In summary, we have found that calculated Curie temperatures and spin-wave stiffness constants agree well with experiment for Fe and Co, while less satisfactory results are obtained for Ni, where the role of the Stoner excitations is much more important as compared to Fe and Co. In addition, the adiabatic approximation is less justified for Ni, and, possibly, correlation effects beyond the LSDA play the more important role for this ferromagnet.

4.2 Rare-earth metals

Rare-earth (RE) metals represent a class of systems where the concept of atomic-like local moments is well justified due to highly localized $4f$ orbitals. The standard LSDA, however, fails to describe correctly their ground-state properties: the equilibrium lattice constants are signifi-

cantly smaller than the experimental ones due to an overestimated $4f$-contribution to cohesion, and the ground-state magnetic structures in the LSDA are qualitatively wrong as well. In the case of Gd in hcp structure, the antiferromagnetic (AFM) stacking of the (0001) atomic planes was predicted [55] in contrast to the observed ferromagnetic (FM) state [56]. The most sophisticated methods beyond the LSDA, which improve the situation, take explicitly into account the on-site Coulomb interaction of the $4f$ electrons, like the LSDA+U scheme [57, 58] and the self-interaction corrected (SIC) LSDA approach [59, 60]. Ground-state magnetic structures of $4f$ electron systems are often non-collinear and incommensurate with the underlying chemical unit cell [56] which presents another complication for *ab initio* techniques.

We have treated two RE metals, namely, hcp Gd [17] and bcc Eu [18], in a simplified manner taking the $4f$ states as a part of the atomic core (with the majority $4f$ level occupied by 7 electrons and the minority $4f$ level empty). The other valence orbitals were included in the standard LSDA. This 'open-core' approach was often employed in selfconsistent spin-polarized calculations of RE-based systems during the last decade [60, 61, 62, 63] and it yielded the correct FM structure of hcp Gd. The theoretical equilibrium Wigner-Seitz radii s ($s_{\text{Gd}} = 3.712$ a.u. with the experimental value of $c/a = 1.597$, $s_{\text{Eu}} = 4.190$ a.u.) are only slightly smaller than the experimental values ($s_{\text{Gd}} = 3.762$ a.u., $s_{\text{Eu}} = 4.238$ a.u.). Different spin configurations were considered for both metals: FM, AFM, and the disordered local moment (DLM) state [21]. The theoretical equilibrium values of s are nearly insensitive to the spin structures and the FM ground state of Gd exhibits a non-negligible energy separation from the AFM and DLM states in contrast to the bcc Eu, where the DLM state is slightly more stable than the FM state.
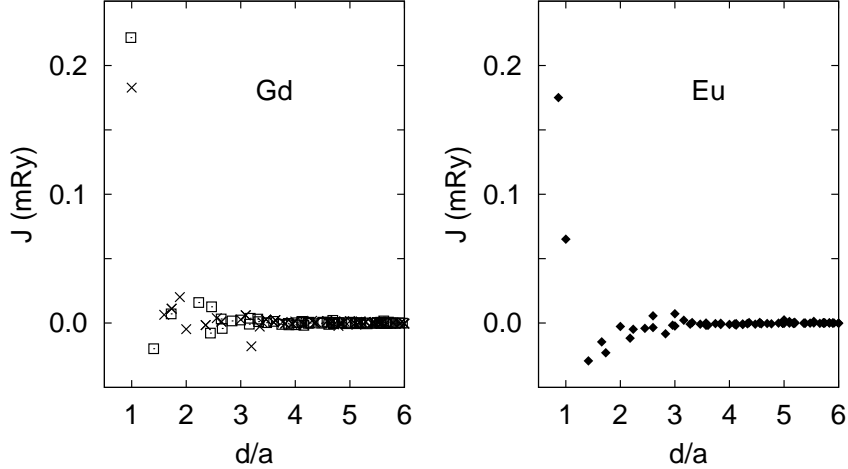
Figure 6: Exchange interactions $J_{\mathbf{RR'}}$ for hcp Gd (left panel) and bcc Eu (right panel) as functions of the distance $|\mathbf{R} - \mathbf{R'}| = d$. The crosses and squares in the left panel refer to pairs of sites $\mathbf{R}$, $\mathbf{R'}$ lying in even (AA) and odd (AB) hcp(0001) planes, respectively.

The exchange interactions in Gd and Eu, derived for the FM state and the theoretical equilibrium Wigner-Seitz radius s, are shown in Fig. 6. Their distance-dependence is qualitatively similar to the $3d$ transition metals, the magnitudes of the dominating nearest-neighbor interactions are, however, smaller by a factor of five, cf. Fig. 1. Moreover, as illustrated in Fig. 7 by calculating the on-site exchange parameter J^0 as a function of the cut-off distance $d_{\max}$ used in the real-space sum in Eq. (8), there is a profound difference between the two $4f$ metals concerning the

oscillating interactions of more distant atoms. In the hcp Gd, they are not strong enough to destroy the FM spin structure, as indicated by the positive converged value of J^0. Note that the negative exchange interaction between the second Gd nearest neighbors is in qualitative agreement with experiment [64]. On the other hand, the contribution of more distant sites to J^0 is very important in the case of bcc Eu and it yields for the converged quantity a negligible resulting value ($J^0 = -0.03\,\text{mRy}$). Such a situation indicates an instability of the FM state with respect to a more complicated spin structure. This feature agrees qualitatively with an experimentally observed helical spin structure, the wave vector of which lies along the $\Gamma - \text{H}$ direction in the bcc BZ [65, 66].
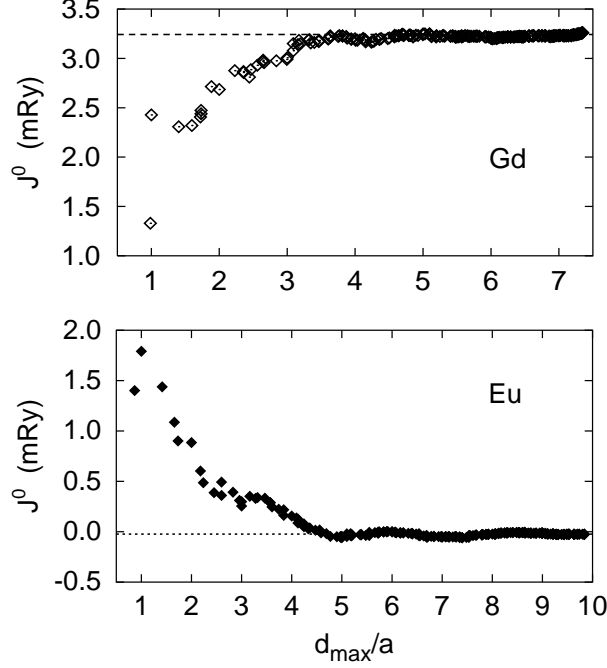
Figure 7: The on-site exchange parameter J^0 for hcp Gd (top panel) and bcc Eu (bottom panel) as a function of the cut-off distance $d_{\max}$ used in the real-space summation in Eq. (8). The horizontal lines mark exact values of J^0 obtained from the sum rule, Eq. (17).

Table 2: Calculated magnetic transition temperatures (T^{MFA} and T^{RPA}) and their comparison with experimental values (T_{exp}) for hcp Gd (Curie temperature) and bcc Eu (Néel temperature). Calculations were performed with experimental values of lattice parameters.

Metal	T^{MFA}[K]	T^{RPA}[K]	T_{exp}[K]
Gd hcp	334	300	293
Eu bcc	151	111	91

Calculations of the magnon spectra and the Curie temperature for hcp Gd require a trivial generalization of Eqs. (6, 9) to the case of two equivalent atoms in the hcp unit cell [67]. The resulting Curie temperatures are given in Tab. 2 together with the experimental value [56] while a comparison of the calculated magnon dispersion law with experiment [56] is presented in Fig. 8. The theoretical magnon spectra included finite temperature of the experiment ($T = 78$ K)

which leads within the RPA to a simple rescaling of the magnon energies proportionally to the temperature-dependent average magnetization [32]. The latter dependence was calculated in the RPA from the classical EHH [67].
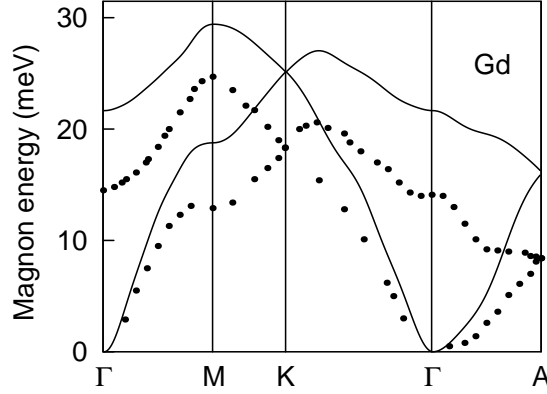

Figure 8: Magnon dispersion law along high-symmetry lines in the Brillouin zone of hcp Gd calculated for $T = 78$ K (lines) and compared to experiment (filled circles - Ref. [56]).

The calculated magnon energies are higher than experimental. A recent theoretical study by Halilov et al. [43, 62] revealed that this effect can be partly explained by assumed collinearity between the localized $4f$-moment and the valence part of the local moment. Inclusion of a possible non-collinearity between the localized and itinerant moments leads to a softening of the magnon energies, reducing them by a factor of 1.5 in the upper part of the spectrum. However, the lower part of the spectrum that is more important for an RPA estimation of the Curie temperature is less influenced by the non-collinearity. On the other hand, the calculated Curie temperatures both in the MFA and in the RPA agree very well with experiment (Tab. 2). This degree of agreement proves that the present approach based on interatomic exchange interactions represents a better starting point to RE magnetism than a theory based on intraatomic exchange integrals formulated in Ref. [68]. The latter scheme provided values of the Curie temperature for Gd in a wide interval between 172 K and 1002 K, depending on further approximations employed.

Determination of the magnetic ground state of Eu from the EHH, Eq. (2), is a difficult task in view of the highly-dimensional manifold of *a priori* possible states as well as a number of qualitatively different spin structures encountered in RE-based systems [56]. Here we consider only spin spirals specified by a single **q**-vector as

$$\bar{\mathbf{e}}_{\mathbf{R}} = (\sin(\mathbf{q} \cdot \mathbf{R}), \, 0, \, \cos(\mathbf{q} \cdot \mathbf{R})) \ , \tag{19}$$

since the spin structure observed for bcc Eu at low temperatures belongs to this class [65, 66]. The minimum of the Hamiltonian H_{eff} corresponds then to the maximum of the lattice Fourier transform $J(\mathbf{q})$, Eq. (6). A scan over the whole BZ reveals that the absolute maximum of $J(\mathbf{q})$ (for the theoretical equilibrium Wigner-Seitz radius $s = 4.19$ a.u.) is obtained for a vector $\mathbf{q} = \mathbf{Q}$ on the $\Gamma - H$ line, namely, at $\mathbf{Q} = (1.69, 0, 0) \, a^{-1}$, see Fig. 9. The magnitude of $\mathbf{Q}$ determines the angle ω between magnetic moments in the neighboring (100) atomic layers. In the present case, it is equal to $\omega = 48°$. Similar values were obtained for the experimental value of the

Wigner-Seitz radius $s_{\mathrm{exp}} = 4.238\,\mathrm{a.u.}$: $\mathbf{Q} = (1.63, 0, 0)\,a^{-1}$, $\omega = 47°$. Both data sets are in surprising agreement with experimental results which report the spin-spiral $\mathbf{q}$-vector inside the $\Gamma - \mathrm{H}$ line and the angle per layer equal to $\omega_{\mathrm{exp}} = 49°$ [65] and $\omega_{\mathrm{exp}} = 47.6 \pm 1.2°$ [66].
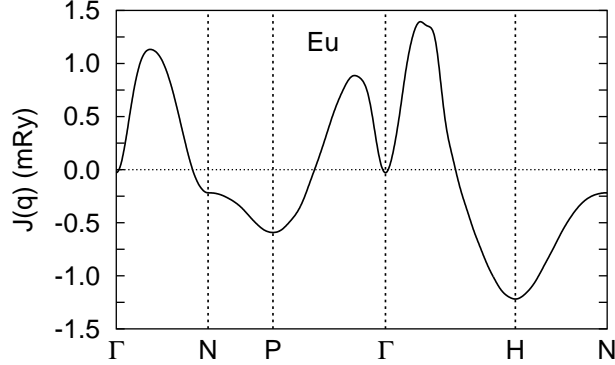

Figure 9: The lattice Fourier transform $J(\mathbf{q})$ of the exchange interactions in bcc Eu along high-symmetry lines in the Brillouin zone.

The resulting maximum $J(\mathbf{Q})$ can be used to get the Néel temperature in the MFA in complete analogy to Eq. (8) [56]:

$$k_{\mathrm{B}} T_{\mathrm{N}}^{\mathrm{MFA}} = \frac{2}{3}\, J(\mathbf{Q})\,, \tag{20}$$

whereas the RPA leads to the following modification of Eq. (9) [32, 69]:

$$\left(k_{\mathrm{B}} T_{\mathrm{N}}^{\mathrm{RPA}}\right)^{-1} = \frac{3}{4}\frac{1}{N}\sum_{\mathbf{q}}\left\{[J(\mathbf{Q}) - J(\mathbf{q})]^{-1} + [W(\mathbf{q},\mathbf{Q})]^{-1}\right\}\,,$$

$$W(\mathbf{q},\mathbf{Q}) = J(\mathbf{Q}) - \frac{1}{2}J(\mathbf{q}+\mathbf{Q}) - \frac{1}{2}J(\mathbf{q}-\mathbf{Q})\,. \tag{21}$$

Both theoretical values and the experimental Néel temperature are given in Tab. 2. The MFA-value is substantially higher than experiment while the RPA reduces the theoretical value of T_{N} significantly so that a good agreement with experiment is obtained.

4.3 Substitutionally disordered alloys

The present real-space approach to exchange interactions can be generalized to substitutionally disordered alloys either by using a supercell technique or by combining it with the coherent-potential approximation (CPA). Both alternatives have their own merits and drawbacks. The CPA takes properly into account the effects of finite lifetime of electronic states due to disorder but it has difficulties to include effects of varying local environments as well as of short-range order (both chemical and magnetic) on electronic properties.

In the following, we sketch the modification of the expression for the exchange interactions, Eq. (13), to a random alloy within the LMTO-CPA formalism [35, 36, 70]. We assume that the lattice sites $\mathbf{R}$ are randomly occupied by alloy components $Q = A, B, \ldots$, with concentrations $c_{\mathbf{R}}^{Q}$. We neglect any correlations between occupations of different lattice sites and we neglect local environment effects, i.e., the LSDA selfconsistent potentials inside $\mathbf{R}$-th cell depend solely on occupation of the site $\mathbf{R}$ by an atom $Q = A, B, \ldots$.

The CPA-configurational average of the auxiliary Green function, Eq. (12), can be written as

$$\langle g_{\mathbf{RR}'}(z) \rangle \;=\; \bar{g}_{\mathbf{RR}'}(z) \;=\; \left\{ [\mathcal{P}(z) - S]^{-1} \right\}_{\mathbf{RR}'} , \tag{22}$$

where the spin index σ is omitted, S is the structure constant matrix and $\mathcal{P}(z)$ is a non-random site-diagonal matrix of coherent potential functions $\mathcal{P}_{\mathbf{R}}(z)$ attached to individual lattice sites which describe effective atoms forming an effective CPA medium. The coherent potential functions satisfy a set of selfconsistency conditions (Soven equation) which guarantees that average single-site scattering due to real atoms with respect to the effective medium vanishes.

The CPA leads also to conditional averages of individual blocks of the Green functions. The site-diagonal block $g_{\mathbf{RR}}(z)$ of the Green function averaged over all alloy configurations with site $\mathbf{R}$ occupied by an atom Q is given by

$$\bar{g}_{\mathbf{RR}}^{Q}(z) \;=\; \bar{g}_{\mathbf{RR}}(z)\, f_{\mathbf{R}}^{Q}(z) \;=\; \tilde{f}_{\mathbf{R}}^{Q}(z)\, \bar{g}_{\mathbf{RR}}(z) , \tag{23}$$

where the prefactors $f_{\mathbf{R}}^{Q}(z)$ and $\tilde{f}_{\mathbf{R}}^{Q}(z)$ are defined as

$$
\begin{aligned}
f_{\mathbf{R}}^{Q}(z) &= \left\{ 1 + \left[P_{\mathbf{R}}^{Q}(z) - \mathcal{P}_{\mathbf{R}}(z) \right] \bar{g}_{\mathbf{RR}}(z) \right\}^{-1} , \\
\tilde{f}_{\mathbf{R}}^{Q}(z) &= \left\{ 1 + \bar{g}_{\mathbf{RR}}(z) \left[P_{\mathbf{R}}^{Q}(z) - \mathcal{P}_{\mathbf{R}}(z) \right] \right\}^{-1} .
\end{aligned}
\tag{24}
$$

Similarly, the site-off-diagonal block $g_{\mathbf{RR}'}(z)$ averaged over all alloy configurations with two sites $\mathbf{R} \neq \mathbf{R}'$ occupied respectively by atomic species Q and Q' is given by

$$\bar{g}_{\mathbf{RR}'}^{QQ'}(z) \;=\; \tilde{f}_{\mathbf{R}}^{Q}(z)\, \bar{g}_{\mathbf{RR}'}(z)\, f_{\mathbf{R}'}^{Q'}(z) . \tag{25}$$

Derivation of the conditionally averaged pair exchange interaction between two sites $\mathbf{R} \neq \mathbf{R}'$ occupied respectively by components Q and Q' can be performed similarly like in the case without substitutional randomness by employing the magnetic force theorem [11] and the so-called vertex-cancellation theorem [71, 72]. It leads to an expression

$$
\begin{aligned}
\bar{J}_{\mathbf{RR}'}^{QQ'} &= -\frac{1}{8\pi i} \int_C \mathrm{tr}_L \left[\Delta_{\mathbf{R}}^{Q}(z)\, \bar{g}_{\mathbf{RR}'}^{QQ',\uparrow}(z)\, \Delta_{\mathbf{R}'}^{Q'}(z)\, \bar{g}_{\mathbf{R}'\mathbf{R}}^{Q'Q,\downarrow}(z) \right] \mathrm{d}z , \\
\Delta_{\mathbf{R}}^{Q}(z) &= P_{\mathbf{R}}^{Q,\uparrow}(z) - P_{\mathbf{R}}^{Q,\downarrow}(z) ,
\end{aligned}
\tag{26}
$$

which is fully analogous to Eq. (13). The conditional average of the on-site exchange interaction, Eq. (17), yields a formula

$$
\begin{aligned}
\bar{J}_{\mathbf{R}}^{0,Q} &= \frac{1}{8\pi i} \int_C \mathrm{tr}_L \Big[\Delta_{\mathbf{R}}^{Q}(z) \left(\bar{g}_{\mathbf{RR}}^{Q,\uparrow}(z) - \bar{g}_{\mathbf{RR}}^{Q,\downarrow}(z) \right) \\
&\qquad\qquad + \Delta_{\mathbf{R}}^{Q}(z)\, \bar{g}_{\mathbf{RR}}^{Q,\uparrow}(z)\, \Delta_{\mathbf{R}}^{Q}(z)\, \bar{g}_{\mathbf{RR}}^{Q,\downarrow}(z) \Big] \mathrm{d}z .
\end{aligned}
\tag{27}
$$

It should be noted, however, that the sum rule for the averaged pair and on-site interactions,

$$\bar{J}_{\mathbf{R}}^{0,Q} = \sum_{\mathbf{R}'Q'} \bar{J}_{\mathbf{RR}'}^{QQ'}\, c_{\mathbf{R}'}^{Q'} , \tag{28}$$

which can be easily obtained from the corresponding sum rule, Eq. (17), valid for any configuration of the alloy, is not exactly satisfied by the expressions (26) and (27). According to our

experience, the two sides of Eq. (28) deviate up to 15% for typical binary transition-metal alloys (FeV, FeAl). This violation of an important sum rule indicates that vertex corrections must be taken into account in averaging exchange interactions in random alloys. On the other hand, the small relative difference of both sides of the sum rule (28) proves that the role of vertex corrections for exchange interactions is less significant than in transport properties, as argued in Ref. [73].

Let us now consider the case of two isolated impurities in a non-magnetic host. The exchange interaction between impurity sites $\mathbf{R} \neq \mathbf{R}'$ can be calculated exactly and compared to the low-concentration limit of the CPA expression, Eq. (26). The latter case corresponds to a binary alloy with $c_{\mathbf{R}}^A \to 0$ and $c_{\mathbf{R}}^B \to 1$ for all lattice sites, with the coherent potential functions $\mathcal{P}_{\mathbf{R}}^\sigma(z) \to P_{\mathbf{R}}^0(z)$ where $P_{\mathbf{R}}^0(z) = P_{\mathbf{R}}^B(z)$ are the non-spin-polarized host potential functions, and with the average Green function substituted by that of the non-random host, $\bar{g}_{\mathbf{RR}'}^\sigma(z) \to g_{\mathbf{RR}'}^0(z)$. Direct calculation of the exchange interaction for two impurities embedded in a crystal gives a result (the so-called two-potential formula [74]) which differs from the low-concentration limit of the CPA expression by matrix quantities $X_{\mathbf{RR}'}^\sigma(z)$ defined in terms of single-site t-matrices of impurities $\tau_{\mathbf{R}}^\sigma(z)$ as

$$X_{\mathbf{RR}'}^\sigma(z) = \left(1 - g_{\mathbf{RR}'}^0(z) \, \tau_{\mathbf{R}'}^\sigma(z) \, g_{\mathbf{R}'\mathbf{R}}^0(z) \, \tau_{\mathbf{R}}^\sigma(z) \right)^{-1} ,$$

$$\tau_{\mathbf{R}}^\sigma(z) = \left[P_{\mathbf{R}}^{A,\sigma}(z) - P_{\mathbf{R}}^0(z) \right] \left\{ 1 + g_{\mathbf{RR}}^0(z) \left[P_{\mathbf{R}}^{A,\sigma}(z) - P_{\mathbf{R}}^0(z) \right] \right\}^{-1} . \tag{29}$$

The quantities $X_{\mathbf{RR}'}^\sigma(z)$ – which enter the impurity-impurity interaction as multiplicative prefactors at the site-off-diagonal blocks $g_{\mathbf{RR}'}^0(z)$ of the host Green function – describe multiple scatterings of electrons between the two impurity sites; their absence in the exchange interaction derived from the low-concentration limit of Eq. (26) reflects a systematic neglect of such multiple-scattering processes in single-site theories like the CPA.
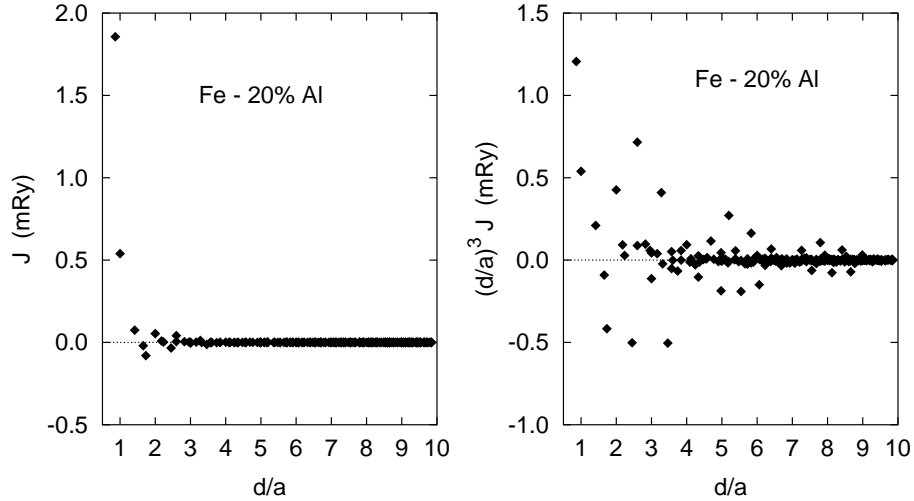

Figure 10: Exchange interactions $\bar{J}_{\mathbf{RR}'}^{\mathrm{FeFe}}$ for a random bcc $\mathrm{Fe}_{0.8}\mathrm{Al}_{0.2}$ alloy as a function of the distance $|\mathbf{R} - \mathbf{R}'| = d$ without (left panel) and with (right panel) a prefactor d^3.

An example of pair exchange interactions is shown in Fig. 10 for Fe-Fe pairs in a disordered bcc $\mathrm{Fe}_{0.8}\mathrm{Al}_{0.2}$ alloy. The interactions are qualitatively similar to those in pure bcc Fe (Fig. 1), but

a more careful analysis of the long-distance behavior reveals an exponentially damped RKKY-like oscillations (Fig. 10, right panel). This feature can be explained by damping of electron states due to the alloy disorder which leads to exponential decay of site-off-diagonal blocks of the averaged Green functions $\bar{g}^{\sigma}_{\mathbf{RR}'}(z)$ with increasing distance $|\mathbf{R}-\mathbf{R}'|$. It should be mentioned that this exponential damping refers only to averaged exchange interactions in contrast to those in each alloy configuration which exhibit a much slower decay for large interatomic separations (see Ref. [73] and references therein).

Calculation of magnon spectra in disordered alloys represents a non-trivial task since the corresponding equation of motion for the two-time Green function for spin operators, obtained from the standard decoupling procedure for higher-order Green functions [32], contains a more complicated type of disorder than purely diagonal disorder. The magnons (and also phonons) in random alloys are featured by simultaneous presence of diagonal, off-diagonal and environmental disorder; the latter is closely related to the Goldstone theorem for these excitations. An extension of the CPA to this case has been studied since early 1970's. Two most recent approaches are based on a cumulant expansion [75] and on an augmented-space formalism [76]; the former scheme is combined with the RPA and provides a value for the Curie temperature. Both formulations are rather complicated which allowed to perform numerical calculations for environmental disorder limited to nearest neighbors only, but they seem promising for future studies with true long-range interactions.

The Curie temperature of a random alloy in the MFA can be obtained in a way similar to that leading to Eq. (8). Let us restrict ourselves to the case of a homogeneous random alloy (with all lattice sites equivalent). In analogy to previous on-site exchange parameters, Eqs. (8, 27), one can introduce quantities

$$\bar{J}^{0,QQ'} = \sum_{\mathbf{R}'Q'} \bar{J}^{QQ'}_{\mathbf{RR}'} \ , \qquad \mathcal{K}^{QQ'} = \bar{J}^{0,QQ'}c^{Q'} \ , \tag{30}$$

where $\mathcal{K}^{QQ'}$ are effective exchange parameters among magnetic moments of the alloy constituents. The Curie temperature is then equal to

$$k_{\mathrm{B}}T_{\mathrm{C}}^{\mathrm{MFA}} = \frac{2}{3}\,\kappa_{\mathrm{max}} \ , \tag{31}$$

where κ_{max} is the maximal eigenvalue of the matrix $\mathcal{K}^{QQ'}$. This type of estimation has been used for diluted magnetic semiconductors as described in Section 4.4.

4.4 Diluted magnetic semiconductors

Diluted magnetic semiconductors (DMS) represent a new class of materials with potential technological applications in spintronics. They have recently attracted much interest because of the hole-mediated ferromagnetism [77, 78]. Curie temperatures higher than the room temperature are desirable for practical applications, whereas the currently prepared samples exhibit the T_{C}'s only slightly above 100 K [78, 79]. The most frequently studied DMS is a III-V-based compound $(\mathrm{Ga}_{1-x}\mathrm{Mn}_x)\mathrm{As}$ in the zinc-blende structure with Mn-concentration in the range $0 < x < 0.1$. Since Mn atoms are in a high-spin state in these systems, the above described formalism is well suited for reliable quantitative investigations of the exchange interactions and the Curie temperatures.
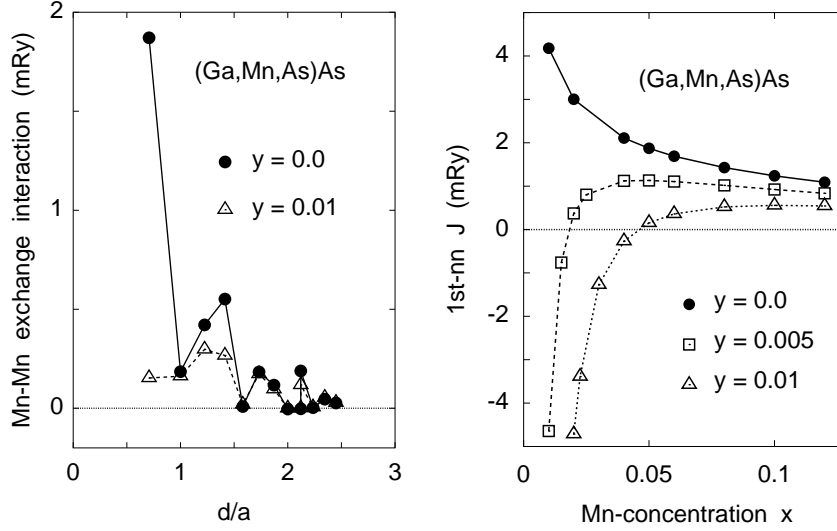
Figure 11: The Mn-Mn exchange interactions in $(\mathrm{Ga}_{0.95-y}\mathrm{Mn}_{0.05}\mathrm{As}_y)\mathrm{As}$ as a function of the Mn-Mn distance d (left panel) and the first nearest-neighbor Mn-Mn interaction in $(\mathrm{Ga}_{1-x-y}\mathrm{Mn}_x\mathrm{As}_y)\mathrm{As}$ (right panel).

The (Ga,Mn)As compound is a substitutionally disordered system with Mn atoms substituting Ga atoms on the cation sublattice. Application of the TB-LMTO-CPA formalism to this system employs so-called empty spheres located at interstitial positions of GaAs semiconductor for matters of space filling, so that the zinc-blende structure is described in terms of four fcc sublattices with substitutional disorder only on the cation sublattice. The pair exchange interactions between Mn atoms $\bar{J}_{\mathbf{RR}'}^{\mathrm{MnMn}}$ in the $(\mathrm{Ga}_{1-x}\mathrm{Mn}_x)\mathrm{As}$ alloy with $x = 0.05$ are shown in Fig. 11 (left panel); interactions between the other components are much smaller and negligible concerning their possible influence on magnetic properties. The first nearest-neighbor interaction is positive and bigger than the (mostly positive) interactions between more distant Mn atoms. Analysis of the behavior of $\bar{J}_{\mathbf{RR}'}^{\mathrm{MnMn}}$ for large interatomic distances reveals exponentially damped RKKY-like oscillations which have two origins: the effect of alloying which introduces an exponential damping in the site-off-diagonal blocks of the averaged Green functions for both spin channels (see Section 4.3), and an additional exponential damping due to a half-metallic character of the system [77], i.e., the alloy Fermi energy lies in a band gap of the minority band (see Section 3.3).

The calculated Curie temperature in MFA for the $(\mathrm{Ga}_{0.95}\mathrm{Mn}_{0.05})\mathrm{As}$ alloy is around 300 K, i.e., substantially higher than the experimental values [78, 79]. A reason for this discrepancy can be found in structural imperfections of the compound which lead to reduction of the number of holes in the valence band. The most probable candidates for such lattice defects are native defects, such as As-antisite atoms [77] and Mn-interstitial atoms [80]. In the following, we demonstrate the influence of the former on the exchange interactions of (Ga,Mn)As compounds [18, 20].

The combined effect of Mn-impurities and As-antisites can be simulated within the CPA using an alloy $(\mathrm{Ga}_{1-x-y}\mathrm{Mn}_x\mathrm{As}_y)\mathrm{As}$ with y denoting the As-antisite concentration. The influence of As-antisites on the Mn-Mn exchange interactions is shown in Fig. 11 (left panel): the positive values of $\bar{J}_{\mathbf{RR}'}^{\mathrm{MnMn}}$ are reduced; the most dramatic reduction is found for the dominating coupling between the nearest-neighbors. The dependence of the nearest-neighbor Mn-Mn interaction on x

and y is shown in Fig. 11 (right panel). For a fixed Mn-concentration x, the interaction decreases monotonously with increasing content of As-antisites y, ending finally at negative values. This change of sign correlates nicely with a predicted instability of the ferromagnetic state with respect to formation of a state featured by disordered directions of the Mn-moments [16, 81].
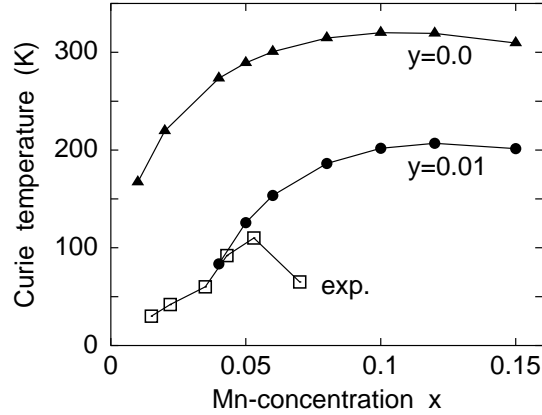

Figure 12: Curie temperatures of $(Ga_{1-x-y}Mn_xAs_y)As$: calculated (full symbols) and experimental [78] (open squares).

The Curie temperatures were estimated in the MFA as described in Sections 2 and 4.3. However, in view of the much bigger Mn-Mn interactions as compared to interactions between other constituent atoms, the Curie temperature comes out equal to

$$k_B T_C^{MFA} = \frac{2}{3} x \sum_{\mathbf{R}'} \bar{J}_{\mathbf{R}\mathbf{R}'}^{MnMn} , \qquad (32)$$

where the lattice sites $\mathbf{R}, \mathbf{R}'$ are confined to the cation fcc sublattice and x denotes the Mn-concentration. The resulting Curie temperatures are summarized in Fig. 12 [16]. The T_C^{MFA} for a fixed x is monotonously decreasing with increasing As-antisite concentration y, in analogy to the y-dependence of the first nearest-neighbor Mn-Mn interaction (Fig. 11, right panel). The T_C for a fixed y exhibits a non-monotonous dependence on the Mn-content x reaching a flat maximum for $x > 0.1$. The latter behavior results from an interplay of two effects: an increase of T_C^{MFA} with increasing x, Eq. (32), and the non-trivial dependence of the first nearest-neighbor Mn-Mn interaction as a function of (x, y), see Fig. 11 (right panel). Note, however, that the next-neighbor exchange couplings also contribute significantly to the Curie temperature, see Eq. (32). A detailed comparison of calculated and measured concentration dependences of the Curie temperature indicates a correlation between the two concentrations x and y in real samples, namely, an increase of the As-antisite concentration with increasing Mn-content [16]. However, this possible explanation of the measured Curie temperatures does not rule out other lattice defects in the system.

Curie temperatures of DMS's have recently been calculated from first principles using alternative approaches [20, 82, 83]. The simplest estimation is based on the total-energy difference ΔE between the DLM state and the ferromagnetic state [16, 82]. The quantity ΔE can be obtained from selfconsistent calculations using the CPA and it can be – within the EHH and the MFA –
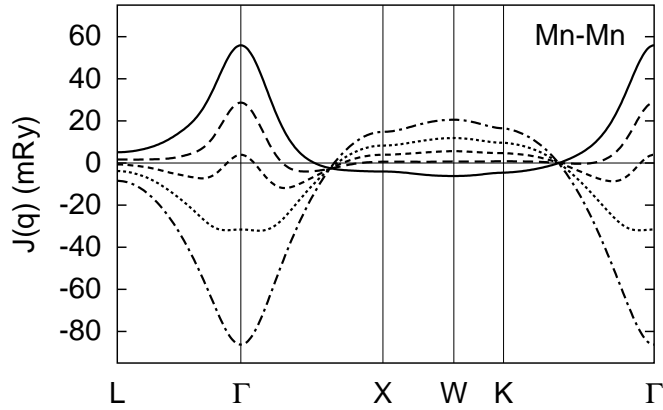
Figure 13: The lattice Fourier transform of the Mn-Mn exchange interaction for $(Ga_{0.95-y}Mn_{0.05}As_y)As$ along high-symmetry lines of the bcc Brillouin zone: $y = 0.0$ (full line), $y = 0.01$ (long dashes), $y = 0.015$ (short dashes), $y = 0.02$ (dotted line), $y = 0.025$ (dashed-dotted line).

identified with the lattice sum in Eq. (32) multiplied by x^2, which yields an expression

$$k_B \tilde{T}_C^{MFA} = \frac{2 \Delta E}{3 x} .$$ (33)

According to our experience for (Ga,Mn)As alloys [16], the values of $\tilde{T}_C^{MFA}$ are higher by 10 to 15% as compared to the values of T_C^{MFA} from Eq. (32).

A combination of the frozen-magnon and supercell approaches was used to study Curie temperatures in (Ga,Mn)As (without structural defects) in the MFA and the RPA [83]. It yielded a non-monotonous dependence of the T_C on the Mn-concentration, very similar to that depicted in Fig. 12 (results for $y = 0$). The RPA values were about 20% smaller than the MFA values; the latter compare well with the present results. It should be noted, however, that the supercell approach was limited to a few special Mn-concentrations ($x = 0.03125, 0.0625, 0.125, 0.25$) and that the first nearest-neighbor Mn-Mn interactions could not be determined due to the special atomic order of the supercells.

Probably the most reliable way of obtaining the Curie temperature from parameters of the EHH is the Monte Carlo simulation. A recent investigation for (Ga,Mn)As alloys proved that the Monte Carlo results yield Curie temperatures only slightly smaller (less than 10%) as compared to the MFA while an RPA estimation of the Curie temperature was found between the MFA and the Monte Carlo values [20]. This success of MFA can be explained by a few special features of the Mn-Mn exchange interactions: they are essentially ferromagnetic, not oscillating, and decaying exponentially with increasing distance, see Fig. 11 (left panel). Their lattice Fourier transforms, shown in Fig. 13, become rather dispersionless, except for a small region around the Γ point, which leads to the small differences among the Curie temperatures evaluated in different ways [20].

Group-IV DMS's, like Mn-doped Ge, have been studied only recently [84, 85], but their Curie temperatures are very similar to those of III-V DMS's. The main difference between the two classes of DMS's lies in positions occupied by Mn atoms: they are located on one fcc sublattice of the zinc-blende structure in the (Ga,Mn)As compound (without native defects) but they
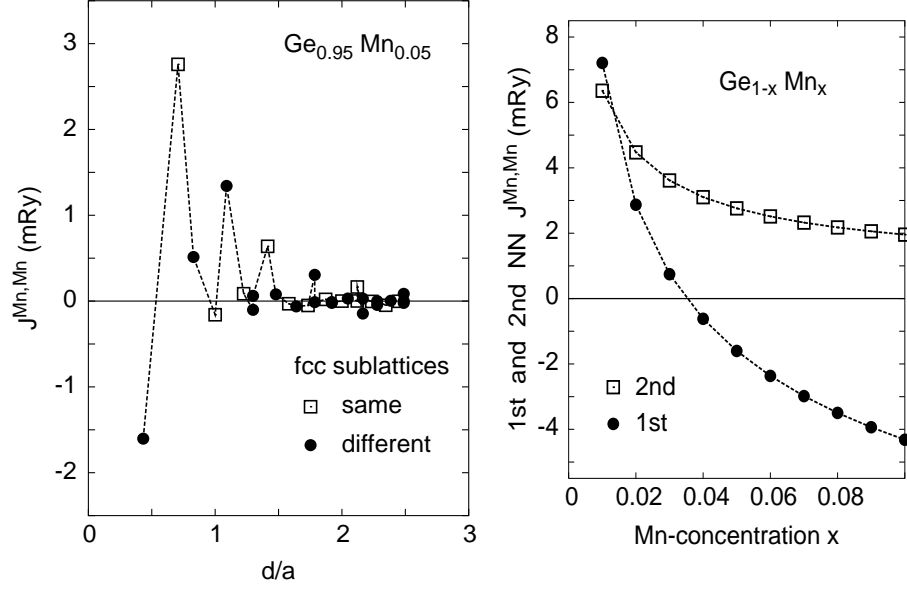
Figure 14: The Mn-Mn exchange interactions in $Ge_{0.95}Mn_{0.05}$ as a function of the Mn-Mn distance d (left panel) and the first and the second nearest-neighbor Mn-Mn interactions in $Ge_{1-x}Mn_x$ (right panel). The pair interactions are divided according to positions of the two Mn atoms on two fcc Ge-sublattices.

occupy lattice sites of two fcc sublattices of the diamond structure in the (Ge,Mn) case. The latter system thus contains Mn-Mn pairs with a short distance which is known to support antiferromagnetic exchange coupling of Mn-moments.
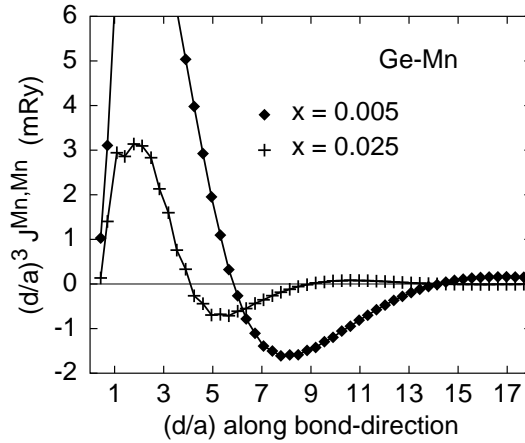
Figure 15: The Mn-Mn exchange interactions multiplied by d^3 in $Ge_{1-x}Mn_x$ as a function of the Mn-Mn distance d for Mn-Mn pairs along the bond direction.

The calculated Mn-Mn exchange interactions in (Ge,Mn) alloys are shown in Fig. 14. It can be seen that the interactions exhibit strong concentration dependence, as illustrated in right panel of Fig. 14 for the first and second nearest-neighbor interactions: for 6% of Mn we find antiferromagnetic coupling between Mn neighbors on different fcc sublattices in a qualitative agreement with results of supercell calculations in Ref. [84]. The negative first nearest-neighbor interaction appears for alloys with more than 3% Mn, whereas the next-neighbor interactions

are essentially ferromagnetic (Fig. 14, left panel). Note that the concentration dependence of the second nearest-neighbor interaction (Fig. 14, right panel) is very similar to that between the first nearest Mn-Mn neighbors in the $Ga_{1-x}Mn_x$As alloy (Fig. 11, right panel).

The asymptotic behavior of $\bar{J}_{\mathbf{RR'}}^{MnMn}$ is presented in Fig. 15 for Mn-Mn pairs along the bond direction, i.e., along a zig-zag line following the [110] direction. Besides the exponential damping of the RKKY-type oscillations, discussed above, one can see a pronounced change of the periods of oscillations with Mn-concentration. This property agrees fully with the RKKY picture which leads to oscillation periods inversely proportional to the characteristic size of the hole of the Fermi surface. It can be also seen that the ferromagnetic character of couplings for $x = 0.025$ is preserved up to a distance of about $4a$ (a is the fcc lattice constant) which is bigger than the average distance of about $3.4a$ between two Mn-impurities.
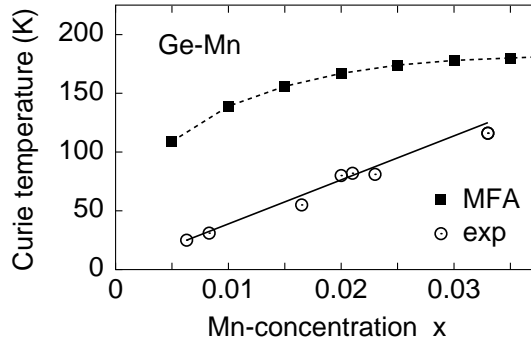
Figure 16: Curie temperatures in $Ge_{1-x}Mn_x$: calculated in MFA and experimental [84].

Curie temperatures in the MFA for $Ge_{1-x}Mn_x$ alloys were calculated according to Eq. (32) with the lattice sum extending over two fcc sublattices occupied by Mn atoms. The concentration dependence is shown in Fig. 16 together with available experimental data [84]. The calculated Curie temperatures increase with Mn-content up to $x \approx 0.03$ where a saturated behavior appears as a consequence of the antiferromagnetic coupling between the first Mn-Mn neighbors (Fig. 14). The measured Curie temperatures increase with Mn-content as well; the difference between the theoretical and experimental data is probably due to Mn-interstitials present in real samples. Their inclusion into theoretical models is under way.

4.5   Two-dimensional ferromagnets

Magnetism of epitaxial ultra-thin transition-metal films on non-magnetic noble- or transition-metal substrates has been studied intensively during the last two decades. Main differences with respect to bulk magnetism lie both in ground-state properties, where non-zero local moments can appear also for other elements besides the five $3d$ transition metals (Cr, Mn, Fe, Co, Ni) [86], and in finite-temperature behavior, where the reduced dimensionality leads to a different universality class as compared to the bulk. In the limit of one-monolayer thickness of the film, one can realize a true two-dimensional magnet on a non-magnetic substrate.

The above formalism can easily be generalized to the two-dimensional case since the basic expression for the pair exchange interactions, Eq. (13), is formulated in the real space. The

magnetic properties resulting from a two-dimensional EHH can be obtained in a similar way like in the bulk case, see Eqs. (6, 7, 8, 9), with the reciprocal-space vector $\mathbf{q}$ replaced by a two-dimensional vector $\mathbf{q}_\parallel$ in the surface Brillouin zone (SBZ) and with the real-space sums restricted to lattice sites $\mathbf{R}, \mathbf{R}'$ of the magnetic film. The site-off-diagonal blocks $g^\sigma_{\mathbf{R}\mathbf{R}'}(z)$ of the Green function in Eq. (13) are determined using the surface Green function technique [35, 36], while the definition of $\Delta_\mathbf{R}(z)$ remains unchanged. The magnon energies are given by

$$E(\mathbf{q}_\parallel) = \frac{4}{M} \left[J(\mathbf{0}_\parallel) - J(\mathbf{q}_\parallel) \right] + \Delta \ , \quad J(\mathbf{q}_\parallel) = \sum_\mathbf{R} J_{\mathbf{0}\mathbf{R}} \exp(i\mathbf{q}_\parallel \cdot \mathbf{R}) \ , \tag{34}$$

where Δ is a magnetic anisotropy energy which is a consequence of relativistic effects (spin-orbit interaction, magnetostatic dipole-dipole interaction). The Curie temperature in the MFA is given by Eq. (8) while the RPA leads to an expression

$$\left(k_B T_C^{RPA} \right)^{-1} = \frac{6}{M} \ \frac{1}{N_\parallel} \sum_{\mathbf{q}_\parallel} \frac{1}{E(\mathbf{q}_\parallel)} \ , \tag{35}$$

where $N_\parallel$ is the number of $\mathbf{q}_\parallel$-vectors used in the SBZ-average.
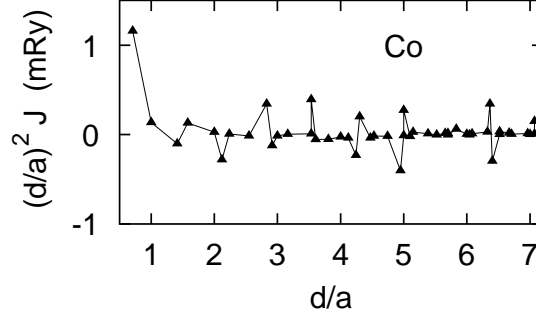

Figure 17: Exchange interactions $J_{\mathbf{R}\mathbf{R}'}$ multiplied by a prefactor d^2 for Co-moments in a Co-overlayer on an fcc Cu(001) substrate as a function of the distance $|\mathbf{R} - \mathbf{R}'| = d$.

The calculated pair exchange interactions $J_{\mathbf{R}\mathbf{R}'}$ in a Co-monolayer on an fcc Cu(001) substrate are shown in Fig. 17. The first nearest-neighbor interaction dominates and the next-neighbor interactions exhibit an RKKY-like oscillatory behavior with an envelope decaying proportionally to $|\mathbf{R} - \mathbf{R}'|^{-2}$, in contrast to the bulk decay proportional to $|\mathbf{R} - \mathbf{R}'|^{-3}$. Note, however, that the present case is not strictly two-dimensional due to the indirect exchange interactions of two Co-overlayer atoms via the Cu-substrate, which becomes weakly polarized in the atomic layers adjacent to the overlayer.

The indirect interaction between the magnetic atoms, which is mediated by the non-magnetic atoms, has important consequences for magnetic properties of magnetic films placed on a non-magnetic substrate and covered by a non-magnetic cap-layer of a finite thickness. As reported in a recent experiment [87], the Curie temperature of fcc(001)-Fe ultrathin films on a Cu(001) substrate varies in a non-monotonous manner as a function of the Cu cap-layer thickness. Such a behavior clearly cannot be explained within a localized picture of magnetism.

Motivated by this finding we performed a systematic study of Fe- and Co-monolayers on an fcc Cu(001) substrate capped by another Cu-layer of varying thickness [13, 15]. Figure 18 presents the magnon spectra in two limiting cases, namely, for an uncovered Fe-overlayer on Cu(001)
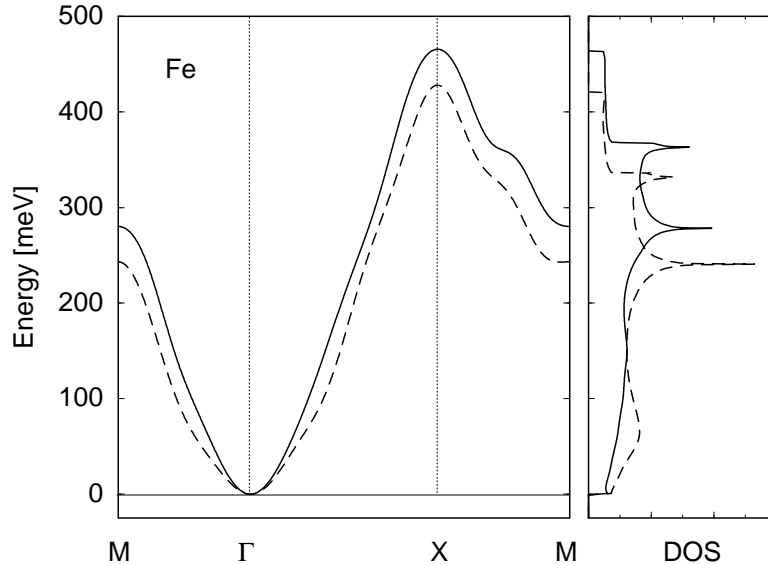
Figure 18: Magnon dispersion laws (left panel) and corresponding densities of states (right panel) for an Fe-layer embedded in fcc Cu (full lines) and an Fe-overlayer on fcc Cu(001) (dashed lines). We have set here $\Delta = 0$ in Eq. (34).

and for an Fe-monolayer embedded in bulk Cu, and figure 19 shows the full dependence of the magnetic moments and the first nearest-neighbor exchange interactions on the cap-layer thickness. The magnon spectra and the magnon densities of states exhibit all typical features of two-dimensional bands with the nearest-neighbor interactions which are here only slightly modified by non-vanishing interactions in next shells. The magnetic moments drop substantially on capping while their sensitivity to increasing cap-layer thickness is rather small. On the other hand, the behavior of the nearest-neighbor exchange interaction is more complicated and it reflects interference effects in the Cu-cap layer. The oscillations visible in right panel of Fig. 19 are due to quantum-well states in the Cu-cap layer formed between the vacuum and the magnetic layer which, in turn, influence properties of the magnetic layer. Note that the values of the nearest-neighbor exchange interaction are significantly enhanced (roughly by a factor 2 or more) as compared with their bulk counterparts (cf. Fig. 1).

Calculations of the Curie temperatures of the two-dimensional ferromagnets represent a more difficult task than in the bulk case. The MFA Curie temperatures of the monolayers are typically of the same order of magnitude as the corresponding bulk temperatures [13] due to the fact that the reduced coordination is approximately compensated by the increase of the exchange interactions. This observation is in a strong disagreement with experimental data which yield the Curie temperatures of the order $150 - 200$ K. This failure is due to the fact that the MFA violates the Mermin-Wagner theorem [88] due to the neglect of collective transverse fluctuations (spin-waves) and it is thus inappropriate for two-dimensional systems.

Application of the RPA to the Curie temperature of a two-dimensional isotropic EHH, Eq. (35) with $\Delta = 0$, yields a vanishing $T_{\mathrm{C}}^{\mathrm{RPA}}$ in agreement with the Mermin-Wagner theorem. Finite values of $T_{\mathrm{C}}^{\mathrm{RPA}}$ require non-zero values of the magnetic anisotropy energy Δ which is taken here as an adjustable parameter. This is not a serious problem as the RPA Curie temperature has
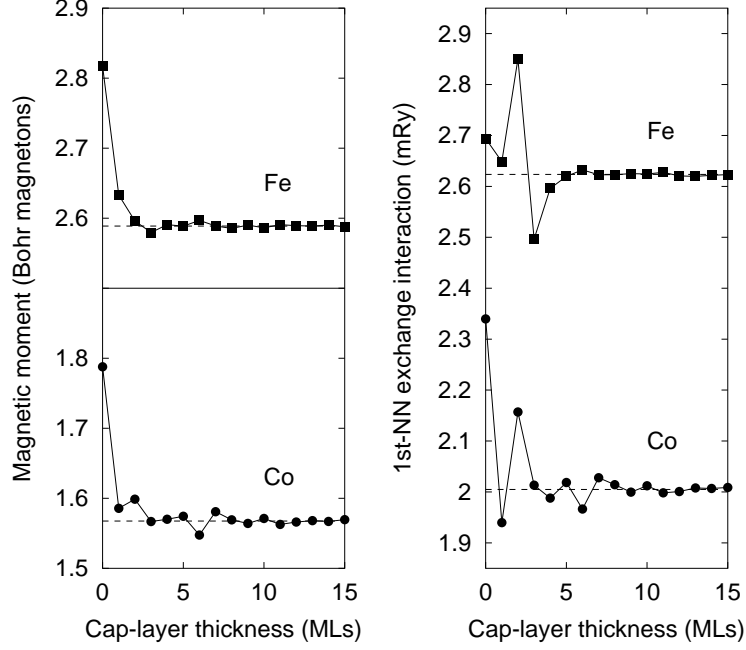
Figure 19: The magnetic moments (left panel) and the first nearest-neighbor exchange interactions (right panel) of the Fe- and Co-monolayers on fcc Cu(001) as a function of the cap-layer thickness. The dashed lines represent the embedded layer limit (infinite cap thickness) while the limit of zero cap thickness corresponds to the uncovered overlayer.

only a weak logarithmic dependence upon Δ [89], and it is thus sufficient to know the order of magnitude of Δ. The latter is typically of the order of the dipolar energy $2\pi(M\mu_B)^2/V$, where V is the atomic volume. In calculations we used $\Delta_{Co} = 0.052$ mRy and $\Delta_{Fe} = 0.140$ mRy.

The calculated RPA Curie temperatures are shown in Fig. 20 (left panel). They are strongly reduced as compared to the corresponding bulk values thereby improving on the MFA results. Nevertheless, they are still too large as compared to experiment. It is unclear whether this is due to some inaccuracy of the theory or to some imperfections of the samples used in experiments. On the other hand, such important experimental facts as the strong influence of the metallic coverage on the Curie temperature [87] are well explained by the present theory. The fluctuations of the Curie temperature are of order of $50 - 70$ K, in a reasonable agreement with experiment. A more detailed analysis of the data reveals that the oscillations of the RPA Curie temperatures follow rather closely the behavior of the spin-stiffness constants, see Fig. 20. The similarity of both trends is due to the fact that the T_C^{RPA} for a two-dimensional system is determined predominantly by low-energy magnons.

It should be noted that an analogous oscillatory behavior of the Curie temperature as a function of the non-magnetic spacer thickness has also been observed for fcc(001)-Co/Cu/Ni trilayers [90]. The latter system has been investigated theoretically in terms of the on-site exchange parameters J_R^0 [91].
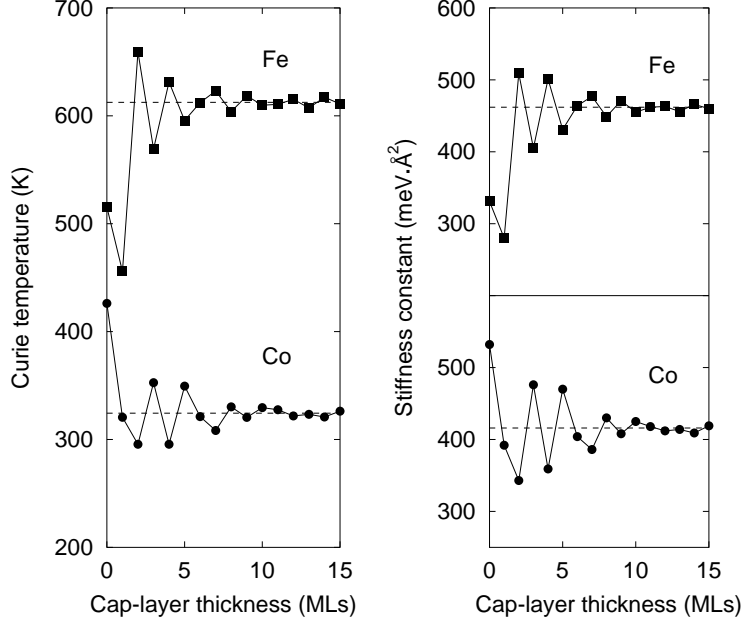
Figure 20: The Curie temperatures (left panel) and the spin-stiffness constants (right panel) of the Fe- and Co-monolayers on fcc Cu(001) as a function of the cap-layer thickness. The dashed lines represent the embedded layer limit (infinite cap thickness) while the limit of zero cap thickness corresponds to the uncovered overlayer case.

4.6 Surfaces of ferromagnets

Reduced coordination at surfaces of transition-metal ferromagnets leads to an enhancement of surface magnetic moments over their bulk values [86]. For the ferromagnetic hcp Gd, an enhancement of its Curie temperature at (0001) surface over the bulk value was observed [92]. Theoretical explanation of the latter fact was provided by total-energy calculations using an LSDA+U approach [93]. An important role was ascribed to a small inward relaxation of the top surface layer. However, more recent works have thrown serious doubts on these conclusions, both on side of experiment [94] and theory [63].

We have recently performed calculations for low-index surfaces of bcc Fe, hcp Co, and hcp Gd [19] focused on layer-resolved local quantities like the magnetic moments and the on-site exchange parameters $J_{\mathbf{R}}^0$, Eq. (17). Note, however, that for inhomogeneous systems like surfaces, a direct relation between the Curie temperatures and the on-site exchange parameters $J_{\mathbf{R}}^0$ cannot be given. Hence, the latter quantities reflect merely the strength of the exchange interaction and its spatial variations in layered systems [91].

Figure 21 presents the results for Fe- and Co-surfaces. It is seen that the well-known surface enhancement of the moments is accompanied by a more complicated layer-dependence of the on-site exchange parameters exhibiting a minimum in the top surface layer and a maximum in the first subsurface layer. A qualitative explanation follows from Eqs. (13, 17) which show that $J_{\mathbf{R}}^0$ reflects the exchange splitting on the $\mathbf{R}$-th site as well as the splittings and number of its neighbors. Hence, the reduction of $J_{\mathbf{R}}^0$ in the top surface layer is due to the reduced coordination, whereas the maximum in the first subsurface position is due to the full (bulk-like)
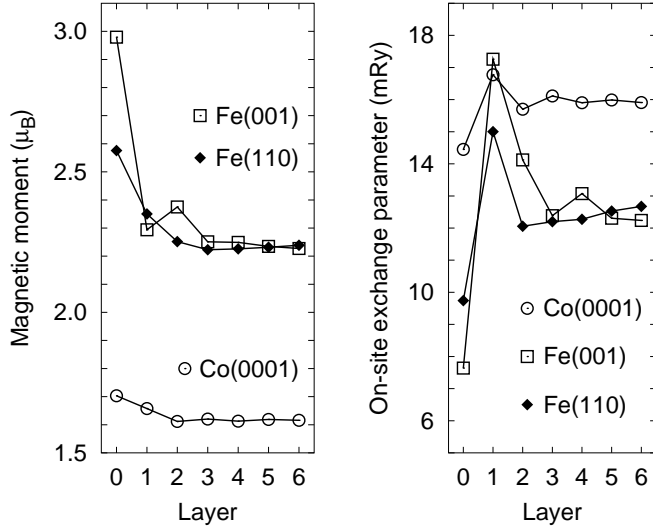
Figure 21: Layer-resolved magnetic moments (left panel) and on-site exchange parameters $J_{\mathbf{R}}^0$ (right panel) at surfaces of bcc Fe and hcp Co. The layer numbering starts from the top surface layer, denoted by 0.

coordination of these sites and the enhanced surface local moments, see Fig. 21. Note that the layer-dependence of the on-site exchange parameters and its explanation are analogous to the case of hyperfine magnetic fields at the nuclei of iron atoms [35, 95].

The Gd(0001) surface was treated in the 'open-core' approach mentioned in Section 4.2. Two models of the surface structure were used: with lattice sites occupying the ideal truncated bulk positions (unrelaxed structure) and with a 3% contraction of the interlayer separation between the two topmost atomic layers (inward relaxation). The magnitude of the contraction was set according to LEED measurements [96] and previous full-potential calculations [63]. The layer-resolved quantities are presented in Figure 22. The layer-resolved magnetic moments exhibit a small surface enhancement followed by Friedel-like oscillations around the bulk value. These oscillations can be resolved also in the layer-dependence of the on-site exchange parameters $J_{\mathbf{R}}^0$ which, however, start with reduced values in the top surface layer due to the reduced coordination, as discussed for Fe- and Co-surfaces. The maximum of the on-site exchange parameters is found in the second subsurface layer, in contrast to the transition-metal surfaces, which can be explained by the reduced Gd-moments in the first subsurface layer. The surface relaxation does not modify investigated layer-dependences substantially: it leads to a small reduction of the local moments and the on-site exchange parameters in the first two top surface layers and a tiny enhancement in the second subsurface layer as compared to the ideal surface.

One can conclude that the surface enhancement of the local magnetic moments of the three ferromagnetic metals is not accompanied by an analogous trend of on-site exchange parameters which might be an indication of a surface-induced enhancement of Curie temperatures. However, a calculation of the pair exchange interactions and an improved treatment of the EHH beyond the MFA remain important tasks for future.
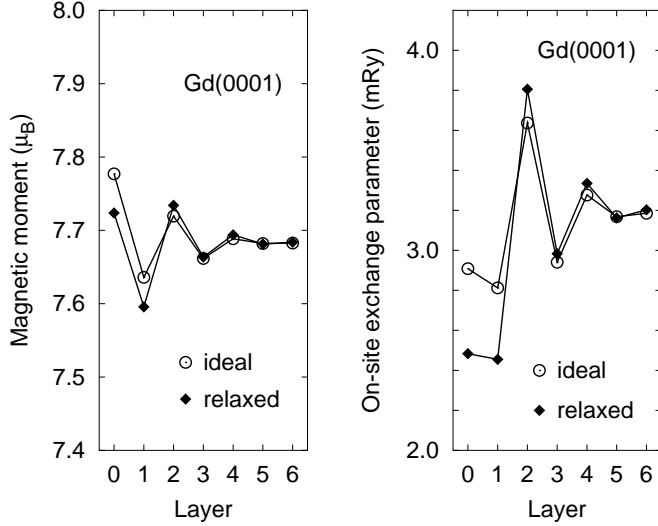
Figure 22: Layer-resolved magnetic moments (left panel) and on-site exchange parameters $J_{\mathbf{R}}^0$ (right panel) at the (0001) surface of hcp Gd as calculated with the lattice sites in the ideal truncated bulk positions and with the top surface layer relaxed towards the bulk. The layer numbering starts from the top surface layer, denoted by 0.

5   Discussion and outlook

Exchange interactions and related quantities can be extracted from selfconsistent electronic structure calculations in a number of different ways; each of them has its own advantages and disadvantages. The simplest approach lies in obtaining the exchange interactions from total-energy differences calculated directly for various (usually collinear) spin configurations [63, 97, 98]. The usefulness of such schemes is, however, rather limited mainly due to a finite number of configurations used for the mapping.

The real-space method presented here allows to get a set of pair interactions even for very distant atoms only from a single selfconsistent calculation. It has therefore been used independently in a number of papers for very different systems [51, 99, 100, 101]. A widely used alternative approach, the so-called frozen-magnon approach, relies on constrained DFT calculations for true spin spirals and subsequent derivation of the coupling constants from the total energies of the spirals [27, 43, 44]. The frozen-magnon approach can be implemented with the magnetic force theorem [83] or can be formulated in terms of torques instead of total energies [102]. The real-space and frozen-magnon approaches are formally equivalent to each other. The quantities that are directly calculated (the pair exchange interactions $J_{\mathbf{RR'}}$ in the former case, the magnon energies $E(\mathbf{q})$'s in the latter) are related to each other by a lattice Fourier transformation, Eq. (6). For this reason, their advantages and disadvantages refer mainly to their computational efficiency. For calculations of spin-wave dispersion curves (for a moderate number of $\mathbf{q}$-points) and of the spin-wave stiffness D, the frozen-magnon approach is superior, for it does not require to perform the Fourier transformation and the delicate analysis explained in Section 3.3. The real-space approach seems to be more efficient for calculations of the Curie temperature, where the MFA estimation can be obtained from Eq. (8) and the sum rule (17), i.e., from a single real-space calculation, whereas a BZ-average of the magnon energies $E(\mathbf{q})$ is required in the

frozen-magnon approach. The real-space technique is better also when a fine scan over the full BZ is needed like, e.g., in RPA calculations of the Curie temperature, Eq. (9), or in searching for instabilities of the ferromagnetic state (see Section 4.2), since the set of calculated $J_{\mathbf{RR'}}$ for typically 200 shells provides a fast and accurate parametrization of $J(\mathbf{q})$, which considerably reduces the computational effort.

The central idea of mapping the infinitesimal changes of single-particle energies onto an effective classical Hamiltonian for localized spins has been used also for a quantitative description of effects beyond the bilinear isotropic exchange interaction in Eq. (2). Higher terms in expansion of the single-particle energies with respect to rotation angles give rise to biquadratic exchange interaction, important especially in metallic multilayers [103]. Inclusion of relativistic effects, leading to anisotropic exchange interaction and Dzialoshinskii-Moriya interaction, has been discussed for bulk systems [52, 104] and thin films [105]. In both cases, the gap in the spin-wave spectrum for zero wavevector can be calculated with accuracy better than used in Section 4.5 for quantity Δ in Eq. (34). The magnetic force theorem and expressions for effective interaction parameters have recently been formulated also for highly correlated systems treated beyond the LSDA [106].

It should be noted, however, that certain aspects of finite-temperature itinerant magnetism cannot be reproduced by effective Hamiltonians with one unit vector per atomic site only. An *ab initio* study based on a model Hamiltonian with bilinear, biquadratic and bicubic terms depending on the magnitude of local magnetic moments was formulated in Ref. [107]. The parametrization of the model was obtained from selfconsistent calculations for a number of spin-spiral states. The calculated Curie temperature of bcc Fe agrees well with experiment while the Curie temperatures of fcc Co and fcc Ni were underestimated by about $20 - 25\%$.

Another *ab initio* approach based on effective Hamiltonians acting on more than one magnetic vector per atom was worked out in Refs. [43, 62]. It is based on a well-defined spatial separability of the *sp*- and *d*-components of the spin density in late 3*d* transition metals leading thus to two spin vectors per atom. Results of this approach for the magnon spectrum of fcc Ni seem to describe qualitatively well finer details in the experimental data around $100 - 150$ meV (sometimes denoted as an 'optical' magnon), which are manifestation of non-adiabatic effects [43]. In the case of heavy RE-metals (Gd through Tm), three moment vectors per site were considered: the conduction electron (*spd*) spin moment vector and the 4*f* electron spin and orbital moment vectors. The effective Hamiltonian in the latter case contains also intrasite spin-orbit coupling interaction and crystal-field terms. A first-principles approach to crystal-field parameters in RE-based systems can be found in Refs. [60, 108].

As mentioned in Section 2, the pair exchange interactions according to Eq. (5) do not contain contributions from constraining magnetic fields which appear as Lagrange multipliers in the constrained DFT. Their effect has been recently addressed in Refs. [24, 26]; it leads to a modification of the pair exchange interactions and related quantities. The changes of the moment directions $\delta\mathbf{u_R}$ and the constraining fields $\mathbf{B_R^\perp}$ satisfy linear relations [24]

$$M_{\mathbf{R}}\,\delta\mathbf{u_R} \;=\; \sum_{\mathbf{R'}} \left(K_{\mathbf{RR'}}\,\delta\mathbf{u_{R'}} \;+\; \chi_{\mathbf{RR'}}\,\mathbf{B_{R'}^\perp} \right) \;, \qquad (36)$$

where $M_{\mathbf{R}}$ denotes the magnitude of $\mathbf{R}$-th local moment in units of μ_{B} and where the exchange-

correlation response function $K_{\mathbf{RR'}}$ and the bare transverse susceptibility $\chi_{\mathbf{RR'}}$ are given by

$$K_{\mathbf{RR'}} = \frac{2}{\pi} \operatorname{Im} \int_{-\infty}^{E_{\mathrm{F}}} dE \int_{\Omega_{\mathbf{R}}} d\mathbf{r} \int_{\Omega_{\mathbf{R'}}} d\mathbf{r'} \, G^{\uparrow}(\mathbf{r}, \mathbf{r'}; E + \mathrm{i}0) \, B_{\mathrm{xc}}(\mathbf{r'}) \, G^{\downarrow}(\mathbf{r'}, \mathbf{r}; E + \mathrm{i}0) ,$$

$$\chi_{\mathbf{RR'}} = \frac{2}{\pi} \operatorname{Im} \int_{-\infty}^{E_{\mathrm{F}}} dE \int_{\Omega_{\mathbf{R}}} d\mathbf{r} \int_{\Omega_{\mathbf{R'}}} d\mathbf{r'} \, G^{\uparrow}(\mathbf{r}, \mathbf{r'}; E + \mathrm{i}0) \, G^{\downarrow}(\mathbf{r'}, \mathbf{r}; E + \mathrm{i}0) . \tag{37}$$

As a consequence of non-zero constraining fields, the exchange parameters $J_{\mathbf{RR'}}$ get renormalized values given explicitly by [24]

$$J_{\mathbf{RR'}}^{\mathrm{ren}} = J_{\mathbf{RR'}} - \frac{1}{2} \left\{ (M - K^T) X^{-1} (M - K) \right\}_{\mathbf{RR'}} , \tag{38}$$

where M, K, X denote, respectively, matrices with elements $M_{\mathbf{R}} \delta_{\mathbf{RR'}}$, $K_{\mathbf{RR'}}$, $\chi_{\mathbf{RR'}}$, and where K^T denotes the transpose of K. The evaluation of Eq. (38) for real systems remains yet to be performed.

Some physical insight into the nature of this renormalization can be obtained for Bravais lattices assuming a sufficiently rigid magnetization within an atomic cell [24]. With a definition of an average exchange splitting on site $\mathbf{R}$,

$$\Delta_{\mathbf{R}} = \frac{2}{M_{\mathbf{R}}} \int_{\Omega_{\mathbf{R}}} d\mathbf{r} \, m(\mathbf{r}) \, B_{\mathrm{xc}}(\mathbf{r}) , \tag{39}$$

where $m(\mathbf{r})$ is the spin density, it can be shown that the renormalization of the pair interactions, Eq. (38), leads to a simple renormalization of the magnon energies $E(\mathbf{q})$ which is significant for high-energy magnons $E(\mathbf{q}) > \Delta$ (where $\Delta = \Delta_{\mathbf{R}}$ for a Bravais lattice). In particular, the spin-wave stiffness constant D does not undergo any renormalization. The Curie temperature evaluated in the RPA becomes renormalized according to a formula

$$\left(k_{\mathrm{B}} T_{\mathrm{C}}^{\mathrm{RPA,ren}} \right)^{-1} = \left(k_{\mathrm{B}} T_{\mathrm{C}}^{\mathrm{RPA}} \right)^{-1} - \frac{6}{M\Delta} , \tag{40}$$

which means that the renormalized Curie temperatures are enhanced as compared to the un-renormalized ones. The values for the bulk cubic $3d$ ferromagnets are summarized in Table 3. It can be seen that the renormalization of exchange parameters improves considerably the agreement between theory and experiment for Fe and Ni, in contrast to Co, where the unrenormalized Curie temperature is closer to experiment than the renormalized one. A quantitative analysis for bulk Gd shows that the effect of constraining fields is completely negligible [26].

Table 3: Curie temperature calculated within the RPA by using the bare ($T_{\mathrm{C}}^{\mathrm{RPA}}$) and renormal-ized ($T_{\mathrm{C}}^{\mathrm{RPA,ren}}$) exchange interactions and their comparison with experimental values ($T_{\mathrm{C,exp}}$).

Metal	$T_{\mathrm{C}}^{\mathrm{RPA}}$[K]	$T_{\mathrm{C}}^{\mathrm{RPA,ren}}$[K]	$T_{\mathrm{C,exp}}$[K]
Fe bcc	950	1057	$1044 - 1045$
Co fcc	1311	1771	$1388 - 1398$
Ni fcc	350	634	$624 - 631$

As is well known, the exact magnon dispersion law is obtained from poles of the dynamical transverse susceptibility while the effective exchange interactions are closely related to the static

transverse susceptibility [26]. Susceptibility calculations within the DFT are, however, quite involved even for systems with perfect three-dimensional translational symmetry [109, 110], which calls for additional approximations. The calculations can be simplified using again the adiabatic approximation and the ASA as done in Ref. [102]. The spin-wave spectrum of bcc Fe calculated from the susceptibility agrees very well with that from a frozen-magnon approach, whereas differences between the two approaches are found in results for fcc Co and fcc Ni [102]. However, for a correct reproduction of the 'optical' magnon branch of fcc Ni (including the lifetime effects), full susceptibility calculations [110] are inevitable.

Susceptibility calculations have been employed in another successful approach to finite-temperature magnetism, based on the DLM state with local magnetic moments pointing to random directions [21, 111]. In contrast to the previous techniques starting from the magnetic ground state and its excitations, the DLM theory is focused on the paramagnetic state whereby no particular form of an effective spin Hamiltonian has to be assumed. The transition temperature is derived from divergence of the susceptibility of the DLM state which is related to a direct correlation function. An efficient evaluation of the latter quantity represents the most difficult part of computations. This mean-field technique has been applied to bulk bcc Fe and fcc Ni [54]; an especially good agreement between the calculated and experimental Curie temperatures has been achieved by including effects of correlations in terms of Onsager cavity fields. Applications to thin transition-metal films have been restricted to the mean-field level [112, 113]; the results for the Curie temperatures reproduce a number of experimentally observed trends with respect to the thickness of magnetic films and of non-magnetic capping layers. In the case of Fe and Co monolayers on a Cu(001) substrate, however, the theory predicts unrealistically high Curie temperatures, in full agreement with the MFA values from the EHH, see Section 4.5 and Ref. [13].

The most important feature of the described *ab initio* approach to exchange interactions lies in its real-space formulation, which opens a way to study long-range interactions encountered in itinerant magnets including systems without three-dimensional translational invariance (random alloys, low-dimensional magnets). The inherent limitation to cases with large local magnetic moments makes the approach especially suitable for applications to systems like transition-metal surfaces and thin films, diluted magnetic semiconductors, rare-earth metals and compounds, etc.

Acknowledgements

References

[1] P. Hohenberg and W. Kohn. *Phys. Rev.*, 136:B864, 1964.

[2] W. Kohn and L. J. Sham. *Phys. Rev.*, 140:A1133, 1965.

[3] U. von Barth and L. Hedin. *J. Phys. C*, 5:1629, 1972.

[4] J. B. Staunton. *Rep. Progr. Phys.*, 57:1289, 1994.

[5] J. Kübler. *Theory of Itinerant Electron Magnetism.* Clarendon Press, Oxford, 2000.

[6] K. Baberschke, M. Donath, and W. Nolting, editors. *Band-Ferromagnetism*, volume 580 of *Lecture Notes in Physics.* Springer, Berlin, 2001.

[7] P. Mohn. *Magnetism in the Solid State.* Springer, Berlin, 2003.

[8] E. Runge and E. K. U. Gross. *Phys. Rev. Lett.*, 52:997, 1984.

[9] N. D. Mermin. *Phys. Rev.*, 137:A1441, 1965.

[10] A. I. Liechtenstein, M. I. Katsnelson, and V. A. Gubanov. *J. Phys. F*, 14:L125, 1984.

[11] A. I. Liechtenstein, M. I. Katsnelson, V. P. Antropov, and V. A. Gubanov. *J. Magn. Magn. Mater.*, 67:65, 1987.

[12] V. P. Antropov, B. N. Harmon, and A. N. Smirnov. *J. Magn. Magn. Mater.*, 200:148, 1999.

[13] M. Pajda, J. Kudrnovský, I. Turek, V. Drchal, and P. Bruno. *Phys. Rev. Lett.*, 85:5424, 2000.

[14] M. Pajda, J. Kudrnovský, I. Turek, V. Drchal, and P. Bruno. *Phys. Rev. B*, 64:174402, 2001.

[15] P. Bruno, J. Kudrnovský, M. Pajda, V. Drchal, and I. Turek. *J. Magn. Magn. Mater.*, 240:346, 2002.

[16] J. Kudrnovský, I. Turek, V. Drchal, F. Máca, J. Mašek, P. Weinberger, and P. Bruno. *J. Superconductivity*, 16:119, 2003.

[17] I. Turek, J. Kudrnovský, G. Bihlmayer, and S. Blügel. *J. Phys.: Condens. Matter*, 15:2771, 2003.

[18] I. Turek, J. Kudrnovský, V. Drchal, P. Bruno, and S. Blügel. *Physica Status Solidi B*, 236:318, 2003.

[19] I. Turek, G. Bihlmayer, S. Blügel, and P. Weinberger. *Czech. J. Phys.*, 53:81, 2003.

[20] G. Bouzerar, J. Kudrnovský, L. Bergqvist, and P. Bruno. *Phys. Rev. B*, 68:081203, 2003.

[21] B. L. Gyorffy, A. J. Pindor, J. Staunton, G. M. Stocks, and H. Winter. *J. Phys. F*, 15:1337, 1985.

[22] P. H. Dederichs, S. Blügel, R. Zeller, and H. Akai. *Phys. Rev. Lett.*, 53:2512, 1984.

[23] L. M. Sandratskii. *J. Phys.: Condens. Matter*, 3:8565, 1991.

[24] P. Bruno. *Phys. Rev. Lett.*, 90:087205, 2003.

[25] A. Oswald, R. Zeller, P. J. Braspenning, and P. H. Dederichs. *J. Phys. F*, 15:193, 1985.

[26] V. P. Antropov. *J. Magn. Magn. Mater.*, 262:L192, 2003.

[27] S. V. Halilov, H. Eschrig, A. Y. Perlov, and P. M. Oppeneer. *Phys. Rev. B*, 58:293, 1998.

[28] V. P. Antropov, M. I. Katsnelson, M. van Schilfgaarde, and B. N. Harmon. *Phys. Rev. Lett.*, 75:729, 1995.

[29] V. P. Antropov, M. I. Katsnelson, B. N. Harmon, M. van Schilfgaarde, and D. Kusnezov. *Phys. Rev. B*, 54:1019, 1996.

[30] Q. Niu and L. Kleinman. *Phys. Rev. Lett.*, 80:2205, 1998.

[31] Q. Niu, X. Wang, L. Kleinman, W.-M. Liu, D. M. C. Nicholson, and G. M. Stocks. *Phys. Rev. Lett.*, 83:207, 1999.

[32] S. V. Tyablikov. *Methods of Quantum Theory of Magnetism.* Plenum Press, New York, 1967.

[33] C. S. Wang, R. E. Prange, and V. Korenman. *Phys. Rev. B*, 25:5766, 1982.

[34] O. K. Andersen and O. Jepsen. *Phys. Rev. Lett.*, 53:2571, 1984.

[35] I. Turek, V. Drchal, J. Kudrnovský, M. Šob, and P. Weinberger. *Electronic Structure of Disordered Alloys, Surfaces and Interfaces.* Kluwer, Boston, 1997.

[36] I. Turek, J. Kudrnovský, and V. Drchal. In H. Dreyssé, editor, *Electronic Structure and Physical Properties of Solids*, volume 535 of *Lecture Notes in Physics*, page 349. Springer, Berlin, 2000.

[37] S. H. Vosko, L. Wilk, and M. Nusair. *Can. J. Phys.*, 58:1200, 1980.

[38] P. Weinberger. *Electron Scattering Theory for Ordered and Disordered Matter.* Clarendon Press, Oxford, 1990.

[39] A. Gonis. *Green Functions for Ordered and Disordered Systems.* North-Holland, Amsterdam, 1992.

[40] O. Gunnarsson, O. Jepsen, and O. K. Andersen. *Phys. Rev. B*, 27:7144, 1983.

[41] P. Bruno. *Phys. Rev. B*, 52:411, 1995.

[42] K. C. Hass, B. Velický, and H. Ehrenreich. *Phys. Rev. B*, 29:3697, 1984.

[43] S. Halilov. In D. J. Singh and D. A. Papaconstantopoulos, editors, *Electronic Structure and Magnetism of Complex Materials*, volume 54 of *Springer Series in Materials Science*, chapter 1, page 1. Springer, Berlin, 2003.

[44] M. van Schilfgaarde and V. P. Antropov. *J. Appl. Phys.*, 85:4827, 1999.

[45] C. K. Loong, J. M. Carpenter, J. W. Lynn, R. A. Robinson, and H. A. Mook. *J. Appl. Phys.*, 55:1895, 1984.

[46] J. W. Lynn. *Phys. Rev. B*, 11:2624, 1975.

[47] H. A. Mook and D. McK. Paul. *Phys. Rev. Lett.*, 54:227, 1985.

[48] G. Shirane, V. J. Minkiewicz, and R. Nathans. *J. Appl. Phys.*, 39:383, 1968.

[49] H. A. Mook, J. W. Lynn, and M. R. Nicklow. *Phys. Rev. Lett.*, 30:556, 1973.

[50] R. Pauthenet. *J. Appl. Phys.*, 53:2029 and 8187, 1982.

[51] D. Spišák and J. Hafner. *J. Magn. Magn. Mater.*, 168:257, 1997.

[52] V. P. Antropov, M. I. Katsnelson, and A. I. Liechtenstein. *Physica B*, 237-238:336, 1997.

[53] R. H. Brown, D. M. C. Nicholson, X. Wang, and T. C. Schulthess. *J. Appl. Phys.*, 85:4830, 1999.

[54] J. B. Staunton and B. L. Gyorffy. *Phys. Rev. Lett.*, 69:371, 1992.

[55] M. Heinemann and W. M. Temmerman. *Phys. Rev. B*, 49:4348, 1994.

[56] J. Jensen and A. R. Mackintosh. *Rare Earth Magnetism.* Clarendon, Oxford, 1991.

[57] B. N. Harmon, V. P. Antropov, A. I. Liechtenstein, I. V. Solovyev, and V. I. Anisimov. *J. Phys. Chem. Solids*, 56:1521, 1995.

[58] A. B. Shick, A. I. Liechtenstein, and W. E. Pickett. *Phys. Rev. B*, 60:10763, 1999.

[59] P. Strange, A. Svane, W. M. Temmerman, Z. Szotek, and H. Winter. *Nature*, 399:756, 1999.

[60] M. Richter. *J. Phys. D*, 31:1017, 1998.

[61] M. S. S. Brooks, L. Nordström, and B. Johansson. *J. Phys.: Condens. Matter*, 3:2357, 1991.

[62] A. Y. Perlov, S. V. Halilov, and H. Eschrig. *Phys. Rev. B*, 61:4070, 2000.

[63] P. Kurz, G. Bihlmayer, and S. Blügel. *J. Phys.: Condens. Matter*, 14:6353, 2002.

[64] P. A. Lindgard. *Phys. Rev. B*, 17:2348, 1978.

[65] N. G. Nereson, C. E. Olsen, and G. P. Arnold. *Phys. Rev.*, 135:A176, 1964.

[66] A. H. Millhouse and K. A. McEwen. *Solid State Commun.*, 13:339, 1973.

[67] P. Franek. Master's thesis, Charles University, Prague, 2003.

[68] M. S. S. Brooks and B. Johansson. In K. H. J. Buschow, editor, *Handbook of Magnetic Materials*, volume 7, chapter 3, page 139. North-Holland, Amsterdam, 1993.

[69] I. Turek, J. Kudrnovský, M. Diviš, P. Franek, G. Bihlmayer, and S. Blügel. *Phys. Rev. B*, (submitted).

[70] J. Kudrnovský and V. Drchal. *Phys. Rev. B*, 41:7515, 1990.

[71] P. Bruno, J. Kudrnovský, V. Drchal, and I. Turek. *Phys. Rev. Lett.*, 76:4254, 1996.

[72] J. Kudrnovský, V. Drchal, I. Turek, P. Bruno, P. Dederichs, and P. Weinberger. In H. Dreyssé, editor, *Electronic Structure and Physical Properties of Solids*, volume 535 of *Lecture Notes in Physics*, page 313. Springer, Berlin, 2000.

[73] P. M. Levy, S. Maekawa, and P. Bruno. *Phys. Rev. B*, 58:5588, 1998.

[74] S. D. Drell and L. Verlet. *Phys. Rev.*, 99:849, 1955.

[75] G. Bouzerar and P. Bruno. *Phys. Rev. B*, 66:014410, 2002.

[76] S. Ghosh, P. L. Leath, and M. H. Cohen. *Phys. Rev. B*, 66:214206, 2002.

[77] H. Akai. *Phys. Rev. Lett.*, 81:3002, 1998.

[78] H. Ohno. *J. Magn. Magn. Mater.*, 200:110, 1999.

[79] K. W. Edmonds et al. *Appl. Phys. Lett.*, 81:4991, 2002.

[80] F. Máca and J. Mašek. *Phys. Rev. B*, 65:235209, 2002.

[81] P. A. Korzhavyi et al. *Phys. Rev. Lett.*, 88:187202, 2002.

[82] K. Sato, P. H. Dederichs, and H. Katayama-Yoshida. *Europhys. Lett.*, 61:403, 2003.

[83] L. M. Sandratskii and P. Bruno. *Phys. Rev. B*, 66:134435, 2002.

[84] Y. D. Park et al. *Science*, 295:651, 2002.

[85] B. T. Jonker et al. cond-mat/0302231.

[86] M. Weinert and S. Blügel. In L. H. Bennett and R. E. Watson, editors, *Magnetic Multilayers*, page 51. World Scientific, Singapore, 1994.

[87] R. Vollmer, S. van Dijken, M. Schleberger, and J. Kirschner. *Phys. Rev. B*, 61:1303, 2000.

[88] N. D. Mermin and H. Wagner. *Phys. Rev. Lett.*, 17:1133, 1966.

[89] P. Bruno. *Mater. Res. Soc. Symp. Proc.*, 321:299, 1992.

[90] A. Ney, F. Wilhelm, M. Farle, P. Poulopoulos, P. Srivastava, and K. Baberschke. *Phys. Rev. B*, 59:R3938, 1999.

[91] E. I. Isaev, L. V. Pourovskii, A. M. N. Niklasson, Yu. Kh. Vekilov, B. Johansson, and I. A. Abrikosov. *Phys. Rev. B*, 65:024435, 2001.

[92] E. D. Tober et al. *Phys. Rev. Lett.*, 81:2360, 1998.

[93] A. B. Shick, W. E. Pickett, and C. S. Fadley. *Phys. Rev. B*, 61:R9213, 2000.

[94] C. S. Arnold and D. P. Pappas. *Phys. Rev. Lett.*, 85:5202, 2000.

[95] S. Blügel. In *Magnetismus von Festkörpern und Grenzflächen*. Forschungszentrum Jülich, 1993.

[96] J. Giergiel, A. W. Pang, H. Hopster, X. Guo, S. Y. Tong, and D. Weller. *Phys. Rev. B*, 51:10201, 1995.

[97] D. Spišák and J. Hafner. *Phys. Rev. B*, 65:235405, 2002.

[98] D. Ködderitzsch, W. Hergert, W. M. Temmerman, Z. Szotek, A. Ernst, and H. Winter. *Phys. Rev. B*, 66:064434, 2002.

[99] R. F. Sabiryanov, S. K. Bose, and O. N. Mryasov. *Phys. Rev. B*, 51:8958, 1995.

[100] S. Frota-Pessoa, R. B. Muniz, and J. Kudrnovský. *Phys. Rev. B*, 62:5293, 2000.

[101] L. Szunyogh and L. Udvardi. *J. Magn. Magn. Mater.*, 198-199:537, 1999.

[102] O. Grotheer, C. Ederer, and M. Fähnle. *Phys. Rev. B*, 63:100401(R), 2001.

[103] O. N. Mryasov, A. J. Freeman, and A. I. Liechtenstein. *J. Appl. Phys.*, 79:4805, 1996.

[104] V. P. Antropov and A. I. Liechtenstein. *Mater. Res. Soc. Symp. Proc.*, 253:325, 1992.

[105] L. Udvardi, L. Szunyogh, K. Palotás, and P. Weinberger. *Phys. Rev. B*, 68:1044XX, 2003.

[106] M. I. Katsnelson and A. I. Lichtenstein. *Phys. Rev. B*, 61:8906, 2000.

[107] N. M. Rosengaard and B. Johansson. *Phys. Rev. B*, 55:14975, 1997.

[108] P. Novák and J. Kuriplach. *Phys. Rev. B*, 50:2085, 1994.

[109] J. Callaway, A. K. Chatterjee, S. P. Singhal, and A. Ziegler. *Phys. Rev. B*, 28:3818, 1983.

[110] S. Y. Savrasov. *Phys. Rev. Lett.*, 81:2570, 1998.

[111] J. B. Staunton, S. S. A. Razee, L. Szunyogh, and B. L. Gyorffy. *Physica B*, 318:316, 2002.

[112] S. S. A. Razee, J. B. Staunton, L. Szunyogh, and B. L. Gyorffy. *Phys. Rev. B*, 66:094415, 2002.

[113] S. S. A. Razee, J. B. Staunton, L. Szunyogh, and B. L. Gyorffy. *Phys. Rev. Lett.*, 88:147201, 2002.